The Pennsylvania State University

The Graduate School

College of Engineering

COGNITIVE HYBRID WIRELESS RELAY NETWORKS

A Thesis in

Electrical Engineering

by

Kyounghwan Lee

Submitted in Partial Fulfillment
of the Requirements
for the Degree of

Doctor of Philosophy

December 2007

The thesis of Kyounghwan Lee was reviewed and approved* by the following:

Aylin Yener
Associate Professor of Electrical Engineering
Thesis Adviser
Chair of Committee

John F. Doherty
Professor of Electrical Engineering

Thomas F. La Porta
Professor of Computer Science and Engineering

Guohong Cao
Associate Professor of Computer Science and Engineering

W. Kenneth Jenkins
Professor of Electrical Engineering
Head of the Department of Electrical Engineering

*Signatures are on file in the Graduate School.

Abstract

Future wireless networks will evolve towards architectures where multiple communication standards or technologies cooperate with each other by sharing the resources and transmitting their information in a cooperative fashion. Such network architectures will be made possible by the use of cognitive radios. This thesis aims to investigate the design and the performance of a new wireless network paradigm termed *cognitive hybrid wireless relay network*. We first consider a simple three-node hybrid wireless relay network where multiple frequency bands available from the source and the relay are mutually orthogonal. Specifically, we investigate the information-theoretic performance and the corresponding optimum resource allocation for various relaying schemes. Convinced by the merit of the hybrid wireless relay network architecture, we next investigate the design of large hybrid wireless relay networks where source nodes communicate to their destinations via intermediate nodes able to detect spectrum holes. We examine the outage and diversity performance of the resulting two-hop system under fairly general channel conditions. Lastly, we consider more general cognitive wireless networks where a number of cognitive users seek to access unused frequency channels licensed to the primary users. In this setup, we propose cooperative spectrum sensing strategies in which cognitive users collaborate to share their decisions regarding spectrum occupancy of primary users.

Table of Contents

List of Tables vii

List of Figures viii

Acknowledgments xi

Chapter 1. Introduction 1

1.1 Multi-Band Relay Channel 3

1.2 Cognitive Wireless Relay Networks 5

1.3 Thesis Road Map 7

Chapter 2. Resource Allocation for the Multi-Band Relay Channel: A Building Block for Hybrid Wireless Networks 8

2.1 Introduction 8

2.2 The Multi-Band Relay Channel (MBRC) 12

2.3 Capacity Bounds and Optimum Resource Allocation 16

2.3.1 Maximization of Capacity Bounds for the Gaussian $(3, 2)$-MBRC 24

2.3.2 Upper Bound On Capacity 29

2.4 Numerical Results 30

2.4.1 Capacity Bounds 30

2.4.2 Guidelines for Hybrid Network Design 32

2.5 Chapter Summary 36

2.6 Appendices 37
2.6.1 Proof of maximizing input distribution 37
2.6.2 Proof of Theorem 2.2 39
2.6.3 Proof of Proposition 2.1 40
2.6.4 Optimum Resource Allocation 43
2.6.5 Iterative Algorithm for Case 3 47

Chapter 3. Iterative Power Allocation Algorithms for Amplify/Compress-and-Forward Multi-Band Relay Channel 49
3.1 Introduction 49
3.2 System Model 51
3.3 Iterative Power Allocation Algorithm 53
3.3.1 Iterative Power Allocation for Amplify-and-Forward 55
3.3.2 Iterative Power Allocation for Compress-and-Forward 56
3.3.3 Convergence of Iterative Algorithm 57
3.4 Numerical Results 58
3.5 Chapter Summary 64
3.6 Appendix 66
3.6.1 Proof of Global Optimality Condition 66

Chapter 4. Cognitive Wireless Relay Networks: Outage and Diversity Performance 68
4.1 Introduction 68
4.2 System Model 71
4.2.1 The Cognitive Wireless Relay Network 71

4.2.2 Spectrum Acquisition 73
4.3 Outage Probability Analysis 76
4.3.1 Intra-Cluster Cooperation 85
4.4 Overlay Cognitive Wireless Relay Networks 88
4.5 Numerical Results 94
4.6 Chapter Summary 97
4.7 Appendices 98
4.7.1 Proof of the conditional outage probability 98
4.7.2 Proof of (4.22) and (4.29) 101

Chapter 5. Throughput Enhancing Cooperative Spectrum Sensing Strategies for Cognitive Radios 104
5.1 Introduction 104
5.2 System Model 106
5.3 Cooperative Spectrum Sensing Strategy 107
5.4 Simulation Results 112
5.5 Chapter Summary 118

Chapter 6. Conclusion 120
6.1 Thesis Summary 120
6.2 Future Research 122

References 124

List of Tables

3.1 Four Cases depending on Channel Conditions 59

5.1 Performance of P_{CR} and P_{FR}: $B = 8$, $P_f = (0.01, 0.05, 0.1, 0.15)$, and $P_d = (0.8, 0.85, 0.9, 0.95)$. 111

5.2 Performance of P_{CR} and P_{FR}: $B = 4, 8, 12$, $P_f = 0.05$, and $P_d = 0.85$. 112

List of Figures

2.1 (k, m) Multi-Band Relay Channel. 12

2.2 Upper and lower bounds of $(3, 2)$-MBRC with power optimization only: SNRs at SD, $\eta_1 = 10$dB and $\eta_2 = 5$dB. 31

2.3 Upper and lower bounds of $(3, 2)$-MBRC with joint power and bandwidth optimization: SNRs at SD, $\eta_1 = 10$dB and $\eta_2 = 5$dB. 32

2.4 Comparison of achievable rates: the new SR ink is better than the current SR link, and the new SD link is better than the current SD link. 33

2.5 Comparison of achievable rates: the new SR link is better than the current SR link, and the new SD link is worse than the current SD link. . . 34

2.6 Optimum bandwidth allocation: the new SR link is better than the current SR link, and the new SD link is worse than the current SD link. . . 35

3.1 Convergence of the iterative algorithm for AF scheme with five different random starting points. 60

3.2 Maximum achievable rates for case I. 61

3.3 Power Allocation for CF of case I. 62

3.4 Power Allocation for AF of case I. 63

3.5 Power Allocation for CF of case III. 64

3.6 Power Allocation for AF of case III. 65

3.7 Comparison of maximum achievable rates. 66

4.1 System model 72

4.2 Tree diagram. 83

4.3 Overlay cognitive wireless relay networks: (s) and (p) stand for the secondary and the primary network, respectively. 89

4.4 Model of cognitive wireless relay network. 95

4.5 Outage probabilities of RDF. 96

4.6 Outage probabilities: $P_{S_i} = 1, \forall i$. 97

4.7 Outage probabilities of RDF for different N. 98

4.8 The number of required cooperating nodes for achieving full-diversity. . 99

5.1 A general cognitive network setup. 105

5.2 Time-slotted Structure. 107

5.3 Frequency channel table before and after cooperative spectrum sharing: SU_i, ith cognitive user. 109

5.4 Probability of successful transmission per slot: $T = 14$, $B = 10$, $C = 10$. 113

5.5 Probability of interference to the primary users per slot: $T = 14$, $B = 10$, $C = 10$. 114

5.6 Probability of missed opportunity for access: $T = 14$, $B = 10$, $C = 10$. . 115

5.7 Throughput per cognitive user: $B = 10$, $C = 4$, $P_f = 0.05$, and $P_d = 0.85$. 116

5.8 Throughput per cognitive user: $T = 14$, $C = 10$, $P_f = 0.05$, and $P_d = 0.85$. 117

5.9 Throughput per cognitive user: $T = 14$, $B = 10$, $C = 10$, $P_f = 0.05$, $P_d = 0.85$. 118

5.10 Throughput per cognitive user: $T = 14$, $B = 10$, $C = 10$, $P_f = 0.01$, $\alpha = 3$. 119

Acknowledgments

I feel grateful that I have so many people whom I would like to express my thanks to. Foremost, I would like to express my deepest thank to Prof. Aylin Yener for her invaluable advice, patience, and assistance throughout my PhD studies. It has been great experience for me to work with her. Her academic guidance and encouragement have always been there for me to complete this long journey.

I also would like to thank to my committee members, Prof. Thomas La Porta, Prof. John F. Doherty, and Prof. Guohong Cao for their time and invaluable comments. I am also grateful to my colleagues, special thanks to Semih Serbetli, Xiang He, Ender Tekin, Min Chen for their invaluable help and discussion. I thank to the members of Korean Buddhism Organization for their support and friendship.

I would like to thank my family for their support and love that are instrumental in completing my PhD studies. Special thanks to Hyeseon for her support, patience, and love.

Chapter 1

Introduction

The rapidly increasing demand for high data rate and reliable communications calls for the efficient design of wireless communication networks at various layers. To this end, wireless communication networks will continue to evolve towards where different radio technologies such as WiFi (IEEE 802.11) and cellular networks can exploit the advantages of each other to improve overall connectivity and the performance of the networks [41, 68]. We call such networks *hybrid wireless networks*. Recent development of multi-band/multi-mode devices and cognitive radios will accelerate the realization of this new network paradigm in the near future [22, 52].

Channel impairments such as multi-path fading, shadowing, and path loss impose challenges on reliable wireless communications. Considerable effort has been dedicated to overcome these challenges via diversity techniques. The idea behind diversity is to send the same data over independent paths, which later are combined in a way of reducing the effect of channel impairments. Diversity techniques exploit spatial, temporal, and frequency dimensions [2, 50, 62]. It has been shown that using multiple antennas at the transmitters and the receivers, i.e., MIMO provides a dramatic increase in spectral efficiency without bandwidth penalty [47, 62]. Even though the promising performance gain of a MIMO system is evident, practical limitations of employing multiple transmit antennas such as size, cost, and hardware complexity of wireless devices stimulate a new

form of spatial diversity without using multiple antennas, i.e., cooperative communications [20, 30, 46, 58].

Cooperative relaying techniques entail a group of terminals, each with single antenna[1], essentially forming a distributed antenna array to provide comparable gains to a MIMO system. An intensive research effort has been dedicated towards investigating the performance of cooperative relaying techniques [6, 12, 20, 21, 24, 26, 29, 30, 39, 40, 42, 43, 46, 57, 58]. Cooperation between the source node and relay nodes offers a number of benefits over a conventional direct transmission scheme. These benefits include robust connectivity [51], decreased interference level [31, 58], improved coverage [55], and capacity increase [6, 20, 30, 46].

Radio spectrum is a scarce resource, which motivates intense research efforts on developing "spectrally efficient techniques" such as efficient transmission schemes, diversity techniques, and recent cooperative relaying techniques. While these techniques improve spectral efficiency of the current communication networks, these do not address the current problems of inefficient radio spectrum utilization and the ever increasing demand for additional radio spectrum, due to the increasing deployment of high speed data networks for services such as mobile internet and multi-media applications. Today's fixed spectrum allocation regulated by government agencies such as FCC will face the shortage of available spectrum for these new services [7]. As such, more flexible open spectrum policies and architectures are needed. To this end, cognitive radios offer a viable solution as they are amenable to employ a more open spectrum policy [19, 45] and allow secondary (cognitive) users access by acquiring a spectrum holes unoccupied by

[1] Cooperative relaying techniques can also be sought in the multi-antenna case [5, 67].

primary (licensed) users. This can help enhance spectrum utilization significantly while reducing white spaces in the spectrum [19].

Motivated by these futuristic aspects of hybrid wireless networks and cooperative relaying techniques with cognitive radios, in this thesis, we aim to investigate the design and the performance of *cognitive hybrid wireless relay networks*.

1.1 Multi-Band Relay Channel

In the first part of the thesis, we focus on seeking the information theoretic limits of the building block of cognitive hybrid wireless relay networks. In particular, we consider the three-node network structure we term the multi-band relay channel (MBRC). In this model, we assume that a source node can communicate over multiple frequency bands to its destination, and a cognitive node that overhears the source transmission acts as a relay node. We assume that the relay node uses decode-and-forward scheme and acquires a spectrum hole successfully before forwarding the source transmission, and thus has dedicated resources to assist the source node.

The frequency bands that the source utilizes as well the ones used by the relay node are mutually orthogonal. The different bands are assumed to represent links that operate with different wireless communication standards. Specifically, we aim to understand the performance limits for MBRC, i.e., information theoretic capacity bounds and find the joint optimum bandwidth and power allocation that maximizes the bounds by solving the resulting max-min optimization problem. We provide sufficient conditions under which the associated max-min problem is equivalent to the supporting plane problem [39], which renders the solution for an arbitrary number of bands. For the case where

the source has two bands and the relay has a single band available to communicate, we find the joint optimum bandwidth and power allocation between these three bands. It is shown that sharing the total available bandwidth, i.e., employing optimum bandwidth allocation between the source bands and the relay band, in addition to optimum power allocation at the source, can improve the capacity significantly.

In order to gain insight into the impact of optimum resource allocation on the construction of a hybrid wireless network, we examine a scenario where new wireless links can be added to the classical frequency division relay network to form a simple hybrid wireless network. Given the channel conditions between nodes, we study how to allocate resources to achieve the higher achievable rate.

Next, we investigate the joint optimum transmit power allocation of the source and the relay node under individual power constraints for MBRC for amplify-and-forward and compress-and-forward. The motivation behind studying these additional schemes is that they may be preferable over schemes that fully decode at the relay from a capacity perspective and/or security requirement. We investigate the joint source and relay power allocation problems that maximize the instantaneous achievable rate under individual power constraints.

These information-theoretic capacity studies are conducted in essence to convince us and the research community at large of the potential benefits of hybrid wireless relay networks. Based on this theoretical evidence as a driving force, we next investigate the design of large hybrid wireless relay networks where source nodes communicate to their destinations via multiple hops facilitated by intermediate cognitive nodes able to detect spectrum holes.

1.2 Cognitive Wireless Relay Networks

When a relay node has dedicated resources, i.e., a frequency channel or time-slot to assist its source node, it is not surprising to find that the existence of the relay node can improve reliability of the source to destination communication that otherwise would be limited by the reliability of the direct channel between the two nodes. When the relay nodes do not have such resources and rely on opportunity to capture the resources unused by other nodes, the diversity performance would differ from the case where relays have dedicated resources. The interesting question then becomes how the diversity performance is affected by the resource acquisition capabilities of the relay nodes. To answer this question, we consider cognitive wireless relay networks which are defined by source nodes, destination nodes, and a group of network clusters each consisting of a number of secondary (cognitive) relay nodes and a pair of primary (licensed) source and destination nodes. Cognitive nodes relay information from the source depending on their geographical proximity and their ability to acquire the spectrum hole successfully.

Specifically, we aim to understand the performance of this system by investigating the impact of spectrum acquisition on the diversity order provided by the cognitive relay nodes employing regenerative decode-and-forward, nonregenerative decode-and-forward, and amplify-and-forward. We analyze the high SNR approximation of the outage performance [29] in order to examine the diversity order of these networks for the general channel condition. Even for the case where the spectrum exists in each cluster, it is shown that full-diversity is not achieved regardless of the relaying schemes due to less than perfect spectrum acquisition capability of the relay nodes. Thus, we set out

to improve the outage performance by incorporating a specific intra-cluster cooperation scheme where neighboring cognitive relay nodes in a cluster collaborate with a desired cognitive relay node. We show that the combination of this intra-cluster cooperation along with the system level cooperation via relaying through cognitive nodes improves the outage performance significantly, and full-diversity can be achieved if the proper number of neighboring relay nodes participate in the intra-cluster cooperation. Also, we investigate the outage probability of an overlay cognitive wireless relay network where a source node belonging to the primary network wishes to communicate to its destination via relaying its information using the primary nodes in each cluster.

In the last part of this thesis, we consider the general cognitive hybrid wireless networks where a number of cognitive users seek to access unused frequency channels licensed to the primary users. In this setup, the main challenge is to design a spectrum sensing strategy and access algorithm which enhance the throughput of the cognitive users as well as limit the interference to the primary users. We study cooperative spectrum sensing strategies in which cognitive users collaborate by sharing their decisions regarding spectrum occupancy of primary users. We show that as compared with the non-cooperative case, this simple cooperative sensing strategy enhances the successful transmission of the cognitive users, leading to improve the throughput of the cognitive users while reducing the interference to the primary users.

1.3 Thesis Road Map

In chapter 2, we investigate the information-theoretic performance of multi-band relay channel (MBRC) and the jointly optimum power and bandwidth allocation strategy maximizing its capacity bounds. In chapter 3, we extend our work to investigate the joint source and relay transmit power optimization for MBRC with different relaying schemes. In chapter 4, we investigate the outage and diversity performance of the cognitive wireless relay network. In chapter 5, throughput enhancing cooperative spectrum sensing strategies are investigated for a general cognitive hybrid wireless network. Finally, chapter 6 presents concluding remarks and directions for future research.

Chapter 2

Resource Allocation for the Multi-Band Relay Channel: A Building Block for Hybrid Wireless Networks

2.1 Introduction

Future wireless networks are expected to enable nodes to communicate over multiple technologies and hops. Recent advances in the development of software defined radios support the vision where agile radios are employed at each node that utilize multiple standards and communicate seamlessly. Indeed, an intense research effort is directed towards having multiple communication standards coexist within one system, e.g. the cellular network and IEEE 802.11 WLAN as in [41, 68]. We refer to a group of nodes capable of employing a number of communication technologies to find the best multi-hop route between the source-destination pairs, as *hybrid wireless networks*.

In this chapter, we consider a simple hybrid wireless network with a source destination pair, and aim at understanding its *performance limits*, i.e., information theoretic rates with optimum resource allocation. In particular, we consider a scenario where a source node can communicate over multiple frequency bands to its destination, and a node that overhears the source transmission acts as a relay. We assume that the frequency bands that the source utilizes as well the ones used by the relay node are mutually orthogonal. The different bands are envisioned to represent links that operate with different wireless communication standards.

There has been considerable research effort up to date towards characterizing the information theoretic capacity of relay channels [6, 10, 20, 26, 64]. Most of the earlier work on relay channel capacity assumes that simultaneous transmission and reception on the same frequency at the relay is possible [10]. Since this is difficult to implement, recent work considers employing orthogonality at the relay via time-division [20, 30, 46], frequency-division [15, 40], or code-division [58]. To compensate the loss of spectral efficiency caused by this architecture and to increase the capacity, optimum resource allocation has been considered in [20, 32, 39, 40, 46]. The optimum power and time slot duration allocation for the time-division relay channel has been considered in [20]. Reference [46] investigates three half-duplex time-division protocols that vary in the method of broadcasting they employ and the existence of receiver collision. The optimum power and time-slot allocation has been investigated for the protocol with the maximum degree of broadcasting and no receiver collision in [20].

We note that resource allocation in wireless relay networks is done by utilizing the received SNR and the channel state information which are typically assumed to be available at the source and the relay node [1,20,32,40,46]. Notably, reference [32] studies optimum power and bandwidth allocation strategies for collaborative transmit diversity schemes for the situation when the source and the relay know the magnitudes of all channel gains. The outage minimization and the corresponding optimum power control are considered when the network channel state is available at the source and the relay [1]. The model considered in this chapter is in accordance with previous work, and utilizes the received SNRs that are available at the source and the relay in order to find optimum resource allocation strategy.

In this chapter, we investigate the optimum resource allocation strategies that maximize the capacity bounds for a simple *hybrid wireless relay network*. The channel model in this chapter can be traced back to a class of orthogonal relay networks first proposed in [40]. The three-node relay network in [40] is composed of two parts: a broadcast channel from the source node to the relay and destination node, and a separate orthogonal link from the relay node to the destination node. The parallel channel counterpart of [40] is later examined in [39]. A sum power constraint is imposed on the source node, and the relay node is restricted to perform a partial decode and forward operation. The sum rate from the source to the destination is then maximized by performing power allocation among different sub-channels and the time sharing factor between the two parts of the network. A supporting plane technique is proposed in [39] to solve the associated max-min optimization problem. The results for the parallel network are then applied to the block fading model [39].

The model considered in this chapter is similar to the parallel relay network in [39], yet, for the hybrid wireless network considered, the rate maximization yields a different optimization problem than [39]. In a hybrid network, in addition to power allocation among different bands, it is conceivable to consider bandwidth allocation as well; and we find that the joint optimum power and bandwidth allocation yields higher rate than power optimization only. It is worth mentioning that dynamic bandwidth allocation is beneficial for a hybrid wireless network even in a scenario of a flat overall band. This is because different systems (standards) may exhibit different received SNR behavior even if the underlying channel gain and noise level are the same. This can be caused, for

example, by different coding schemes or different requirements on feedback. Thus, one system will not, in general, be invariably better than all the others over all links.

At the outset, the joint power and bandwidth optimization appears challenging. Luckily, the resulting max-min optimization problem, we show, conforms to a set of sufficient conditions that render the solution manageable, even for an arbitrarily large number of bands. The technique that we can use under these sufficient conditions is the supporting plane technique used in [39]. We remark that the sufficient conditions are general enough that a class of utility functions can be optimized using the technique although our focus is on the information theoretic rates. This implies that the optimization technique used in this chapter can be incorporated as a building block in a variety of resource allocation settings.

Lastly, in order to gain insight into the impact of optimum resource allocation on the construction of a hybrid wireless network, we examine a scenario where new wireless links can be added to the classical frequency division relay network to form a simple hybrid wireless network. Given the channel conditions between nodes, we study how to allocate resources to achieve the higher achievable rate. We observe that the source node is encouraged to communicate over the best network by dedicating all resources exclusively when condition of source-to-relay (SR) link and source-to-destination (SD) link of the new network is better (or worse) than that of SD link and SR link of the current network. Otherwise, it is beneficial to share resource between the current network and the new network to achieve a higher rate.

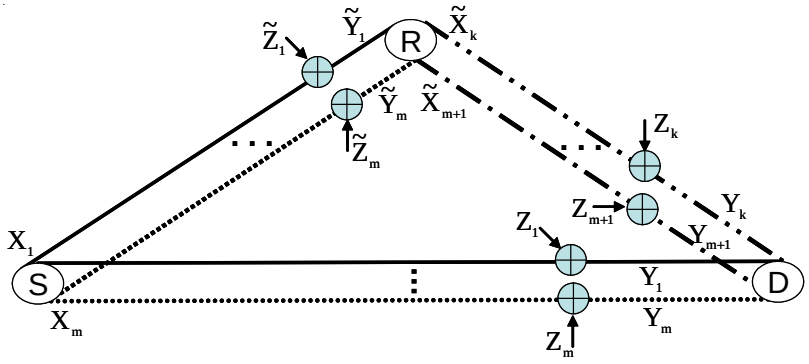

Fig. 2.1. (k, m) Multi-Band Relay Channel.

2.2 The Multi-Band Relay Channel (MBRC)

We consider the multi-band relay channel (MBRC), which models a three-node hybrid wireless network where multiple frequency bands available from the source and the relay are mutually orthogonal. In particular, the situation where there are m channels available for the source node and $k-m$ for the relay node, shown in Figure 2.1, is termed the (k, m)-MBRC.

The source node transmits information over m orthogonal channels to the relay and the destination node. The relay node uses a decode-and-forward scheme [10]. The (k, m)-MBRC input-output signal model is thus given by

$$\tilde{\mathbf{Y}}_{\mathbf{SR}} = \mathbf{X}_{\mathbf{S}} + \tilde{\mathbf{Z}}_{\mathbf{SR}} \tag{2.1}$$

$$\mathbf{Y}_{\mathbf{RD}} = \tilde{\mathbf{X}}_{\mathbf{R}} + \mathbf{Z}_{\mathbf{RD}} \tag{2.2}$$

$$\mathbf{Y}_{\mathbf{SD}} = \mathbf{X}_{\mathbf{S}} + \mathbf{Z}_{\mathbf{SD}} \tag{2.3}$$

- $\mathbf{X_S} = [X_1, X_2, \cdots, X_m]^{\mathrm{T}}$ and $\tilde{\mathbf{X}}_\mathbf{R} = [\tilde{X}_{m+1}, \tilde{X}_{m+2}, \cdots, \tilde{X}_k]^{\mathrm{T}}$ are the transmitted signal vectors from the source node and the relay node, respectively.

- $\mathbf{Y_{SD}} = [Y_1, Y_2, \cdots, Y_m]^{\mathrm{T}}$ and $\tilde{\mathbf{Y}}_\mathbf{SR} = [\tilde{Y}_1, \tilde{Y}_2, \cdots, \tilde{Y}_m]^{\mathrm{T}}$ are the received signal vectors at the destination node and the relay node when the signal is transmitted from the source node.

- $\mathbf{Y_{RD}} = [Y_{m+1}, Y_{m+2}, \cdots, Y_k]^{\mathrm{T}}$ is the received signal vector at the destination from the relay.

- $\tilde{\mathbf{Z}}_\mathbf{SR} = [\tilde{Z}_1, \cdots, \tilde{Z}_m]^{\mathrm{T}}$ is the zero-mean independent additive white Gaussian noise (AWGN) vector with covariance matrix $E[\tilde{\mathbf{Z}}_\mathbf{SR}\tilde{\mathbf{Z}}_\mathbf{SR}^{\mathrm{T}}] = \mathrm{diag}\{\tilde{N}_1/2, \cdots, \tilde{N}_m/2\}$ at the relay node.

- $\mathbf{Z_{SD}} = [Z_1, Z_2, \cdots, Z_m]^{\mathrm{T}}$ and $\mathbf{Z_{RD}} = [Z_{m+1}, \cdots, Z_k]^{\mathrm{T}}$ are the zero-mean independent AWGN vectors with covariance matrices $E[\mathbf{Z_{SD}}\mathbf{Z_{SD}}^{\mathrm{T}}] = \mathrm{diag}\{N_1/2, \cdots, N_m/2\}$, and $E[\mathbf{Z_{RD}}\mathbf{Z_{RD}}^{\mathrm{T}}] = \mathrm{diag}\{N_{m+1}/2, \cdots, N_k/2\}$ at the destination node.

$[\cdot]^{\mathrm{T}}$ denotes the transpose operation, and $\mathrm{diag}\{a_1, \cdots, a_n\}$ is an $n \times n$ diagonal matrix. Since channels are independent, the channel transition probability mass function is:

$$\begin{aligned} &P(y_1, y_2, \cdots, y_m, y_{m+1}, \cdots, y_k, \tilde{y}_1, \tilde{y}_2, \cdots, \tilde{y}_m | x_1, x_2, \cdots, x_m, \tilde{x}_{m+1}, \cdots, \tilde{x}_k) \\ &\qquad = \prod_{i=1}^{m} P(y_i, \tilde{y}_i | x_i) \prod_{j=m+1}^{k} P(y_j | \tilde{x}_j) \end{aligned} \tag{2.4}$$

and we have the following theorem.

Theorem 2.1. *The upper and lower bounds for the capacity of* (k, m)*-MBRC are:*

$$C_{low} = \max_{\substack{S\in\{1,\ldots,m\} \\ S^c=\{1,\ldots,m\}/S}} \left[\sup_{P(\cdot)} \min \left\{ \sum_{i\in S} I(X_i;Y_i) + \sum_{i=m+1}^{k} I(\tilde{X}_i;Y_i), \sum_{i\in S} I(X_i;\tilde{Y}_i) \right\} + \sup_{P(\cdot)} \sum_{i\in S^c} I(X_i;Y_i) \right] \tag{2.5}$$

$$C_{up} = \sup_{P(\cdot)} \min \left\{ \sum_{i=1}^{m} I(X_i;Y_i) + \sum_{i=m+1}^{k} I(\tilde{X}_i;Y_i), \sum_{i=1}^{m} I(X_i;\tilde{Y}_i,Y_i) \right\} \tag{2.6}$$

where $I(X;Y)$ is the mutual information between X and Y. The input distribution $P(\cdot)$ is given by

$$P(x_1, x_2, \cdots, x_m, \tilde{x}_{m+1}, \cdots, \tilde{x}_k) = P(x_1)P(x_2)\cdots P(\tilde{x}_k) \tag{2.7}$$

Proof. The lower bound is obtained by taking the maximum of all possible transmission rates given the total number of bands, i.e., the lower bound includes all possible transmission schemes which depend on whether the transmission from the source band(s) are decoded at the relay.

We define S as the set of bands in which the transmission from the source is decoded at the relay. S^c is the complement of S, and includes the set of bands for direct

communication. For (k, m)-MBRC, the lower bound is given by

$$C_{\text{low}} = \max_{\substack{S\in\{1,\ldots,m\} \\ S^c=\{1,\ldots,m\}/S}} \Big\{ C_{\text{DF}}\left(\mathbf{X}_S, \tilde{\mathbf{X}}_{\{m+1,\ldots,k\}}, \tilde{\mathbf{Y}}_S, \mathbf{Y}_{S\cup\{m+1,\ldots,k\}}\right) + C_{\text{DT}}\left(\mathbf{X}_{S^c}, \mathbf{Y}_{S^c}\right) \Big\} \tag{2.8}$$

where $\mathbf{X}_S$ is the transmitted signal vector from the source and $\mathbf{X}_{S^c}$ is the transmitted signal vector from the source intended for direct transmission. Similarly, $\tilde{\mathbf{X}}_{\{m+1,\ldots,k\}}$ is the transmitted signal from the relay. $\tilde{\mathbf{Y}}_S$ is the received signal vector at the relay. $\mathbf{Y}_{S\cup\{m+1,\ldots,k\}}$ is the received signal vector at the destination. $\mathbf{Y}_{S^c}$ is the received signal vector at the destination as a result of direct transmission. $C_{DF}(\cdot)$ and $C_{DT}(\cdot)$ are given by

$$C_{\text{DF}}(\cdot) = \sup_{P\left(\boldsymbol{x}_S, \tilde{\boldsymbol{x}}_{\{m+1,\ldots,k\}}\right)} \min \Big\{ I\left(\mathbf{X}_S, \tilde{\mathbf{X}}_{\{m+1,\ldots,k\}}; \mathbf{Y}_{S\cup\{m+1,\ldots,k\}}\right), I\left(\mathbf{X}_S; \tilde{\mathbf{Y}}_S | \tilde{\mathbf{X}}_{\{m+1,\ldots,k\}}\right) \Big\} \tag{2.9}$$

$$C_{\text{DT}}(\cdot) = \sup_{P(\boldsymbol{x}_{S^c})} I\left(\mathbf{X}_{S^c}, \mathbf{Y}_{S^c}\right) \tag{2.10}$$

where $P\left(\boldsymbol{x}_S, \tilde{\boldsymbol{x}}_{\{m+1,\ldots,k\}}\right)$ is the input joint distribution with respect to S. Similarly, $P\left(\boldsymbol{x}_{S^c}\right)$ is the input joint distribution with respect to S^c. We note that (2.9) can be readily obtained by using the results in [10] by taking $X = \mathbf{X}_S$, $\tilde{X} = \tilde{\mathbf{X}}_{\{m+1,\ldots,k\}}$, $\tilde{Y} = \tilde{\mathbf{Y}}_S$, and $Y = \mathbf{Y}_{S\cup\{m+1,\ldots,k\}}$. Applying the same approach, we obtain the following

from the cut set bound [11].

$$C_{\text{up}} = \sup_{P(\cdot)} \min \Big\{ I\left(\mathbf{X}_S, \tilde{\mathbf{X}}_{\{m+1,...,k\}}; \mathbf{Y}_{S\cup\{m+1,...,k\}}\right), \\ I\left(\mathbf{X}_S; \mathbf{Y}_{S\cup\{m+1,...,k\}}, \tilde{\mathbf{Y}}_S | \tilde{\mathbf{X}}_{\{m+1,...,k\}}\right) \Big\} \tag{2.11}$$

where $P(\cdot) = P\left(x_1, ..., x_m, \tilde{x}_{m+1}, ..., \tilde{x}_k\right)$. Following a similar approach to [40], (2.7) can be shown to maximize the mutual information in (2.9)-(2.11) (See Appendix 2.6.1.), and the optimization over (2.7) leads to (2.5)-(2.6). □

2.3 Capacity Bounds and Optimum Resource Allocation

In the remainder of the chapter, we will consider optimum resource allocation on the bounds obtained for the MBRC, i.e., for hybrid wireless networks where the source node has access to distinct bands (standards) and a second node that overhears the source information relays to the destination using additional orthogonal bands.

We have the input-output signal model given by (2.1) under source and relay power constraints.

$$E\left[X_i^2\right] \leq \alpha_i P_s, \quad i = 1, ..., m \tag{2.12}$$

$$E\left[\tilde{X}_i^2\right] \leq \zeta_i P_r \quad i = m+1, ..., k \tag{2.13}$$

where P_s and P_r are the total available power at the source and relay node. α_i and ζ_i are the nonnegative power allocation parameters for each orthogonal band at the source and relay node, and $\sum_{i=1}^{m} \alpha_i = \sum_{i=m+1}^{k} \zeta_i = 1$. Unlike [1, 20], we do not have a total power constraint between the source and the relay and assume each has its own battery.

We assume the system has total bandwidth W. We define the received SNRs at the relay and the destination over channel $i = 1, .., k$ as,

$$\chi_i \triangleq \frac{P_s}{\tilde{N}_i W}, \qquad \eta_i \triangleq \frac{P_s}{N_i W}, \quad i = 1, ..., m \tag{2.14}$$

$$\rho_i \triangleq \frac{P_r}{N_i W}, \quad i = m+1, ..., k \tag{2.15}$$

Note that the actual received SNR values are the scaled versions of (2.14)-(2.15) depending on the power and bandwidth allocation. For example, the actual received SNR at the relay from channel 1, which is allocated α_1 fraction of the source power and ϕ_1 fraction of the bandwidth, simply $\frac{\alpha_1 \chi_1}{\phi_1}$. Given the received SNRs which are available at the source and relay, our aim is to find the optimum resource allocation parameters that maximize capacity lower bound in terms of the transmitted power and the total bandwidth for (k, m)-MBRC, which leads to optimally allocating the source power among m source bands, the relay power among $k - m$ relay bands, and the total bandwidth among k bands. We can obtain the capacity lower and upper bounds of the Gaussian (k, m)-MBRC from Theorem 2.1 as follows.

Theorem 2.2. *The upper and lower bounds for the capacity of the Gaussian (k, m)-MBRC are:*

$$C_{low}^{MBRC} = \max_{\substack{S\in\{1,\ldots,m\} \\ S^c\in\{1,\ldots,m\}/S}} \max_{\substack{0\le\alpha_i,\phi_i,\zeta_i\le 1 \\ \sum_{i=1}^{m}\alpha_i=1 \\ \sum_{i=1}^{k}\phi_i=1 \\ \sum_{i=m+1}^{k}\zeta_i=1}} \min\left\{ \sum_{i\in S}\phi_i\log\left(1+\alpha_i\frac{\eta_i}{\phi_i}\right) + \sum_{i=m+1}^{k}\phi_i\log\left(1+\zeta_i\frac{\rho_i}{\phi_i}\right) + \right.$$

$$\left. \sum_{i\in S^c}\phi_i\log\left(1+\alpha_i\frac{\eta_i}{\phi_i}\right), \quad \sum_{i\in S}\phi_i\log\left(1+\alpha_i\frac{\chi_i}{\phi_i}\right) + \sum_{i\in S^c}\phi_i\log\left(1+\alpha_i\frac{\eta_i}{\phi_i}\right) \right\} \tag{2.16}$$

$$C_{up}^{MBRC} = \max_{\substack{0\le\alpha_i,\phi_i,\zeta_i\le 1 \\ \sum_{i=1}^{m}\alpha_i=1 \\ \sum_{i=1}^{k}\phi_i=1 \\ \sum_{i=m+1}^{k}\zeta_i=1}} \min\left\{ \sum_{i=1}^{2}\phi_i\log\left(1+\alpha_i\frac{\eta_i}{\phi_i}\right) + \sum_{i=m+1}^{k}\phi_i\log\left(1+\zeta_i\frac{\rho_i}{\phi_i}\right), \right.$$

$$\left. \sum_{i=1}^{2}\phi_i\log\left(1+\alpha_i\frac{\eta_i+\chi_i}{\phi_i}\right) \right\} \tag{2.17}$$

Proof. See Appendix 2.6.2. □

For each broadcast channel, if the relay node sees a higher received SNR than the destination node, then a superposition coding scheme [11] is used to convey independent information to the relay node, which can not be decoded by the destination directly. The relay node then collects this information from all the channels where superposition coding is used, and transmits it to the destination at the appropriate rate.

Based on whether the relay node is utilized by a certain channel (band), we note that there are 2^m possible schemes. We observe that these 2^m schemes are not exclusive

to each other, since a superposition coding scheme may be reduced to a direct source-to-destination transmission if no band is allocated to the relay-to-destination link. We also note that which scheme yields the largest rate is completely decided by the SNR relationship, namely the component-wise relationship between the received SNRs of the source-to-relay links, i.e., $\chi_1, ..., \chi_m$ and the received SNRs of the source-to-destination links, i.e., $\eta_1, ..., \eta_m$.

If $\chi_j \leq \eta_j$, $j = 1, ..., m$, then for any bandwidth allocation, the signal received by the relay over this broadcast channel can be viewed as a degraded version of the signal received by the destination. Therefore, direct link transmission should be used for this band, regardless of what scheme is used for the other bands. On the other hand, if $\eta_j < \chi_j$, then the relay node can always learn something more than the destination node over this band, and uses the superposition code scheme, and, although the superposition scheme may be reduced to a direct link transmission scheme, optimizing under this scheme does not incur any rate loss. Based on these observations, we conclude that there is no need to examine all the schemes to find the best rate and the corresponding resource allocation. That is, practically, the system checks the received SNRs and chooses one of 2^m schemes satisfying the relationship of the received SNRs to communicate and the rate with optimized resource allocation for the chosen scheme is the maximum achievable rate, and the corresponding resource allocation is the globally optimum solution.

Next, we maximize the capacity lower bound in (2.16). To achieve this goal, we introduce the following general max-min optimization problem.

$$\max_{(c_1,c_2)\in\mathbf{B}_1} \min\{c_1, c_2\} \tag{2.18}$$

$$\text{where } \mathbf{B}_1 = \{(G_1(\underline{R}), G_2(\underline{R})) : \underline{R} \in \mathbf{C}_0\} \tag{2.19}$$

$$\mathbf{C}_0 = \{\text{all feasible values of } \underline{R}\} \tag{2.20}$$

We note that $G_1(\underline{R})$ and $G_2(\underline{R})$ can be any utility function with the resource allocation parameter vector, $\underline{R}$.

Proposition 2.1. *If $G_1(\underline{R})$ and $G_2(\underline{R})$ are non-negative and concave over the convex set $\mathbf{C}_0$, there must exist $0 \leq \beta \leq 1$ such that maximizing the following equation is equivalent to (2.18).*

$$G(\beta, \underline{R}) = \beta G_1(\underline{R}) + (1-\beta)G_2(\underline{R}),\ 0 \leq \beta \leq 1. \tag{2.21}$$

Proof. See Appendix 2.6.3. □

Note that the optimization problem in (2.18) corresponds to finding $\underline{R}$ and β maximizing the minimum of two end points in $G(\beta, \underline{R})$. One possible technique to solve the max-min optimization problem in (2.18) is given by the following proposition [39], which we will also utilize.

Proposition 2.2 ([39], Proposition 1)**.** *The relationship between optimum resource allocation parameters $\underline{R}^*$ and the corresponding optimum point β^* is given by the following.*

Case 1 : If $\beta^* = 1$ *and* $G_1(\underline{R}^*) < G_2(\underline{R}^*)$

Case 2 : If $\beta^* = 0$ *and* $G_1(\underline{R}^*) > G_2(\underline{R}^*)$

Case 3 : Neither case 1 nor 2 occurs; under this case, $0 \leq \beta^* \leq 1$ *and* $G_1(\underline{R}^*) = G_2(\underline{R}^*)$

Now, we can restate our max-min optimization problem given in Theorem 2.2 as:

$$\max_{(c_1,c_2)\in \mathbf{B}_1} \min\{c_1, c_2\} \tag{2.22}$$

$$\text{where } \mathbf{B}_1 = \{(C_1(\underline{R}), C_2(\underline{R})) : \underline{R} \in \mathbf{C}_0\} \tag{2.23}$$

$$\mathbf{C}_0 = \{(\alpha_1, ..., \alpha_m, \zeta_{m+1}, ..., \zeta_k, \phi_1, ..., \phi_k) : 0 \leq \alpha_i, \zeta_i, \phi_i \leq 1, \tag{2.24}$$

$$\sum_{i=1}^{m} \alpha_i = 1, \sum_{i=m+1}^{k} \zeta_i = 1, \sum_{i=1}^{k} \phi_i = 1\} \subset \Re^{2k}$$

where $C_1(\underline{R})$ and $C_2(\underline{R})$ are the first and the second term of max-min optimization problem in (2.16). Next, we need to prove that $C_1(\underline{R})$ and $C_2(\underline{R})$ are concave over $\mathbf{C}_0$ in (2.24). Define

$$F(x_1, \ldots, x_n, y_1, \ldots, y_n) = \sum_{i\in D} x_i \log\left(1 + y_i \frac{t_i}{x_i}\right), \quad t_i > 0,\ x_i \geq 0,\ y_i \geq 0,\ i = 1, ..., n \tag{2.25}$$

$$D = \{i : x_i > 0,\ i = 1, ..., n\} \tag{2.26}$$

It is easy to see that $F(x_1, \ldots, x_n, y_1, \ldots, y_n)$ is continuous over $\{x_i \geq 0,\ y_i \geq 0,\ i = 1, ..., n\}$. Then, we have the following proposition.

Proposition 2.3. *$F(x_1, ..., x_n, y_1, ..., y_n)$ is concave over $x_i \geq 0$ and $y_i \geq 0,\ i = 1, ..., n$.*

Proof. Due to the continuity of $F(\cdot)$, we only need to prove that $F(\cdot)$ is concave over the interior of the region, which is $\{x_i > 0,\ y_i > 0, i = 1, ..., n\}$. This is done by examining the Hessian, $\mathbf{H}$, of (2.25). First, we find the second order derivatives of (2.25) with respect to x_i and y_i as follows.

$$\frac{\partial^2 F(\cdot)}{\partial {x_i}^2} = \frac{-t_i^2 y_i^2}{x_i(t_i y_i + x_i)^2} \tag{2.27}$$

$$\frac{\partial^2 F(\cdot)}{\partial {y_i}^2} = \frac{-t_i^2 x_i}{(t_i y_i + x_i)^2} \tag{2.28}$$

$$\frac{\partial^2 F(\cdot)}{\partial x_i \partial y_i} = \frac{t_i^2 y_i}{(t_i y_i + x_i)^2} \tag{2.29}$$

We note that $\frac{\partial^2 F(\cdot)}{\partial x_i \partial x_j} = \frac{\partial^2 F(\cdot)}{\partial y_i \partial y_j} = \frac{\partial^2 F(\cdot)}{\partial x_i \partial y_j} = 0, \forall i \neq j$.

The Hessian is the $2n \times 2n$ block diagonal matrix with the following 2×2 matrix in its ith diagonal.

$$A_i = \begin{bmatrix} \frac{\partial^2 F(\cdot)}{\partial {x_i}^2} & \frac{\partial^2 F(\cdot)}{\partial x_i \partial y_i} \\ \frac{\partial^2 F(\cdot)}{\partial y_i \partial x_i} & \frac{\partial^2 F(\cdot)}{\partial {y_i}^2} \end{bmatrix} \quad i = 1, ..., n \tag{2.30}$$

It is readily seen that A_i is singular. Since $\frac{\partial^2 F(\cdot)}{\partial {x_1}^2} < 0$ for $y_1 > 0$ from (2.27), $\mathbf{H}$ is the negative semi-definite. Thus, $F(\cdot)$ is concave over $x_i > 0$ and $y_i > 0,\ i = 1, ..., n$. Since $F(\cdot)$ is continuous over $x_i \geq 0,\ y_i \geq 0,\ i = 1, ..., n$, $F(\cdot)$ is concave over $x_i \geq 0$ and $y_i \geq 0,\ i = 1, ..., n$. □

We note that for any choice of set $S \in \{1, ..., m\}$, $C_1(\underline{R})$ corresponds to $F(\cdot)$ in (2.25) with $x_i = \phi_i$, $i = 1, ..., k$, $y_i = \alpha_i$, $i = 1, ..., m$, $y_i = \zeta_i$, $i = m+1, ..., k$, $t_i = \eta_i$,

$i = 1, ..., m$, and $t_i = \rho_i$, $i = m+1, ..., k$. For $C_1(\underline{R})$, the Hessian is a $2k \times 2k$ block diagonal matrix. Similarly, $C_2(\underline{R})$ corresponds to $F(\cdot)$ with $x_i = \phi_i$, $i = 1, ..., m$, $y_i = \alpha_i$, $i = 1, ..., m$, $t_i = \chi_i$, $i \in S$, and $t_i = \eta_i$, $i \in S^c$. For $C_2(\underline{R})$, the Hessian is a $2m \times 2m$ block diagonal matrix.

Remark 2.1. *Since $F(\cdot)$ is concave over the set $x_i \geq 0$ and $y_i \geq 0$, $i = 1, ..., n$, it is also concave over any convex subset of it. Thus, $C_1(\underline{R})$ and $C_2(\underline{R})$ are concave over $\underline{R} \in \mathbf{C}_0$.*[1] *This establishes that the local optimum for (2.22) is also the global optimum [3, Theorem 3.4.2, pp. 125-126].*

Remark 2.2. *We further find that $F(\cdot)$ is strictly concave over any convex subset of $x_i > 0$ ($y_i > 0$), $i = 1, ..., n$, jointly when $y_i > 0$ ($x_i > 0$), $i = 1, ..., n$, are held constant. Note that, when all $y_i > 0$, $i = 1, ..., n$, are held constant, i.e., $y_i = c_i$, we have $F(\cdot)$ as a function of x_i, $i = 1, ..., n$. In this case, it is easily seen that the Hessian is the $n \times n$ diagonal matrix in which ith diagonal term is given by $\frac{\partial^2 F(\cdot)}{\partial {x_i}^2} = \frac{-t_i^2 c_i^2}{x_i (t_i c_i + x_i)^2}$, $c_i > 0$, $i = 1, ..., n$. Since now all of the diagonal terms are strictly negative when $x_i > 0$, $i = 1, ..., n$, $F(\cdot)$ is strictly concave over all $x_i > 0$, $i = 1, ..., n$, jointly when all $y_i > 0$, $i = 1, ..., n$, are held constant. Similarly, $F(\cdot)$ is strictly concave over $y_i > 0$, $i = 1, ..., n$, jointly when all $x_i > 0$, $i = 1, ..., n$, are held constant. Since if a function is strictly concave over a set, it is also strictly concave over any convex subset of that set, the preceding argument implies that $F(\cdot)$ is strictly concave over any convex subset of $x_i > 0$ ($y_i > 0$), $i = 1, ..., n$, when all $y_i > 0$ ($x_i > 0$), $i = 1, ..., n$, are held constant. This fact will be useful in the sequel.*

[1] *It is readily seen that the sum constraints define a convex set.*

Based on Proposition 2.1 and Proposition 2.3, the methodology given in Proposition 2.2 can be applied to our max-min optimization problem in (2.22) for an arbitrary (k, m). That said, in the remainder of the chapter, we will examine the optimum resource allocation for $(3, 2)$-MBRC where the source has two bands and the relay has a single band available to communicate and uses its own full power P_r. We find this network model representative and meaningful because of the following two observations. First, if there is more than one band available for the link between the relay and the destination, then only the best band among them will be used. This can be seen by fixing the overall band for this link and performing joint power and bandwidth optimization. Therefore, as long as the relay-to-destination SNRs are different, which is usually the case in practice, (k, m)-MBRC will have the same resource allocation parameters as those of $(m + 1, m)$-MBRC. Secondly, the case with $m > 2$ is similar to the case with $m = 2$ except that there are more schemes to choose from. Therefore, we focus on the $(3, 2)$-MBRC in the sequel.

2.3.1 Maximization of Capacity Bounds for the Gaussian $(3, 2)$-MBRC

For $(3, 2)$-MBRC, there are four schemes to choose from. Let us label them Scheme I through IV. From Theorem 2.2, the upper and lower bounds for the capacity of the

Gaussian $(3,2)$-MBRC are given by

$$C_{\text{low}}^{\text{MBRC}} = \max_{\substack{0\le\alpha_i,\phi_i\le 1 \\ \sum_{i=1}^{2}\alpha_i=1 \\ \sum_{i=1}^{3}\phi_i=1}} \min\left\{ \sum_{i=1}^{2} \phi_i \log\left(1+\alpha_i\frac{\eta_i}{\phi_i}\right) + \phi_3 \log\left(1+\frac{\rho_3}{\phi_3}\right), \right. \tag{2.31}$$

$$\left. \phi_1 \log\left(1+\alpha_1\frac{\kappa}{\phi_1}\right) + \phi_2 \log\left(1+\alpha_2\frac{\nu}{\phi_2}\right) \right\}$$

$$C_{\text{up}}^{\text{MBRC}} = \max_{\substack{0\le\alpha_i,\phi_i\le 1 \\ \sum_{i=1}^{2}\alpha_i=1 \\ \sum_{i=1}^{3}\phi_i=1}} \min\left\{ \sum_{i=1}^{2} \phi_i \log\left(1+\alpha_i\frac{\eta_i}{\phi_i}\right) + \phi_3 \log\left(1+\frac{\rho_3}{\phi_3}\right), \right.$$

$$\left. \sum_{i=1}^{2} \phi_i \log\left(1+\alpha_i\frac{\eta_i+\chi_i}{\phi_i}\right) \right\} \tag{2.32}$$

where $(\kappa,\nu) = (\chi_1,\chi_2)$, (χ_1,η_2), (η_1,χ_2), and (η_1,η_2) for scheme I to IV, respectively. Each scheme materializes as a function of the received SNRs as follows.

- Scheme I: $S = \{1,2\}$; the scenario where transmission from the source node over both links are decoded at the relay node. This scheme is chosen if $\eta_1 \le \chi_1$ and $\eta_2 \le \chi_2$.
- Scheme II: $S = \{1\}$; the scenario where transmission from the source node over band 1 is decoded at the relay node while band 2 is used for direct transmission only. This scheme is chosen if $\eta_1 \le \chi_1$ and $\eta_2 \ge \chi_2$.

- Scheme III: $S = \{2\}$; the scenario where transmission from the source node over band 2 is decoded at the relay node while band 1 is used for direct transmission only. This scheme is chosen if $\eta_1 \geq \chi_1$ and $\eta_2 \leq \chi_2$.

- Scheme IV: $S = \{\phi\}$; the scenario where transmissions from the source node from both bands are used only for direct transmission. This scheme is chosen if $\eta_1 \geq \chi_1$ and $\eta_2 \geq \chi_2$.

We define $\underline{R}^* = (\alpha_1, \alpha_2, \phi_1, \phi_2, \phi_3)$ as the optimum resource allocation parameters for (2.31). $C_1(\underline{R})$ and $C_2(\underline{R})$ are the first and second term in (2.31). From (2.31), we note that the capacity for scheme IV is given by

$$C_{\text{direct}}^{\text{MBRC}} = \max_{\substack{0 \leq \alpha_i, \phi_i \leq 1 \\ \sum_{i=1}^{2} \alpha_i = 1 \\ \sum_{i=1}^{2} \phi_i = 1}} \left\{ \phi_1 \log\left(1 + \alpha_1 \frac{\eta_1}{\phi_1}\right) + \phi_2 \log\left(1 + \alpha_2 \frac{\eta_2}{\phi_2}\right) \right\} \tag{2.33}$$

In this case, the max-min optimization problem reduces to a maximization problem and it is readily shown that the optimum resource allocation for the rate of scheme IV is given by

$$\underline{R}^* = \begin{cases} (1, 0, 1, 0, 0) & \text{if } \eta_1 > \eta_2 \\ (0, 1, 0, 1, 0) & \text{if } \eta_1 < \eta_2 \end{cases} \tag{2.34}$$

For schemes I, II, III, once the appropriate scheme is decided upon, parameters (κ, ν) can be substituted into (2.31) accordingly and we can examine $\underline{R}^*$ for each of the cases in Proposition 2.2.

Case 1: $\beta^* = 1$, and $\underline{R}^*$ maximizes $C_1(\underline{R})$.

This case holds if the following condition is satisfied.

$$\sum_{i=1}^{2} \phi_i^* \log\left(1+\alpha_i^* \frac{\eta_i}{\phi_i^*}\right) + \phi_3^* \log\left(1+\frac{\rho_3}{\phi_3^*}\right) < \phi_1^* \log\left(1+\alpha_1^* \frac{\kappa}{\phi_1^*}\right) + \phi_2^* \log\left(1+\alpha_2^* \frac{\nu}{\phi_2^*}\right) \tag{2.35}$$

and, we obtain

$$\underline{R}^* = \begin{cases} \left(1, 0, 1-\frac{\rho_3}{\rho_3+\eta_1}, 0, \frac{\rho_3}{\rho_3+\eta_1}\right) & \text{if } \eta_1 > \eta_2 \\ \left(0, 1, 0, 1-\frac{\rho_3}{\rho_3+\eta_2}, \frac{\rho_3}{\rho_3+\eta_2}\right) & \text{if } \eta_1 < \eta_2 \end{cases} \tag{2.36}$$

The received SNRs must satisfy

$$\frac{\eta_1}{\rho_3+\eta_1} \log\left(1+\frac{\kappa(\rho_3+\eta_1)}{\eta_1}\right) > \log(1+\rho_3+\eta_1) \quad \text{for } \eta_1 > \eta_2 \tag{2.37}$$

$$\frac{\eta_2}{\rho_3+\eta_2} \log\left(1+\frac{\nu(\rho_3+\eta_2)}{\eta_2}\right) < \log(1+\rho_3+\eta_2) \quad \text{for } \eta_1 < \eta_2 \tag{2.38}$$

Proof. See Appendix 2.6.4. □

Case 2: $\beta^* = 0$, and $\underline{R}^*$ maximizes $C_2(\underline{R})$.

This case holds if the following condition is satisfied.

$$\sum_{i=1}^{2} \phi_i^* \log\left(1+\alpha_i^* \frac{\eta_i}{\phi_i^*}\right) + \phi_3^* \log\left(1+\frac{\rho_3}{\phi_3^*}\right) > \phi_1^* \log\left(1+\alpha_1^* \frac{\kappa}{\phi_1^*}\right) + \phi_2^* \log\left(1+\alpha_2^* \frac{\nu}{\phi_2^*}\right) \tag{2.39}$$

and, we obtain

$$\underline{R}^* = \begin{cases} (1, 0, 1, 0, 0) & \text{if } \kappa > \nu, \eta_1 > \kappa \\ (0, 1, 0, 1, 0) & \text{if } \kappa < \nu, \eta_2 > \nu \end{cases} \tag{2.40}$$

Proof. See Appendix 2.6.4. □

Remark 2.3. *By substituting the appropriate parameters for* (κ, ν) *for each scheme into (2.40), we observe that case 2 does not ever materialize for schemes I, II, III.*

Case 3: $0 \leq \beta^* \leq 1$, and $\underline{R}^*$ maximizes $\beta^* C_1(\underline{R}) + (1-\beta^*)C_2(\underline{R})$ for a fixed β^*.

This case occurs when (2.35) or (2.39) do not hold. The closed form solution for this optimization problem does not exist. Thus, we have to rely on an iterative algorithm. We propose to use alternating maximization algorithm that calls for optimizing $\boldsymbol{\alpha} = \{\alpha_1, \alpha_2\}$ in one stage, followed by optimizing $\boldsymbol{\phi} = \{\phi_1, \phi_2, \phi_3\}$ in the next stage. The iterations are obtained by finding KKT points of the corresponding optimization problem with the variable vector $\boldsymbol{\alpha}$ or $\boldsymbol{\phi}$. We note that the objective function is not differentiable at the boundary of the feasible region, i.e., for $\phi_i = 0$, $i = 1, 2, 3$ and the corresponding KKT points are not defined. Thus, we need to introduce a small positive value, ε, and define a modified feasible region as illustrated in (2.67) and (2.68) that excludes the boundary point. Every time an iteration reaches the boundary of the new feasible region, we expand the feasible region by successively reducing ε so that we can continue with the iterations until convergence. The detailed description of the following proposed iterative algorithm and proof of its convergence to the global optimum solution is given in Appendix 2.6.5:

Step 1: – Initialization: For initial values of β^*, μ, λ, ω_i, $i = 1, 2, 3$, ψ_i, $i = 1, 2$, assign values to ϕ_1, ϕ_2, ϕ_3, such that $\phi_1 + \phi_2 + \phi_3 = 1$.

- Iteration n: Update $\alpha_i(n), i = 1, 2$ by finding the solution of KKT condition of (2.78) with respect to $\alpha_i, i = 1, 2$; find $\mu(n)$ and $\psi_i(n)$, $i = 1, 2$ such that $\alpha_1(n) + \alpha_2(n) = 1$ and $\alpha_i(n) \geq \varepsilon$, $i = 1, 2$.
- Iteration $n + 1$: Update $\phi_1(n + 1)$, $\phi_2(n + 1)$, and $\phi_3(n + 1)$ by finding the solution of KKT condition of (2.78) with respect to ϕ_i, $i = 1, 2, 3$; find $\lambda(n+1)$ and $\omega_i(n + 1)$, $i = 1, 2, 3$ such that $\phi_1(n + 1) + \phi_2(n + 1) + \phi_3(n + 1) = 1$, and $\phi_i(n) \geq \varepsilon$, $i = 1, 2, 3$.
- Repeat step 1 until the optimum β^* is found by $C_1(\underline{R}^*) = C_2(\underline{R}^*)$ in (2.79).

Step 2: If the iteration does <u>not</u> reach the boundary of the feasible region of (2.67) and (2.68), the algorithm terminates.

Step 3: Otherwise, set $\varepsilon = \varepsilon/d$, $d > 1$ in (2.67) and (2.68) and repeat steps (1) to (2) by using the KKT points from the previous iteration as the initial points.[2]

We reiterate that based on the scheme at hand, we would substitute the correct parameters for $(\kappa, \nu) \in \{(\chi_1, \chi_2), (\chi_1, \eta_2), (\eta_1, \chi_2)\}$ to find the optimum resource allocation strategy.

2.3.2 Upper Bound On Capacity

Recall that the upper bound given by (2.17) is obtained by the max-flow min-cut theorem. The maximization for the upper bound follows same steps to that of the lower bound. In general, the upper bound is not tight. One exception is that for $(3, 2)$-MBRC, since case 2 for schemes I, II, and III is not possible, the optimum resource allocation

[2]For numerical results, we use $d = 2$.

parameters $\underline{R}^*$ maximize $C_1(\underline{R})$ (case 1) or $C_1(\underline{R}) = C_2(\underline{R})$ (case 3). There exists a ρ_3' such that $C_1(\underline{R}^*) < C_2(\underline{R}^*)$ if $\rho_3 < \rho_3'$, otherwise $C_1(\underline{R}^*) = C_2(\underline{R}^*)$. Since the first term of the upper bound in (2.32) is the same as $C_1(\underline{R})$, we know that for $(3,2)$-MBRC, $\underline{R}^*$ maximizes $C_{\text{low}}^{\text{MBRC}} = C_{\text{up}}^{\text{MBRC}}$ for $\rho_3 < \rho_3'$ and the resulting optimized rate is the capacity of $(3,2)$-MBRC. A similar observation was made for the frequency division relay network, i.e., when one band exists from the source in [40]. It is interesting to observe that the same observation extends to the multi-band case.

2.4 Numerical Results

2.4.1 Capacity Bounds

In this section, we present numerical results to support our analysis described in section 2.3. Specifically, for $(3,2)$-MBRC, we plot the capacity lower bound (LB) obtained by optimum resource allocation as well as the capacity upper bound (UB) with the same resource allocation parameters. For comparison purposes, we also consider the case where overall bandwidth W is equally divided between the three bands and only optimum power allocation is done.

Figure 2.2 shows the upper bound (UB) and the lower bound (LB) for $(3,2)$-MBRC with optimum power allocation only. When the source-to-relay (SR) SNRs χ_1 and χ_2 are smaller than or equal to the source-to-destination (SD) SNRs η_1 and η_2 respectively, the lower bound does not increase and saturate even if the relay-to-destination (RD) SNR ρ_3 increases. This is expected, since using the relay is not beneficial when the source to relay channel is worse than the source to destination channel.

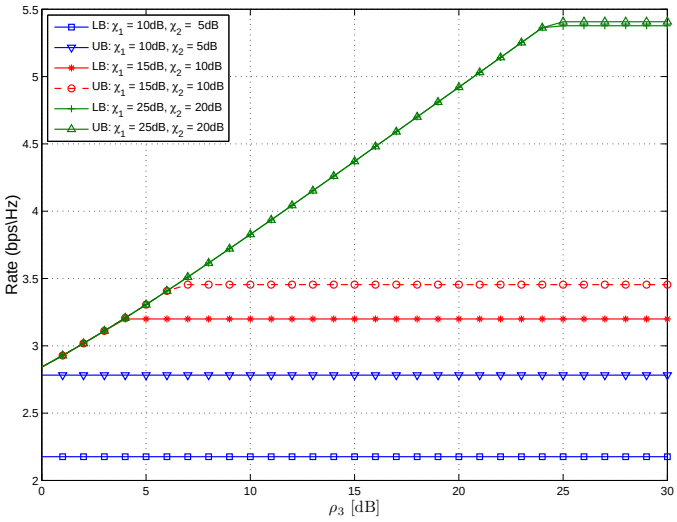

Fig. 2.2. Upper and lower bounds of $(3, 2)$-MBRC with power optimization only: SNRs at SD, $\eta_1 = 10$dB and $\eta_2 = 5$dB.

In contrast, when χ_1 and χ_2 are larger than η_1 and η_2 respectively, the lower bound increases as ρ_3 increases and saturates after a certain threshold of ρ_3. This threshold becomes larger as the quality of the SR links improve as compared to the SD links, i.e., as χ_1 and χ_2 get larger compared to η_1 and η_2. Indeed, the fact that we can achieve higher rates when the SR channel is better than the SD channel is intuitively pleasing as the power allocation becomes more effective when we have a better SR channel. It is noticeable that the upper and lower bounds approach each other as the SR link quality improves as compared to that of SD.

Figure 2.3 shows the upper and lower bounds for $(3, 2)$-MBRC with joint optimum power and bandwidth allocation. We observe that the lower bound does not saturate when the SR links are better than the SD links. This additional improvement is thanks

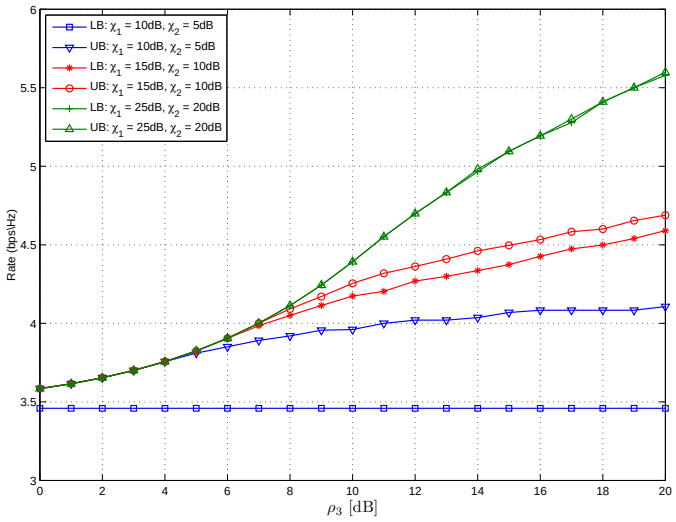

Fig. 2.3. Upper and lower bounds of $(3, 2)$-MBRC with joint power and bandwidth optimization: SNRs at SD, $\eta_1 = 10$dB and $\eta_2 = 5$dB.

to the dynamic bandwidth allocation. By comparing Figure 2.2 and Figure 2.3, we observe that the achievable rate of MBRC with joint optimum power and bandwidth is always larger than that of power optimization only, sometimes by a significant margin. This points to the advantage of joint power and bandwidth optimization, promoting the idea of different wireless technologies lending each other frequency resources to improve capacity.

2.4.2 Guidelines for Hybrid Network Design

When a new wireless link becomes available at the source in addition to the existing single band relay network, a hybrid wireless network can be formed. In this case, a meaningful question is how to allocate resources between links in order to maximize the data rate. It is evident that the resource allocation strategy is a function of the channel

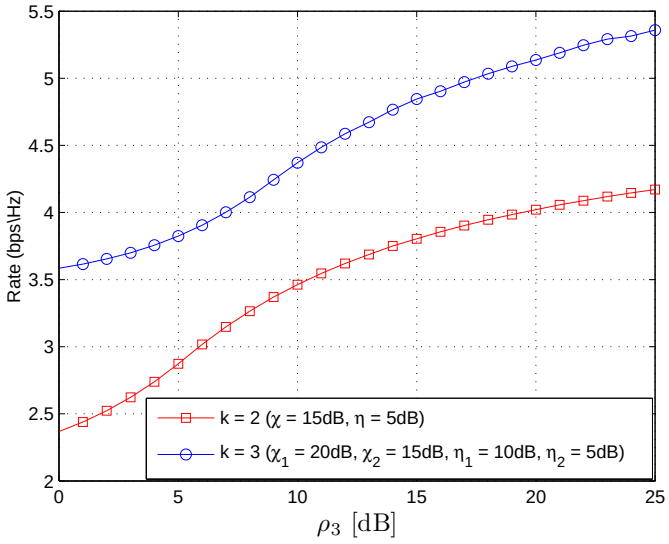

Fig. 2.4. Comparison of achievable rates: the new SR ink is better than the current SR link, and the new SD link is better than the current SD link.

quality of the available links (SD/SR/RD). To answer this question, we compare the achievable rates with optimum resource allocation for $k = 2$ and 3 and observe the effect of adding a new link on the maximum achievable rate.

Figure 2.4 shows the achievable rates when the new SR ink is better than the current SR link, and the new SD link is better than the current SD link. Comparing $k = 3$ and $k = 2$, we observe that the achievable rate of $k = 3$ is better than that of $k = 2$. This is because the new link is better than the current link, and all resources are allocated to the new link. If the new links were worse, the maximum achievable rates would stay the same since all resources would be allocated to the current link.

Figure 2.5 shows the achievable rates when the new SR link is better than the current SR link, and the new SD link is worse than the current SD link. We observe that

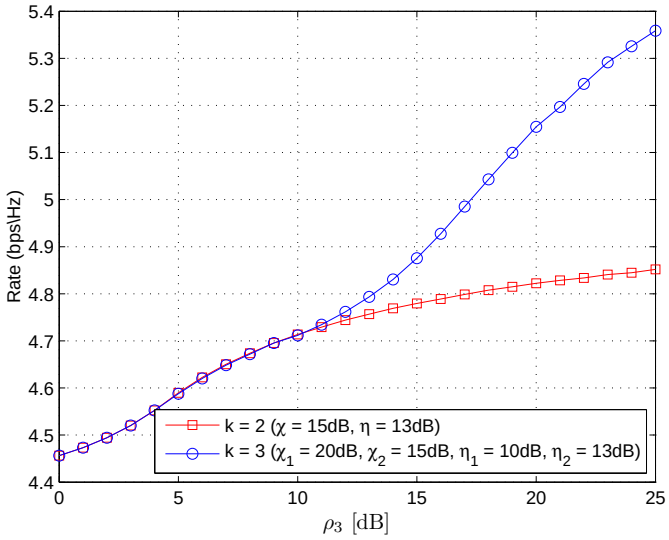

Fig. 2.5. Comparison of achievable rates: the new SR link is better than the current SR link, and the new SD link is worse than the current SD link.

the achievable rates for $k = 2$ and 3 are almost same for low RD SNR. This is because when the RD link is poor, the relay becomes less useful, and most of bandwidth and power are allocated into channel with the best direct link. As the RD SNR increases, we observe that the achievable rate for $k = 3$ is larger than that of $k = 2$. This is because it is optimum resource allocation that we allocate more bandwidth and power to the new link with the best SR link. The observation is justified by examining bandwidth allocation (the power allocation follows a similar pattern) for $k = 3$ shown in Figure 2.6. We see that more bandwidth is allocated to the current link (ϕ_2 for $k = 3$) for low received RD SNR. More bandwidth is allocated to the new link (ϕ_1 for $k = 3$) when the RD link becomes better. We also observe that case 1 and case 3 of our proposed optimum resource allocation occur depending on the RD SNR: with both SR SNRs better

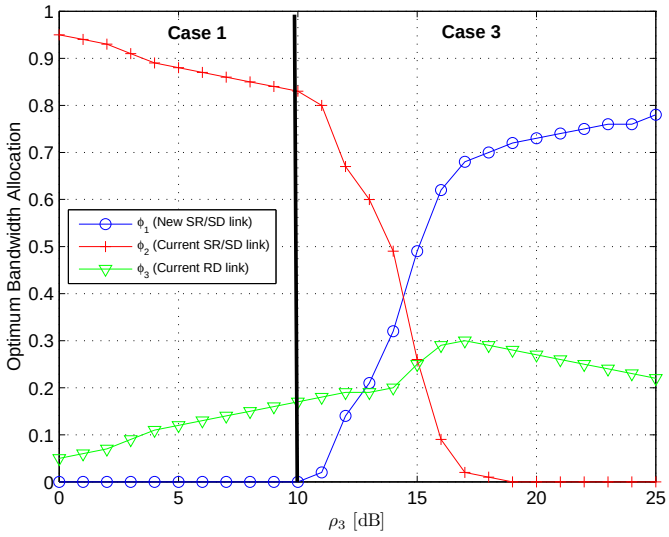

Fig. 2.6. Optimum bandwidth allocation: the new SR link is better than the current SR link, and the new SD link is worse than the current SD link.

than both SD SNRs, case 1 occurs at low RD SNR (from 0dB to 10dB), otherwise, the optimum resource allocation corresponds to case 3. We note that the optimum resource allocation scheme would be reversed if the new SR link were worse than the current SR link, and the new SD link were better than the current SD link.

We note that the given received SNRs in the numerical results correspond to scheme I (i.e., $\eta_i \leq \chi_i, i = 1, 2$). Similarly, we can examine the effect of adding a new link under different received SNR relationship between η_i and χ_i which corresponds to scheme II or scheme III, and we could readily apply the optimum resource allocation solution found in section 2.3.1.

2.5 Chapter Summary

In this chapter, we have investigated the optimum resource allocation for a hybrid three-node relay network where the source, with the help of a relay node, communicates to the destination via multiple orthogonal channels (MBRC). In particular, we have studied joint optimum power and bandwidth allocation strategies that maximize the bounds on the capacity, which results in a max-min optimization problem. We have solved this problem using a supporting plane technique [39]. In particular, we have provided sufficient conditions for when this max-min optimization problem can be solved using this technique. It is worthwhile to mention that these sufficient conditions are general enough so that other utility functions that rely on SNR can be considered as well as the information theoretic rates considered in this chapter.

For $(3, 2)$-MBRC, we have found the joint power and bandwidth allocation. We have observed that the upper and lower bounds approach each other as the source to relay channel condition improves as compared to the source to destination channel condition, and joint power and bandwidth optimization always yields better performance than power optimization only.

Our numerical results have also investigated the scenario where a new link at the source becomes available for an existing frequency division relay network, and the power and bandwidth resources are to be reallocated. We have observed that the source node is encouraged to communicate over the best link by dedicating all resources when the new SR link and SD link are better (or worse) than that of the current SD link and SR

link. Otherwise, it is beneficial to share resources between the current link and the new link to achieve the higher rate.

The simple MBRC investigated in this chapter can be considered as a building block for more complex hybrid wireless networks. From the system design point of view, we conclude that, for this two-hop, simple network, higher achievable rates can be obtained by optimally allocating resources between multiple standards. It would be of interest to gain an understanding of the set of conditions under which using multiple communication links (standards) and optimum sharing of resources would be beneficial for multi-hop hybrid wireless networks.

2.6 Appendices

2.6.1 Proof of maximizing input distribution

Proof. $C_{\mathrm{DF}}(\cdot)$ in (2.9) is given by

$$C_{\mathrm{DF}}(\cdot) = \sup_{P(\cdot)} \min\{I(X_1, \cdots, X_m, \tilde{X}_{m+1}, \tilde{X}_{m+2}, \cdots, \tilde{X}_k; Y_1, \cdots, Y_k), \\ I(X_1, \cdots, X_m; \tilde{Y}_1, \cdots, \tilde{Y}_m | \tilde{X}_{m+1}, \cdots, \tilde{X}_k)\} \qquad (2.41)$$

where $P(\cdot) = P(x_1, x_2, \cdots, x_m, \tilde{x}_{m+1}, \cdots, \tilde{x}_k)$. We need to provide the input distribution that maximizes both terms in (2.41). For the first term of (2.41), we have

$$I(X_1, \cdots, X_m, \tilde{X}_{m+1}, \tilde{X}_{m+2}, \cdots, \tilde{X}_k; Y_1, \cdots, Y_k) \tag{2.42}$$

$$= H(Y_1, \cdots, Y_k) - H(Y_1, \cdots, Y_k | X_1, \cdots, X_m, \tilde{X}_{m+1}, \cdots, \tilde{X}_k) \tag{2.43}$$

$$\leq \sum_{i=1}^{k} H(Y_i) - \left(\sum_{i=1}^{m} H(Y_i|X_i) + \sum_{i=m+1}^{k} H(Y_i|\tilde{X}_i) \right) = \sum_{i=1}^{m} I(X_i; Y_i) + \sum_{i=m+1}^{k} I(\tilde{X}_i; Y_i) \tag{2.44}$$

The inequality follows directly from the fact that independence bounds entropy and that we have the channel transition probability mass function given in (2.4). Obviously, (2.43) becomes equality when we have $P(\cdot) = P(x_1)P(x_2)\cdots P(\tilde{x}_k)$. For the second term of (2.41), we have

$$I(X_1, \cdots, X_m; \tilde{Y}_1, \cdots, \tilde{Y}_m | \tilde{X}_{m+1}, \cdots, \tilde{X}_k) \tag{2.45}$$

$$= H(\tilde{Y}_1, \cdots, \tilde{Y}_m | \tilde{X}_{m+1}, \cdots, \tilde{X}_k) - H(\tilde{Y}_1, \cdots, \tilde{Y}_m | X_1, \cdots, X_m, \tilde{X}_{m+1}, \cdots, \tilde{X}_k) \tag{2.46}$$

$$\leq \sum_{i=1}^{m} H(\tilde{Y}_i | \tilde{X}_{m+1}, \tilde{X}_{m+2}, \cdots, \tilde{X}_k) - \sum_{i=1}^{m} H(\tilde{Y}_i | X_i) = \sum_{i=1}^{m} I(X_i; \tilde{Y}_i) \tag{2.47}$$

and (2.46) becomes equality when $P(\cdot) = P(x_1)P(x_2)\cdots P(\tilde{x}_k)$. The same argument holds for C_{up}. □

2.6.2 Proof of Theorem 2.2

Proof. Theorem 2.2 can be readily obtained from Theorem 2.1 by directly applying the following mutual information.

$$I(X_i;Y_i) = H(Y_i) - H(Y_i \mid X_i) = H(Y_i) - H(Z_i) \tag{2.48}$$

$$\leq \frac{1}{2}\log\left(2\pi e\left(\alpha P_s + \frac{N_i}{2}\right)\right) - \frac{1}{2}\log\left(2\pi e\frac{N_i}{2}\right) \tag{2.49}$$

$$= W\phi_i \log\left(1 + \frac{\alpha_i P_s}{N_i W\phi_i}\right) = W\phi_i \log\left(1 + \alpha_i \frac{\eta_i}{\phi_i}\right) \tag{2.50}$$

$$I(X_i;\tilde{Y}_i,Y_i) = H(\tilde{Y}_i,Y_i) - H(\tilde{Y}_i,Y_i|X_i) = H(\tilde{Y}_i,Y_i) - H(\tilde{Z}_i,Z_i) \tag{2.51}$$

$$\leq \frac{1}{2}\log\left(2\pi e\left(\frac{\alpha_i P_s N_i}{2} + \frac{\alpha_i P_s \tilde{N}_i}{2} + \frac{\tilde{N}_i N_i}{4}\right)\right) - \frac{1}{2}\log\left(2\pi e\frac{\tilde{N}_i}{2}\frac{N_i}{2}\right) \tag{2.52}$$

$$= W\phi_i \log\left(1 + \frac{\alpha_i P_s}{N_i W\phi_i} + \frac{\alpha_i P_s}{\tilde{N}_i W\phi_i}\right) = W\phi_i \log\left(1 + \alpha_i \frac{\eta_i + \chi_i}{\phi_i}\right) \tag{2.53}$$

The remaining terms are obtained following the same steps. Letting W be 1 without loss of generality, we get (2.16) and (2.17). □

2.6.3 Proof of Proposition 2.1

Proof. Suppose that both $G_1(\underline{R})$ and $G_2(\underline{R})$ are non-negative and concave over convex set $\mathbf{C}_0$. Then, we claim that the optimization problem (2.18) can be relaxed as follows.

$$\max_{(c_1,c_2)\in\mathbf{B}} \min\{c_1, c_2\} \tag{2.54}$$

$$\text{where } \mathbf{B} = \text{dominance closure}\{\text{convex closure}\{\mathbf{B}_1\}\} \tag{2.55}$$

$$\mathbf{B}_1 = \{(G_1(\underline{R}), G_2(\underline{R})) : \underline{R} \in \mathbf{C}_0\} \tag{2.56}$$

$$\mathbf{C}_0 = \{\text{all feasible values of } \underline{R}\} \tag{2.57}$$

$$\text{dominance closure}\,\{\mathbf{A}\} := \text{closure}\left\{ \bigcup_{(x,y)\in\mathbf{A}} \{\text{rectangular}(x,y)\} \right\} \tag{2.58}$$

$$\text{where rectangular}(x,y) = \{(a,b) : 0 \le a \le x, 0 \le b \le y\} \tag{2.59}$$

To see that, we devise the following notion of dominance: pair (a, b) is said to be dominated by (c, d) if $a \le c$ and $b \le d$. We say a set $\mathbf{A}_1$ is dominated by the other set $\mathbf{A}_2$, or $\mathbf{A}_1 \triangleleft \mathbf{A}_2$ if every point in $\mathbf{A}_1$ is dominated by some point in $\mathbf{A}_2$. Since $G_1(\underline{R})$ and $G_2(\underline{R})$ are concave over $\mathbf{C}_0$,we realize $\mathbf{B}_1$ dominates its convex closure $\bar{\mathbf{B}}_1$. Furthermore, from the definition of dominance closure in (2.58), it is easy to see $\mathbf{B} \triangleleft \bar{\mathbf{B}}_1$. Since $\mathbf{B} \triangleleft \bar{\mathbf{B}}_1$ and $\bar{\mathbf{B}}_1 \triangleleft \mathbf{B}_1$, we have $\mathbf{B} \triangleleft \mathbf{B}_1$. We note that adding dominated points to $\mathbf{B}_1$ does not change the value of optimization problem (2.18), which allows us to consider problem (2.54) instead.

Set $\mathbf{B}$ has the following properties: (1) It is a closed convex set. To see that, consider two points in $\mathbf{B}$: $(a_1, b_1) \in \text{rectangular}(x_1, y_1)$ and $(a_2, b_2) \in \text{rectangular}(x_2, y_2)$.

Then we must have $(\lambda a_1+(1-\lambda)a_2, \lambda b_1+(1-\lambda)b_2) \in \text{rectangular}(\lambda x_1+(1-\lambda)x_2, \lambda y_1+(1-\lambda)y_2)$. (2) Consider any supporting plane of this set, which is a line in $\Re^2$ in this case. The slope of this line can not be both positive and finite. Otherwise, suppose the supporting plane passes through point (x, y) in $\mathbf{B}$, then rectangular(x, y) defined by (2.59), will not be in $\mathbf{B}$.

We then observe that (2.54) must be solved when $c_1 = c_2 \neq 0$ and (c_1, c_2) is at the boundary of $\mathbf{B}$. The maximum of (2.54) should be attained at the boundary of $\mathbf{B}$ since every interior point of $\mathbf{B}$ must be dominated by some point at its boundary. Also, there must be such a point on the boundary with $c_1 = c_2$. We then show that the point with $c_1 = c_2 \neq 0$ must be a local maximal point. This is because any improvement over this point would require increasing $c1, c2$ simultaneously. Suppose such improved point exists. Then it will be strictly separated from set $\mathbf{B}$ by the support plane passing through (c_1, c_2), since no supporting plane has finite positive slope. Since $\mathbf{B}$ is a closed convex set and $\min\{x, y\}$ is a concave function over $\Re^2$, any local maximum must be globally optimal [3, Theorem 3.4.2, pp. 125-126]. This completes our claim that optimality must be attained at the diagonal line. We observe that this point may not be in $\mathbf{B}_1$. Therefore, it may not be parameterizable by $\underline{R}$. This necessitates consideration of the three cases as we will show later.

Since optimality must be attained at the boundary of the convex set $\mathbf{B}$, we observe that (2.54) is equivalent to (2.60) for a certain β.

$$\max_{(c_1,c_2)\in\mathbf{B}} \beta c_1 + (1-\beta)c_2,\ 0 \leq \beta \leq 1 \tag{2.60}$$

(2.60) can be solved by examining three cases: $\beta = 0$, $\beta = 1$, $0 < \beta < 1$.

For $\beta = 1$ and $\beta = 0$, we have

$$\max_{\underline{R} \in \mathbf{C}_0} G_1(\underline{R}),\ \beta = 1; \quad \max_{\underline{R} \in \mathbf{C}_0} G_2(\underline{R}),\ \beta = 0 \tag{2.61}$$

For $0 < \beta < 1$, we prove below that problem (2.60) is equivalent to problem (2.62). Let the optimal solution of problem (2.60) be (c_1^*, c_2^*). Since $0 < \beta < 1$, (c_1^*, c_2^*) can not be dominated by any point in $\mathbf{B}$ other than itself. (If such a point exists, it would be separated from $\mathbf{B}$ by the supporting plane passing through (c_1^*, c_2^*).) Since $\mathbf{B} \triangleleft \mathbf{B}_1$ and $\mathbf{B} \supset \mathbf{B}_1$, we must have $(c_1^*, c_2^*) \in \mathbf{B}_1$. This means we can solve problem (2.62) instead.

$$\max_{(c_1, c_2) \in \mathbf{B}_1} \beta c_1 + (1 - \beta) c_2,\ 0 < \beta < 1 \tag{2.62}$$

Since all points in $\mathbf{B}_1$ can be parameterized by $\underline{R}$, problem (2.62) is equivalent to (2.63). β is adjusted until the solution to (2.63) yields $G_1(\underline{R}) = G_2(\underline{R})$.

$$\max_{\underline{R} \in \mathbf{C}_0} \beta G_1(\underline{R}) + (1 - \beta) G_2(\underline{R}),\ 0 < \beta < 1 \tag{2.63}$$

In summary, we proved that there must exist a $\beta \in [0, 1]$ such that (2.18) is equivalent to (2.60) if $G_1(\underline{R})$ and $G_2(\underline{R})$ are non-negative and concave over convex set $\mathbf{C}_0$. Depending on the value of β, we find that there are three cases for the max-min optimization (2.60) as given in Proposition 2.2. □

2.6.4 Optimum Resource Allocation

Proof. We provide the proof for optimum resource allocation for $(3,2)$-MBRC. To do so, we utilize the following theorem which we restate here with our notation for convenience:

Theorem 2.3 ([4], Proposition 3.9, pp. 219-221)**.** *Suppose that* $F : \mathfrak{R}^{\mathfrak{n}} \mapsto \mathfrak{R}$ *is continuously differentiable and concave on the set* X*, a Cartesian product of sets* X_i*, where each* X_i *is a closed convex subset of* $\mathfrak{R}^{\mathfrak{n_i}}$ $(n_1 + \cdots + n_m = n)$*. Furthermore, suppose that for* $\mathbf{x} = \{\mathbf{x_1}, ..., \mathbf{x_m}\}$*,* $\mathbf{x_i} \in \mathfrak{R}^{\mathfrak{n_i}}$*,* $F(\mathbf{x})$ *is a strictly concave function of each* $\mathbf{x_i}$*, when the other components of* $\mathbf{x}$ *are held constant. Let* $\{\mathbf{x}(t)\}$ *be the sequence generated by the iterative algorithm obtained by optimizing* $F(\mathbf{x})$ *over one vector variable at a time. Then, every limit point of* $\{\mathbf{x}(t)\}$ *maximizes* $F(\mathbf{x})$ *over* X*.*

For a fixed $0 \leq \beta^* \leq 1$, the objective function of our max-min problem corresponds to

$$F(\mathbf{x}) = \beta^* C_1(\mathbf{x}) + (1 - \beta^*) C_2(\mathbf{x}) \tag{2.64}$$

where $\mathbf{x}$ corresponds to $\underline{R} = (\alpha_1, \alpha_2, \phi_1, \phi_2, \phi_3)$.

Based on Proposition 2.3, we know that the objective function (2.64) of our max-min optimization problem given in (2.31) is concave over the constraint set X, which is a Cartesian product of the following two sets, X_1 and X_2 which are closed convex subset of $\mathfrak{R}^{\mathfrak{n_i}} (n_1 = 2, n_2 = 3)$.

$$X_1 = \left\{ \boldsymbol{\alpha} = (\alpha_1, \alpha_2) : 0 \leq \alpha_1, \alpha_2 \leq 1, \quad \sum_{i=1}^{2} \alpha_i = 1 \right\} \tag{2.65}$$

$$X_2 = \left\{ \boldsymbol{\phi} = (\phi_1, \phi_2, \phi_3) : 0 \leq \phi_1, \phi_2, \phi_3 \leq 1, \quad \sum_{i=1}^{3} \phi_i = 1 \right\} \tag{2.66}$$

Also, for the interior points of the feasible region of $\underline{R}$, we note that (2.64) is strictly concave over $\boldsymbol{\alpha}(\boldsymbol{\phi})$ when $\boldsymbol{\phi}(\boldsymbol{\alpha})$ are fixed, see Remark 2.2. We note that the objective function (2.64) is not differentiable at the boundary of the feasible region, i.e., for $\phi_i = 0$, $i = 1, 2, 3$. Therefore, we can not directly apply Theorem 2.3. We define a modified feasible region as follows.

$$X_{1_{\text{new}}} = \left\{ \boldsymbol{\alpha} = (\alpha_1, \alpha_2) : \varepsilon \leq \alpha_1, \alpha_2 \leq 1, \quad \sum_{i=1}^{2} \alpha_i = 1 \right\} \tag{2.67}$$

$$X_{2_{\text{new}}} = \left\{ \boldsymbol{\phi} = (\phi_1, \phi_2, \phi_3) : \varepsilon \leq \phi_1, \phi_2, \phi_3 \leq 1, \quad \sum_{i=1}^{3} \phi_i = 1 \right\} \tag{2.68}$$

with a small $\varepsilon > 0$. Since (2.64) is continuously differentiable over the new feasible region given by (2.67) and (2.68), we can now apply Theorem 2.3. Thus, we can devise an iterative algorithm to maximize the function, by maximizing over $\boldsymbol{\alpha}$ for fixed $\boldsymbol{\phi}$ ($\boldsymbol{\phi}$ for fixed $\boldsymbol{\alpha}$) and then maximizing $\boldsymbol{\phi}$ for fixed $\boldsymbol{\alpha}$ ($\boldsymbol{\alpha}$ for fixed $\boldsymbol{\phi}$). The iterative method, by Theorem 2.3, will converge to the maximizer of $F(\mathbf{x})$ over (2.67) and (2.68), which is the global optimum. If the iterative algorithm converges to a point that is at the boundary of the new feasible region given by (2.67) and (2.68), we need to reduce ε further and repeat the iteration using the KKT points from the previous iteration as the initial point. By repeating this procedure, the iterative algorithm converges to the global optimum solution.

For case 1 ($\beta^* = 1$ in (2.64)) and case 2 ($\beta^* = 0$ in (2.64)), we provide the closed form solution below. For case 3 ($0 \leq \beta^* \leq 1$ in (2.64)), we provide iterative algorithm in Appendix 2.6.5.

Case 1: $\underline{R}^*$ maximizes $C_1(\underline{R})$. Using $\alpha_1 = 1 - \alpha_2 = \alpha$ and $\phi_2 = 1 - \phi_1 - \phi_3$, $C_1(\underline{R})$ in (2.31) can be rewritten as

$$C_1(\alpha, \phi_1, \phi_3) = \phi_1 \log\left(1 + \frac{\alpha\eta_1}{\phi_1}\right) + (1 - \phi_1 - \phi_3)\log\left(1 + \frac{(1-\alpha)\eta_2}{(1-\phi_1-\phi_3)}\right) + \phi_3 \log\left(1 + \frac{\rho_3}{\phi_3}\right) \quad (2.69)$$

Differentiating (2.69) with respect to ϕ_1, we obtain $\phi_1 = \frac{\alpha\eta_1(1-\phi_3)}{\alpha\eta_1+(1-\alpha)\eta_2}$. Observe that $0 \leq \phi_1 \leq 1$ for $0 \leq \alpha \leq 1$ and $0 \leq \phi_3 \leq 1$. Substituting this expression for ϕ_1 into (2.69), we obtain

$$C_1(\alpha, \phi_3) = (1 - \phi_3)\log\left(1 + \frac{\alpha\eta_1 + (1-\alpha)\eta_2}{(1-\phi_3)}\right) + \phi_3 \log\left(1 + \frac{\rho_3}{\phi_3}\right) \quad (2.70)$$

For fixed ϕ_3, we can maximize (2.70) in terms of α by

$$\alpha^* = \begin{cases} 1 & \text{if } \eta_1 > \eta_2, \\ 0 & \text{if } \eta_1 < \eta_2 \end{cases} \quad (2.71)$$

Substituting (2.71) into (2.70), we have

$$C_1(\phi_3) = (1 - \phi_3)\log\left(1 + \frac{\max(\eta_1, \eta_2)}{(1-\phi_3)}\right) + \phi_3 \log\left(1 + \frac{\rho_3}{\phi_3}\right) \quad (2.72)$$

Maximizing (2.72) with respect to ϕ_3 leads to $\rho_3/(\rho_3 + \max(\eta_1, \eta_2))$. The optimum power allocation parameter in (2.71) indicates that one of channels whose received SNR at the destination is smaller is not used. Thus, for the case where $\eta_1 > \eta_2$, $\phi_2^* = 0$. On the other hand, for the case where $\eta_1 < \eta_2$, $\phi_1^* = 0$. Thus, using $\sum_{i=1}^{3} \phi_i = 1$, the optimum resource allocation parameter for case 1 is given by (2.36). By Remark 2.1, this is the global optimum solution. The condition of the received SNRs given by (2.37) and (2.38) for case 1 to occur can be readily found by substituting (2.36) into (2.35).

Case 2: $\underline{R}^*$ maximizes $C_2(\underline{R})$. Using $\phi_2 = 1 - \phi_1 - \phi_3$ and $\alpha_1 = 1 - \alpha_2 = \alpha$, $C_2(\underline{R})$ in (2.31) can be rewritten as

$$C_2(\alpha, \phi_1, \phi_3) = \phi_1 \log\left(1 + \alpha\frac{\kappa}{\phi_1}\right) + (1 - \phi_1 - \phi_3)\log\left(1 + (1-\alpha)\frac{\nu}{(1 - \phi_1 - \phi_3)}\right) \tag{2.73}$$

Differentiating (2.73) with respect to ϕ_1, we obtain $\phi_1 = \frac{\alpha\kappa(1-\phi_3)}{\alpha\kappa+(1-\alpha)\nu}$. Observe that $0 \leq \phi_1 \leq 1$ for $0 \leq \alpha \leq 1$ and $0 \leq \phi_3 \leq 1$. Substituting the expression for ϕ_1 into (2.73), we obtain

$$C_2(\alpha, \phi_3) = (1 - \phi_3)\log\left(1 + \frac{\alpha\kappa + (1-\alpha)\nu}{(1 - \phi_3)}\right) \tag{2.74}$$

For fixed ϕ_3, we can maximize (2.74) in terms of α by

$$\alpha^* = \begin{cases} 1 & \text{if } \kappa > \nu, \\ 0 & \text{if } \kappa < \nu. \end{cases} \tag{2.75}$$

For $\kappa > \nu$, ϕ_3^* should maximize the following:

$$(1-\phi_3)\log\left(1+\frac{\kappa}{(1-\phi_3)}\right) \tag{2.76}$$

It can be readily shown that $\phi_3^* = 0$ is the optimum value. Also, since $\alpha^* = 1$, ϕ_2^* should be zero. Thus, for $\kappa > \nu$, $\underline{R}^* = (1,0,1,0,0)$. Substituting $\underline{R}^* = (1,0,1,0,0)$ into (2.39), $\eta_1 > \kappa$ should be met for case 2 to occur. Similarly, it can be readily shown that for $\kappa < \nu$, $\underline{R}^* = (0,1,0,1,0)$ and $\eta_2 > \nu$ should be met for case 2 to occur. Thus, we obtain (2.40). By Remark 2.1, this is the global optimum solution. □

2.6.5 Iterative Algorithm for Case 3

Proof. For case 3, $\underline{R}^*$ maximizes the following.

$$C(\beta^*, \underline{R}) = \beta^* C_1(\underline{R}) + (1-\beta^*)C_2(\underline{R}),\ 0 \le \beta^* \le 1 \tag{2.77}$$

Since the closed form solution does not exist for case 3, we rely on the iterative algorithm given in Theorem 2.3. As we noted in Appendix 2.6.4, (2.77) is not differentiable at the boundary of the feasible region. Thus, we start with the new feasible region given in (2.67) and (2.68). Then, the Lagrangian is

$$\mathcal{L} = \beta^*\left(\sum_{i=1}^{2}\phi_i\log\left(1+\frac{\alpha_i\eta_i}{\phi_i}\right)+\phi_3\log\left(1+\frac{\rho_3}{\phi_3}\right)\right)+(1-\beta^*)\left(\sum_{i=1}^{2}\phi_i\log\left(1+\frac{\alpha_i\tau_i}{\phi_i}\right)\right)-$$
$$\lambda\left(\sum_{i=1}^{3}\phi_i-1\right)-\mu\left(\sum_{i=1}^{2}\alpha_i-1\right)+\sum_{i=1}^{3}\omega_i\phi_i+\sum_{i=1}^{2}\psi_i\alpha_i \tag{2.78}$$

where $\tau_1 = \kappa$, $\tau_2 = \nu$, and λ and μ are Lagrange multipliers corresponding to sum constraints for bandwidth and power allocation, respectively. ω_i and ψ_i are inequality constraints for bandwidth and power allocation, respectively, i.e., $\alpha_i \geq \varepsilon$, $i = 1, 2$ and $\phi_i \geq \varepsilon$, $i = 1, 2, 3$. For a fixed β^*, we start with values of ϕ_1, ϕ_2, and ϕ_3 such that $\sum_{i=1}^{3} \phi_i = 1$ and find the optimum $\boldsymbol{\alpha}$ such that $\alpha_1 + \alpha_2 = 1$. In iteration n, we update $\boldsymbol{\alpha}(n)$ by optimizing the objective function over $\boldsymbol{\alpha}$ while keeping the total power constraints satisfied, and fixing $\boldsymbol{\phi} = \boldsymbol{\phi}(n-1)$. In iteration $n+1$, $\boldsymbol{\phi}(n+1)$ is found by optimizing the objective function with respect to $\boldsymbol{\phi}$ while keeping the bandwidth constraints satisfied, and fixing $\boldsymbol{\alpha} = \boldsymbol{\alpha}(n)$. By Remark 2.1, Remark 2.2, and Theorem 2.3, this algorithm converges to the global optimum solution. Note that the optimum solution, $(\boldsymbol{\alpha^*}, \boldsymbol{\phi^*})$, satisfies (see Proposition 2.2):

$$\sum_{i=1}^{2} \phi_i^* \log\left(1 + \alpha_i^* \frac{\eta_i}{\phi_i^*}\right) + \phi_3^* \log\left(1 + \frac{\rho_3}{\phi_3^*}\right) = \phi_1^* \log\left(1 + \alpha_1^* \frac{\kappa}{\phi_1^*}\right) + \phi_2^* \log\left(1 + \alpha_2^* \frac{\nu}{\phi_2^*}\right) \tag{2.79}$$

□

Chapter 3

Iterative Power Allocation Algorithms for Amplify/Compress-and-Forward Multi-Band Relay Channel

3.1 Introduction

Relay networks have attracted considerable attention for their potential of improving the performance of wireless systems [20,30,39]. This performance gain is offered by exploiting the inherent broadcasting nature of the wireless channel and the spatial diversity in a distributed fashion. It has been shown that a even more significant performance improvement can be achieved by optimum resource allocation, i.e., transmit power, bandwidth, or transmission time slot duration in these networks [20,39,43,46,59]. The optimum relay transmit power allocation is investigated in [59] for various relaying transmission schemes for a relay assisted F/TDMA network with multiple source-destination pairs where all channels of all sources nodes and relay nodes are orthogonal. The bandwidth and power allocation for the relay networks where a single source and destination pair with multiple relay nodes is investigated in [43]. In a similar setting, power allocation with partial channel side information is considered in [8, 9, 42].

In chapter 2, we have considered the multi-band relay channel (MBRC), which models a three-node hybrid wireless network where multiple frequency bands available from the source and the relay are mutually orthogonal. In particular, we have studied

jointly optimum power and bandwidth allocation strategies that maximize the bounds on the capacity of (k, m)-MBRC employing decode-and-forward (DF), where there are m channels available for the source node and $k - m$ for the relay node. We have focused on maximization of the capacity bounds of the simple MBRC where two source bands exist from the source and one from the relay-to-destination. We have found that joint power and bandwidth optimization yields better performance than power optimization only.

In this chapter, we investigate the *jointly* optimum power allocation of the source and the relay node for MBRC when the sharing of the bandwidth is not possible. We focus on two relay transmission schemes that do not decode the information at the relay: amplify-and-forward (AF) and compress-and-forward (CF). Our motivation for focusing on these transmission schemes is their advantage over DF. AF is known to provide the same multiplexing gain and better diversity order than DF [30]. CF can also outperform DF [20].

We investigate the transmit source and relay power allocation problems that maximize the instantaneous achievable sum rate under individual power constraints. The solution for each scheme is reached by essentially the same iterative algorithm with the associated variables varying depending on the scheme. The proposed algorithms are convergent, and we observe numerically, the convergence to the optimum point.

We observe that CF always performs better than AF. We also note the difference in the power allocation strategy between CF and AF: in CF, the relay and source power allocation are independent, while in AF, they affect and compensate each other to yield the maximum rate.

3.2 System Model

We consider the three-node relay network where multiple frequency bands available from the source and the relay are mutually orthogonal, i.e., the multi-band relay channel (MBRC). In particular, the situation where there are m channels available for the source node and m for the relay node, is termed the $(2m, m)$-MBRC, which is the case where $k = 2m$ in Figure 2.1. We assume that the source transmits information over several frequency channels, which is received by the destination and the relay. The relay forwards the received signal from the source after appropriate processing to the destination over the orthogonal frequency channels. The signal received by the relay and destination in the ith orthogonal channel of the source node is given by

$$Y_i = h_{sd_i} X_i + Z_i, \quad i = 1, ..., m \tag{3.1}$$

$$\tilde{Y}_i = h_{sr_i} X_i + \tilde{Z}_i, \quad i = 1, ..., m \tag{3.2}$$

where X_i is the transmitted signal by the source node in channel i. Z_i and $\tilde{Z}_i$ are the independent additive white Gaussian noise (AWGN) with unit variance at the destination and the relay, respectively. We let h_{sd_i} and h_{sr_i} denote the channel gains from the source node to the destination node and the relay node in channel i.

Similarly, the signal received by the destination node from the relay is given by

$$Y_i = h_{rd_i} \tilde{X}_i + Z_i, \quad i = m + 1, ..., 2m \tag{3.3}$$

where $\tilde{X}_i$ is the symbol transmitted by the relay node in channel i. Z_i, $i = m+1, ..., 2m$ is the independent AWGN with unit variance at the destination. We let h_{rd_i} denote the channel gain from the relay node to the destination node in channel i. We consider the joint source and relay transmit power optimization under the following individual power constraints.

$$E\left[X_i^2\right] \leq \alpha_i P_s \quad i = 1, ..., m \tag{3.4}$$

$$E\left[\tilde{X}_i^2\right] \leq \zeta_i P_r \quad i = m+1, ..., 2m \tag{3.5}$$

where P_s and P_r are the total available power at the source and relay node. α_i and ζ_i are the non-negative power allocation parameters for each orthogonal band at the source and relay node, and $\sum_{i=1}^{m} \alpha_i = \sum_{i=m+1}^{2m} \zeta_i = 1$.

We assume that the system has total bandwidth W, which is divided equally among $2m$ bands. Then, we define the received SNRs at the relay and destination over channel $i = 1, ..., 2m$ as

$$\chi_i \triangleq P_s |h_{sr_i}|^2, \quad i = 1, ..., m \tag{3.6}$$

$$\eta_i \triangleq P_s |h_{sd_i}|^2, \quad i = 1, ..., m \tag{3.7}$$

$$\rho_i \triangleq P_r |h_{rd_i}|^2, \quad i = m+1, ..., 2m \tag{3.8}$$

where we assume that the bandwidth is equally divided and the all noise variances are set to one.

We consider two relay transmission schemes that do not decode the information received at the relay. In particular, we consider:

- Amplify-and-Forward (AF): The relay node forwards the scaled version of the noisy copy of the source signal it received to the destination node [30].

- Compress-and-Forward (CF): The relay node compresses the received signal using Wyner-Ziv lossy source coding [69] and forwards to the destination [20, 26].[1]

3.3 Iterative Power Allocation Algorithm

In this chapter, we investigate the optimum source and relay transmit power allocation that maximizes the instantaneous achievable sum rate for amplify-and-forward (AF) and compress-and-forward (CF) under individual power constraints. Then, the resulting optimization problem can be stated as

$$\max_{0\leq\alpha_i,\,\zeta_i\leq 1} \quad I_{AF/CF} \tag{3.9}$$

$$\text{s. t.} \quad \sum_{i=1}^{m}\alpha_i = 1, \qquad \sum_{i=m+1}^{2m}\zeta_i = 1 \tag{3.10}$$

where $I_{AF/CF}$ is the achievable rate of $(2m, m)$-MBRC of AF and CF transmission schemes. We note that the resulting optimization problem does not have closed form solutions. We thus rely on an iterative algorithms to converge to the optimum point of the corresponding problem.

The common theme is that for each of two schemes we have an optimization problem that has identical characteristics, and we propose to use alternating maximization algorithm discussed in chapter 2 that calls for optimizing $\boldsymbol{\alpha} = \{\alpha_1, ..., \alpha_m\}$ in one stage,

[1] Compress-and-Forward is also called Estimate-and-Forward [1, 10].

followed by optimizing $\boldsymbol{\zeta} = \{\zeta_{m+1}, ..., \zeta_{2m}\}$ in the next stage. The Lagrangian for the optimization problem is given by

$$\mathcal{L} = I_{AF/CF} - \mu \left(\sum_{i=1}^{m} \alpha_i - 1 \right) - \nu \left(\sum_{i=m+1}^{2m} \zeta_i - 1 \right) \tag{3.11}$$

where μ and ν are the Lagrangian multipliers for the source and relay transmit power, respectively. In particular, we find that, for AF and CF, the updates that the iterative algorithm employs for each iteration are given by

$$\zeta_i^* = \left[\frac{-r_1}{2r_2} + \frac{1}{2} \sqrt{\left(\frac{r_1}{r_2} \right)^2 - \frac{4r_0}{r_2}} \right]^+ \tag{3.12}$$

$$\alpha_i^* = \left[-\frac{1}{s_2} + \left(R + \sqrt{Q^3 + R^2} \right)^{1/3} + \left(R - \sqrt{Q^3 + R^2} \right)^{1/3} \right]^+ \tag{3.13}$$

where R and Q are given by

$$R = \frac{9s_1 s_2 - 27s_0 - 2s_2^3}{54}, \quad Q = \frac{3s_1 - s_2^2}{9} \tag{3.14}$$

where s_2, s_1, s_0, r_2, r_1, and r_0 are given differently for each relay transmission scheme. The updates given by (3.12) and (3.13) are obtained simply from the first order optimality conditions for each channel. Thus, simply taking the derivative of the objective function for each scheme with respect to α_i and ζ_i and equating it to zero and after algebraic manipulation, we can obtain (3.12) and (3.13) that can be used for each scheme. The parameters s_2, s_1, s_0, r_2, r_1, and r_0, will be later determined for each relay scheme.

The proposed iterative algorithm calls for optimizing one variable at a time while fixing the values of the rest. We start with initial set of α_i and ζ_i and update each one of them by using (3.12) and (3.13) while keeping the transmit power constraints satisfied. The proposed iterative algorithm is given by

Initialization: For initial values of μ and ν, assign values to ζ_i, $\forall i$, such that $\sum_{i=m+1}^{2m} \zeta_i = 1$.

for $i = 1 : m$ **do**

$\alpha_i(n) = \alpha_i^*(\zeta_{m+i}(n-1))$;

$\mu(n)$ such that $\sum_{i=1}^{m} \alpha_i(n) = 1$

end

for $i = m+1 : 2m$ **do**

$\zeta_i(n+1) = \zeta_i^*(\alpha_{i-m}(n))$;

$\nu(n+1)$ such that $\sum_{i=m+1}^{2m} \zeta_i(n+1) = 1$

end

Update $I_{AF/CF}$

Algorithm 1: Iterative Power Allocation Algorithm

3.3.1 Iterative Power Allocation for Amplify-and-Forward

In amplify-and-forward (AF) scheme, the received signal at the relay over channel i is amplified by the gain, g_i. Thus, the transmitted signal at the relay over channel i is given by

$$\tilde{X}_{m+i} = g_i Y_i, \quad i = 1, ..., m \tag{3.15}$$

where $g_i = \sqrt{\frac{\zeta_{m+i}P_r}{|h_{sr_i}|^2\alpha_i P_s+1}}$, $i = 1, ..., m$. The amplifying gain, g_i, is used to maintain power constraints at the relay [30]. The achievable sum rate of $(2m, m)$-MBRC for AF is given by

$$I_{AF} = \frac{1}{2m}\sum_{i=1}^{m}\log\left(1+\alpha_i\eta_i+\frac{\alpha_i\chi_i\zeta_{m+i}\rho_{m+i}}{1+\alpha_i\chi_i+\zeta_{m+i}\rho_{m+i}}\right) \tag{3.16}$$

where the factor $1/2m$ accounts for the fact that information is conveyed over $2m$ frequencies. The logarithm is base 2. In this case, the parameters yielding iterations (3.12) and (3.13) are given by

$$s_2 = \frac{1+\rho_{m+i}\zeta_{m+i}}{\eta_i}+\frac{2+2\rho_{m+i}\zeta_{m+i}}{\chi_i}-\frac{1}{2m\mu} \tag{3.17}$$

$$s_1 = \frac{2+3\rho_{m+i}\zeta_{m+i}+\rho_{m+i}^2\zeta_{m+i}^2}{\eta_i\chi_i}+\frac{(\rho_{m+i}\zeta_{m+i}+1)^2}{\chi_i^2}-\frac{2+2\rho_{m+i}\zeta_{m+i}}{2m\mu\chi_i} \tag{3.18}$$

$$s_0 = \frac{(\zeta_{m+i}\rho_{m+i}+1)^2}{\eta_i\chi_i^2}-\frac{(\zeta_{m+i}\rho_{m+i}+1)^2}{2m\mu\chi_i^2}-\frac{\zeta_{m+i}\rho_{m+i}(1+\zeta_{m+i}\rho_{m+i})}{2m\mu\eta_i\chi_i} \tag{3.19}$$

$$r_2 = 2m\nu\left(\rho_{m+i}^2+(\eta_i+\chi_i)\rho_{m+i}^2\alpha_i\right) \tag{3.20}$$

$$r_1 = 2m\nu\left(2\rho_{m+i}+2\eta_i\chi_i\rho_{m+i}\alpha_i^2+(2\eta_i\rho_{m+i}+3\chi_i\rho_{m+i})\alpha_i+\chi_i^2\rho_{m+i}\alpha_i^2\right) \tag{3.21}$$

$$r_0 = 2m\nu\left(1+(\eta_i+2\chi_i)\alpha_i+(2\eta_i\chi_i+\chi_i^2)\alpha_i^2+\eta_i\chi_i^2\alpha_i^3\right)-\chi_i\rho_{m+i}\alpha_i(1+\alpha_i\chi_i) \tag{3.22}$$

3.3.2 Iterative Power Allocation for Compress-and-Forward

In compress-and-forward (CF), the relay node forwards a compressed version of its channel output to the destination node [10, 20, 26]. This information is used as side information at the destination. This scheme achieves gains comparable to MIMO

transmission [26]. The achievable sum rate of $(2m, m)$-MBRC for CF is given by

$$I_{CF} = \frac{1}{2m}\sum_{i=1}^{m}\log\left(1+\alpha_i\eta_i+\frac{\alpha_i\chi_i}{1+\sigma_{Wi}^2}\right) \tag{3.23}$$

where σ_{Wi}^2 is given by

$$\sigma_{Wi}^2 = \frac{\alpha_i(\eta_i+\chi_i)+1}{\zeta_{m+i}\rho_{m+i}(\alpha_i\eta_i+1)} \tag{3.24}$$

Then, the corresponding variables are given by

$$s_2 = 1+\frac{2(\eta_i+\chi_i)+\rho_{m+i}(2\eta_i+\chi_i)\zeta_{m+i}}{(\eta_i+\chi_i)^2+\eta_i\rho_{m+i}(\eta_i+\chi_i)\zeta_{m+i}}+\frac{\eta_i^2(1+2\chi_i)+\eta_i^2\rho_{m+i}(1+\chi_i)\zeta_{m+i}}{2m\mu((\eta_i+\chi_i)^2+\eta_i\rho_{m+i}(\eta_i+\chi_i)\zeta_{m+i})} \tag{3.25}$$

$$s_1 = \frac{2(\eta_i+\chi_i)+\rho_{m+i}(2\eta_i+\chi_i+1)\zeta_{m+i}}{(\eta_i+\chi_i)^2+\eta_i\rho_{m+i}(\eta_i+\chi_i)\zeta_{m+i}}+\frac{2\eta_i(\eta_i+\chi_i)(1+\zeta_{m+i}\rho_{m+i})}{2m\mu((\eta_i+\chi_i)^2+\eta_i\rho_{m+i}(\eta_i+\chi_i)\zeta_{m+i})} \tag{3.26}$$

$$s_0 = \frac{2m\mu+\eta_i+\rho_{m+i}(\eta_i+\chi_i)\zeta_{m+i}}{2m\mu((\eta_i+\chi_i)^2+\eta_i\rho_{m+i}(\eta_i+\chi_i)\zeta_{m+i})} \tag{3.27}$$

$$r_2 = 2m\nu\left(\rho_{m+i}^2+\eta_i\rho_{m+i}^2\alpha_i\right) \tag{3.28}$$

$$r_1 = 2m\nu\left(2\rho_{m+i}+(2\eta_i+\chi_i)\alpha_i\rho_{m+i}\right) \tag{3.29}$$

$$r_0 = 2m\nu\left(1+(\eta_i+\chi_i)\alpha_i\right)+\alpha_i\chi_i\rho_{m+i} \tag{3.30}$$

3.3.3 Convergence of Iterative Algorithm

The objective function of the each relaying scheme is concave in each variable, but not jointly concave. First we note that each iteration of the algorithms discussed in this section increases the objective function as the function is concave in each variable. Also,

the maximum achievable sum rate as a result of each optimization problem is bounded from above. Thus the proposed iterative algorithms are convergent. In addition, they are guaranteed to converge to the optimum point if it is unique [65].

In general, the nonconvexity of the problem prevents us from making a claim of convergence of the algorithm to the global optimum. As is common with nonconvex problems, we run multiple iteration by choosing multiple initial random transmit power and find the best of the points. Note that we are guaranteed global optimality if the received SNRs satisfy the following condition:

$$\left[\eta_i, \chi_i, \zeta_{m+i} : \frac{\partial^2 I}{\partial \alpha_i^2}\frac{\partial^2 I}{\partial \zeta_{m+i}^2} - \left(\frac{\partial^2 I}{\partial \alpha_i \partial \zeta_{m+i}}\right)^2 \geq 0\right] \tag{3.31}$$

where $i \in [1, m]$ and I is the achievable sum rate of each scheme. This is because, for the received SNRs satisfying (3.31), the objective function becomes concave for the feasible region (3.10) and is strictly concave over $\boldsymbol{\alpha}(\boldsymbol{\zeta})$ when $\boldsymbol{\zeta}(\boldsymbol{\alpha})$ are fixed. Since the achievable sum rate of each scheme is also continuously differentiable over the feasible region of α_i and ζ_{m+i}, we can guarantee the convergence to the global optimum solution.

Proof. See Appendix 3.6.1. □

3.4 Numerical Results

In this section, we present numerical results to support our analysis. Specifically, we plot the maximum achievable sum rate for each scheme and the corresponding transmit source and relay power allocation. For numerical results, the number of orthogonal

Table 3.1. Four Cases depending on Channel Conditions

Case	I	II	III	IV
χ_1	30dB	20dB	30dB	20dB
η_1	15dB	10dB	10dB	15dB
χ_2	20dB	30dB	20dB	30dB
η_2	10dB	15dB	15dB	10dB

channels from the source and the relay is each assumed to be two, i.e., $(4, 2)$-(MBRC). We fix the source-to-the destination (SD) SNRs (η_1 and η_2) and the source-to-relay (SR) SNRs (χ_1 and χ_2) while changing the relay-to-destination (RD) SNRs in each channel by the same amount, i.e., $\rho_3 = \rho_4 = \rho$.

Table 3.1 shows the four cases considered in numerical results. In case I, SR and SD links of channel 1 is better than those of channel 2. In case II, SR and SD links of channel 1 is worse than those of channel 2. In case III, SR link of channel 1 is better than that of channel 2 and SD link of channel 1 is worse than that of channel 2. In case IV, SR link of channel 1 is worse than that of channel 2 and SD link of channel 1 is better than that of channel 2. We note that SR links are better than SD links for all four cases.

Figure 3.1 shows the convergence of the proposed iterative algorithm to the optimum resource allocation for AF. Starting with random initial power allocation for each trial, we observe that each time converges to the same value. Same observation is valid for CF.

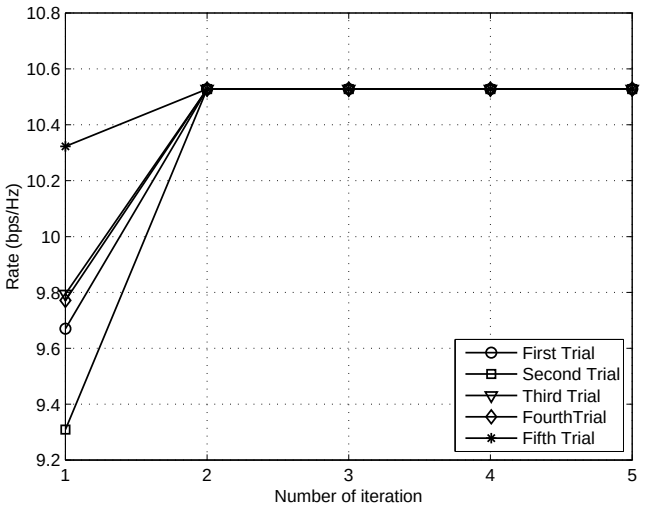

Fig. 3.1. Convergence of the iterative algorithm for AF scheme with five different random starting points.

Figure 3.2 shows the maximized achievable rates of two relay transmission schemes with optimum power allocation for case I. We can observe that CF is always better than AF.

Figure 3.3 shows the transmit source and relay power allocation of CF scheme for case I. We observe that almost equal source power is allocated to the SR/SD links. A slightly more source power is allocated to the channel with higher SD SNR. For relay power allocation, as RD SNRs become better, more relay power is allocated to the channel with higher SR SNR. For better SR link, the relay node can provide the more useful side information to the destination. Thus, allocating more relay power to the channel with higher SR SNR can help the reliable decodability at the destination node in CF scheme.

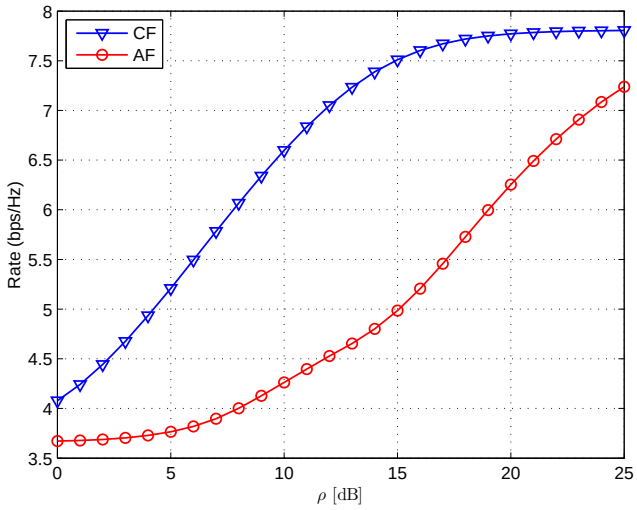

Fig. 3.2. Maximum achievable rates for case I.

Figure 3.4 shows the transmit source and relay power allocation of AF scheme for case I. In this case, the power allocation strategies between two schemes are same. At the low RD SNRs, more source power is allocated to the channel with larger SD SNR because in this case, relay is not going to be helpful and allocating more source power to the channel with better SD SNR yields higher rate. As the RD SNRs become better, more source power is allocated to the channel with smaller SR SNR. This is to ensure that relay node can be helpful for that link. That is, allocating more source power to the channel with smaller SR SNR will help the relay receive the correct message from the source. With the relatively smaller power, the link with higher SNR can do the same. For relay power allocation, more relay power is allocated to the channel with smaller SR SNR at low RD SNRs. As the RD SNRs become better, more relay power is allocated to the channel with larger SR SNR.

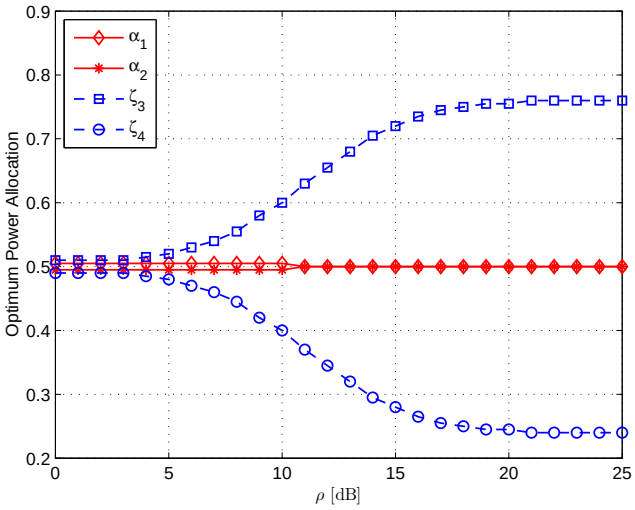

Fig. 3.3. Power Allocation for CF of case I.

For case II, since the channel conditions are opposite to the case I, the source and relay power allocation strategy is the same with case I with changing the role of channel 1 and channel 2.

Figure 3.5 shows the transmit source and relay power allocation of CF scheme for case III. We observe that almost equal source power is allocated to the SR/SD links. A slightly more source power is allocated to the channel with larger SD SNR. For relay power allocation, as RD SNRs become better, more relay power is allocated to the channel with larger SR SNR. We note that the power allocation of CF for case III is almost identical to that of case I except for the role change between α_1 and α_2 because case III is identical to case I with switching the role of SR channel 1 and 2.

Figure 3.6 shows the transmit source and relay power allocation of AF scheme for case III. In this case, the power allocation strategies between two schemes are same. At

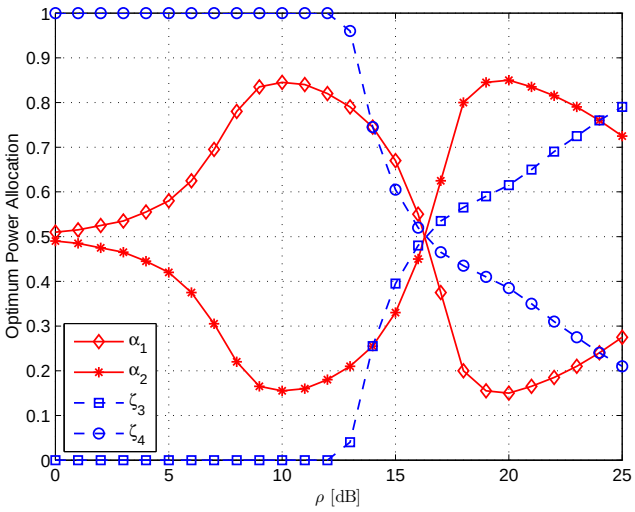

Fig. 3.4. Power Allocation for AF of case I.

the low RD SNR, more source power is allocated to the channel with worse SD link. As the RD SNRs becomes better, more power is allocated to the channel with better SR SNR. For relay power allocation, more relay power is allocated to the channel with larger SR SNR at low RD SNRs. As the RD SNRs become better, relay power starts to be allocated to the channel with worse SR links. For case IV, since the channel conditions are opposite to the case III, the source and relay power allocation strategy is the same with case III with changing the role of channel 1 and channel 2.

From the discussion so far, we note that the power allocation strategy between CF and AF are different. In CF, the relay power and source power allocation are decoupled and we end up allocating more power to the better channel. On the other hand, in AF, the source and relay power allocation affect and compensate each other to yield maximum rate.

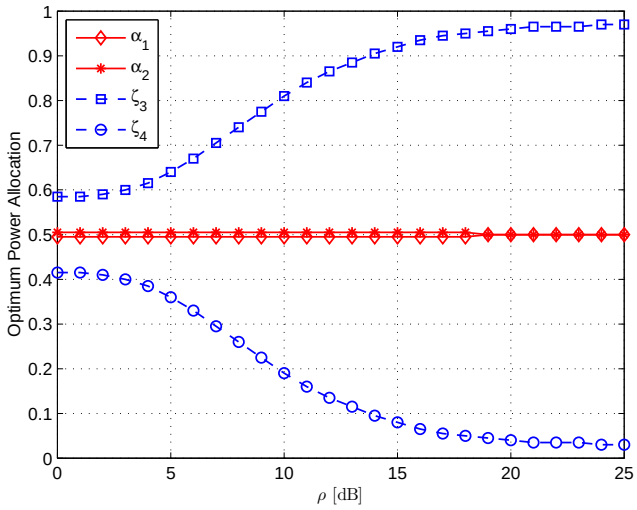

Fig. 3.5. Power Allocation for CF of case III.

So far, we have considered the cases where SR links are always better than SD links. Switching each SNR of SR and SD for each channel, we have the same four cases as Table I except that SD links are now better than SR links.

Figure 3.7 shows the maximized achievable rates of two relay transmission schemes with optimum power allocation when SD links are better than SR links. Although the rates obtained are very close, we can note that CF is still the better than AF.

3.5 Chapter Summary

In this chapter, we have investigated the optimum source and relay power allocation problem for amplify-and-forward (AF) and compress-and-forward (CF) for multi-band relay channels (MBRC) where the source node communicates to the destination with the help of a relay node via multiple orthogonal channels. For each scheme, we

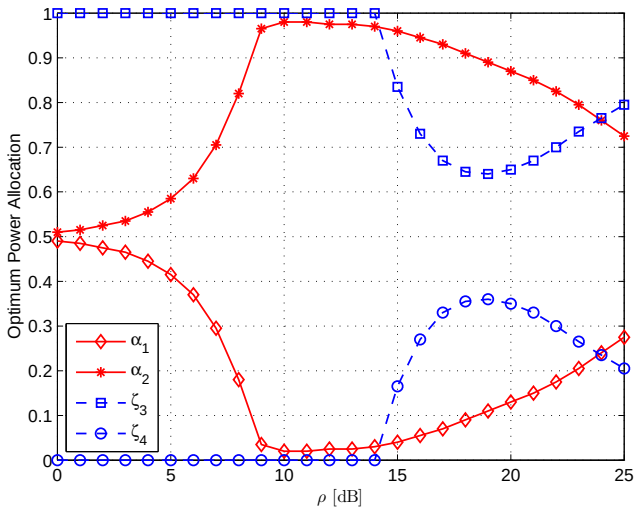

Fig. 3.6. Power Allocation for AF of case III.

have proposed an iterative power allocation algorithm based on alternating minimization to maximize the achievable sum rate. For numerical results, we have considered different cases depending on channel conditions of the source-to-relay and the source-to-destination. It is shown that CF is always better than AF. We have observed that CF and AF may yield different power allocation strategies. Proposed algorithms result in the optimum resource allocation, and thus can provide insight in choosing the best relay forwarding scheme under given channel conditions.

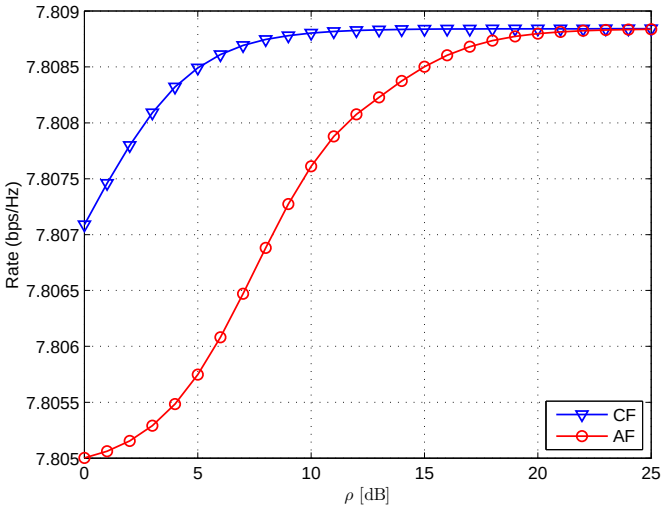

Fig. 3.7. Comparison of maximum achievable rates.

3.6 Appendix

3.6.1 Proof of Global Optimality Condition

Proof. The Hessian, $\mathbf{H}$, of the achievable sum rates in (3.16) and (3.23) is the $2m \times 2m$ block diagonal matrix with the following 2×2 matrix in its ith diagonal.

$$A_i = \begin{bmatrix} \dfrac{\partial^2 I}{\partial \alpha_i^2} & \dfrac{\partial^2 I}{\partial \alpha_i \partial \zeta_{m+i}} \\ \dfrac{\partial^2 I}{\zeta_{m+i} \partial \alpha_i} & \dfrac{\partial^2 I}{\zeta_{m+i}^2} \end{bmatrix} \quad i = 1, ..., m \tag{3.32}$$

Since $\mathbf{H}$ is a block diagonal matrix, $\mathrm{Det}(\mathbf{H}) = \prod_{i=1}^{m} \mathrm{Det}(A_i)$, where $\mathrm{Det}(\cdot)$ is the determinant of a matrix. Thus, we can find the eigenvalues of $\mathbf{H}$ from the following equation.

$$\prod_{i=1}^{m} \left(\lambda_i^2 - B_i \lambda_i + C_i \right) = 0 \tag{3.33}$$

where B_i and C_i are given by

$$B_i = \frac{\partial^2 I}{\partial \alpha_i^2} + \frac{\partial^2 I}{\zeta_{m+i}^2} \tag{3.34}$$

$$C_i = \frac{\partial^2 I}{\partial \alpha_i^2}\frac{\partial^2 I}{\zeta_{m+i}^2} - \left(\frac{\partial^2 I}{\partial \alpha_i \partial \zeta_{m+i}}\right)^2 \tag{3.35}$$

We note that B_i is the trace of A_i and C_i is the determinant of A_i. We note that λ_i has two values (i.e., λ_{i1} and λ_{i2}). Thus, we have total number of $2m$ eigenvalues. From (3.33), we have the following equality equations

$$\lambda_{i1} + \lambda_{i2} = B_i \tag{3.36}$$

$$\lambda_{i1}\lambda_{i2} = C_i \tag{3.37}$$

We note that B_i is always strictly negative since $\frac{\partial^2 I}{\partial \alpha_i^2}$ and $\frac{\partial^2 I}{\zeta_{m+i}^2}$ are strictly negative for all the received SNRs, η_i, χ_i, ρ_{m+i}, and both α_i and ζ_{m+i}. Thus, we can conclude that λ_{i1} and λ_{i2} are always negative when (3.31) is satisfied. Hence, if (3.31) is satisfied, the achievable sum rate of each scheme is concave function over the feasible region and is strictly concave over $\boldsymbol{\alpha}(\boldsymbol{\zeta})$ when $\boldsymbol{\zeta}(\boldsymbol{\alpha})$ are held constant. Since the achievable sum rate of each scheme is also continuously differentiable over the feasible region of α_i and ζ_{m+i}, by Theorem 2.3, we can apply the proposed iterative algorithm and convergence to the global optimum is always guaranteed in this case. □

Chapter 4

Cognitive Wireless Relay Networks: Outage and Diversity Performance

4.1 Introduction

As the deployment of high speed wireless networks for services such as mobile internet and multi-media applications continues to increase, the demand for spectrum is expected to grow rapidly in the near future. Currently, the radio spectrum is regulated and the licensed spectrum bands are not "shared". On the other hand, licensed resources may not be in use continuously, leading to possible under-utilization of the spectrum [7]. In a more flexible scenario, one can envision that the licensed resources, whenever not in use, can be captured and used by additional users, increasing the efficiency of spectrum use. To this end, cognitive radios, which are amenable to employ a more open spectrum policy have attracted considerable attention recently [19, 45]. The IEEE 802.22 working group on Wireless Regional Area Networks (WRAN) has worked on standardizing the opportunistic utilization of white spaces in the UHF/VHF TV band [53].

A cognitive radio allows a secondary (cognitive) user to access and uses a spectrum hole unoccupied by a primary (licensed) user. This can help enhance spectrum utilization significantly while reducing the white spaces in the spectrum [19]. A requirement for this system is seamless operation; thus, the cognitive users must detect the presence of the spectrum hole, or, equivalently, detect the presence of a primary user's

transmission [19, 56]. The common approach for this is to use an energy detector: the performance of energy detection for spectrum sensing has been investigated for various channel conditions in [14, 25, 63]. Recent research effort has investigated cooperative spectrum sensing where a group of neighboring nodes cooperate with a desired cognitive user to improve the spectrum sensing performance. It has been shown that the cooperative spectrum sensing provides more reliable and robust detection of the presence of primary users [16, 17, 44, 49, 61].

There has been considerable research effort in various other directions of cognitive radios. Design of decentralized cognitive MAC for opportunistic spectrum access network in which distributed cognitive users independently search for spectrum opportunities while minimizing the interference to primary users was studied in [70]. Spectrum allocation using graph-theory for opportunistic spectrum access was investigated in [71]. Simple capacity analysis for two types of cognitive radios depending on whether the cognitive radios can expand or contract their spectral bandwidth was shown in [60]. The achievable rate for the cognitive radio channel modeled as a two-sender and two-receiver interference channel was obtained in [13]. The channel capacity for a cognitive user operating within a primary band was evaluated to identify the limits of spectrum sharing in fading environment [18].

The notion of cognitive radios opportunistically capturing spectrum and communicating wirelessly, although mostly thought of in the context of cellular systems up to date, is equally intriguing for multi-hop wireless networks. As wireless networks continue to evolve towards allowing mobile nodes to communicate without the need for infrastructure, relay networks, where a source node is assisted by intermediate nodes, can offer

a significant performance gain [23, 28–30, 46, 58]. Thus, inspired by the performance advantage of wireless relay networks, as well as the promise of opportunistic spectrum utilization, in this chapter, we consider *cognitive wireless relay networks*.

The cognitive wireless relay network we consider consists of a source, a destination, and a group of network clusters each of which consists of a number of secondary (cognitive) relay nodes and one pair of primary source and destination nodes. The cognitive nodes relay information for the source node belonging to the secondary network in an opportunistic fashion by acquiring spectrum unused by a primary node. Three relaying schemes, regenerative decode-and-forward (RDF), nonregenerative decode-and-forward (NDF) and amplify-and-forward (AF) are considered. Our aim is to understand the performance of this system by investigating the impact of spectrum acquisition and the statistical existence of spectrum holes on the diversity order provided by the cognitive relay nodes. Thus, we analyze the high SNR approximation of the outage performance [29] in order to examine the diversity order of the cognitive wireless network. Even for the case where the spectrum hole exists with probability one, we find that full-diversity is not achieved. Motivated by this performance deficiency, we propose an intra-cluster cooperation scheme which exploits the idea of cooperative spectrum sensing [17] to improve the spectrum acquisition capability. It is shown that if we allow neighboring nodes in each cluster to collaborate with the potential relay node, the outage performance is improved and full diversity can be achieved if a proper number of neighboring nodes participate in the intra-cluster cooperation. We next investigate the outage performance of an overlay cognitive wireless relay network where a source node belonging to the primary network

wishes to communicate to its destination via relaying its information using the primary nodes in each cluster.

4.2 System Model

4.2.1 The Cognitive Wireless Relay Network

We consider a cognitive wireless relay network where a source node communicates with a destination node via a number of relay nodes. The relay nodes are secondary (cognitive) users and are grouped in clusters, based on their geographical proximity. The source and destination as well as a number of cognitive relay nodes in each cluster belong to the secondary network. Each cluster consists of a number of cognitive relay nodes (a potential relay node and neighboring relay nodes) and at least one node belonging to the primary network, which has a right to use its dedicated resources when active. The system model is depicted in Figure 4.1.

Among the cognitive nodes in a cluster, one is chosen as a potential relay node and can assist the source node, if the potential node is able to relay the message from the source, *and* acquires the spectrum hole unoccupied by the primary user successfully. We consider three relaying techniques:

- Regenerative Decode-and-Forward (RDF): When the transmission from the source is received reliably at the relay node, the relay node decodes the signal, re-encodes it with the same codebook used in the source node and transmits the signal to the destination [29].

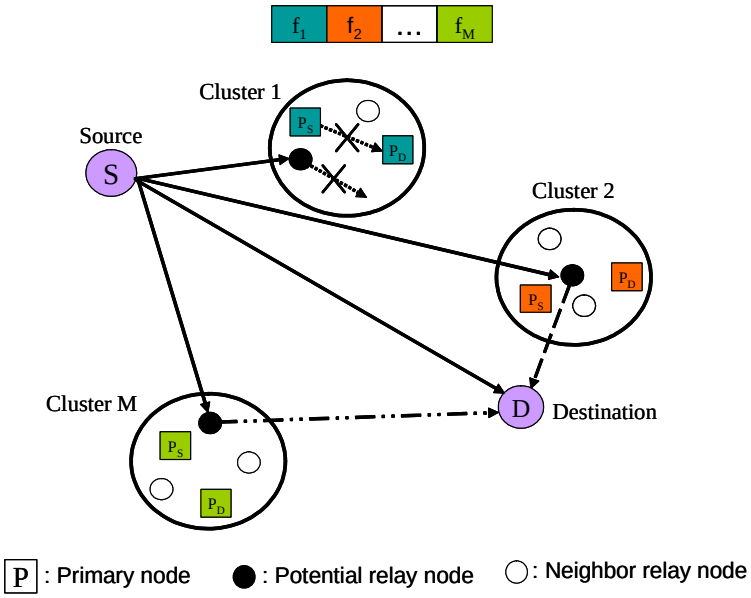

Fig. 4.1. System model

- Nonregenerative Decode-and-Forward (NDF): The relay node decodes the signal from the source reliably, but re-encodes it using a different and independent codebook than that of source [29].

- Amplify-and-Forward (AF): The relay node forwards a scaled version of the noisy copy of the source signal it received to the destination node [30].

Note that for a RDF or a NDF relay node to relay the source signal, it needs to decode the signal reliably, whereas this is not necessary for AF. We assume that each pair of primary nodes in a cluster communicates over an orthogonal frequency band with bandwidth W. Further, we assume that the channel from source-to-relay node is orthogonal to the channels of relays-to-destination.

The source broadcasts its message (X_s) to each cluster and the destination node. The received signals at each relay and the destination are given as:

$$Y_{r_i} = h_{sr_i} X_s + N_{sr_i}, \quad Y_d = h_{sd} X_s + N_{sd} \tag{4.1}$$

The relay nodes relay to the destination node over the acquired spectrum. The received signal at the destination from the successful potential relay node, over channel i, is given by

$$Y_{d_i} = h_{r_i d} X_{r_i} + N_{r_i d} \tag{4.2}$$

where X_{r_i} is the transmitted signal from the successful potential relay node i. N_{sr_i}, N_{sd}, and $N_{r_i d}$ are zero-mean, independent, circularly symmetric, complex Gaussian random variables with variance N_0. h_{sr_i}, h_{sd}, and $h_{r_i d}$ are the fading coefficients and modeled as zero-mean, independent, circularly symmetric complex Gaussian random variables with variances $1/\lambda_{sr_i}$, $1/\lambda_{sd}$, and $1/\lambda_{r_i d}$, respectively. The source and relays all transmit with power P. We define the received SNR at the relay and the destination as:

$$\chi_i = \gamma |h_{sr_i}|^2, \quad \eta = \gamma |h_{sd}|^2, \quad \rho_i = \gamma |h_{r_i d}|^2 \tag{4.3}$$

where the transmit SNR is given by $\gamma = P/N_0 W$.

4.2.2 Spectrum Acquisition

Since the potential relay nodes are cognitive users, it is important that each potential relay node detects the unused spectrum hole, or equivalently, detecting the

absence of transmission signal from primary source node in each cluster. Primary node in cluster i transmits its information (X_{p_i}) to the corresponding destination with transmit power P_{p_i}. Then, the spectrum detection problem is a hypothesis testing problem with the following two hypotheses:

$$Y_{p_i r_i} = \begin{cases} N_{p_i r_i}, & H_0 \\ h_{p_i r_i} X_{p_i} + N_{p_i r_i}, & H_1 \end{cases} \tag{4.4}$$

where subscript i represents ith cluster. H_0 corresponds to the event where a spectrum hole is available and H_1 corresponds to the event where a spectrum hole is not available. $Y_{p_i r_i}$ is the signal received by a potential relay node from the primary source node in ith cluster. X_{p_i} is the transmitted signal from the primary node in ith cluster. $N_{p_i r_i}$ is the received AWGN noise with variance N_0 at the potential relay. $h_{p_i r_i}$ is the fading coefficient and modeled as a zero-mean, circularly symmetric complex Gaussian random variable with variance $1/\lambda_{p_i r_i}$. The received SNR at the potential relay node in cluster i when the primary node transmits is given by

$$\gamma_{p_i} = \frac{P_{p_i} |h_{p_i r_i}|^2}{N_0 W} \tag{4.5}$$

We assume that each potential relay node performs energy detection which is widely used for detecting unknown signals in noise [14, 16, 17, 25, 63]. The decision statistic of

the energy detection has the following distribution [14].

$$Y_i \sim \begin{cases} \chi^2_{2u}, & H_0 \\ \chi^2_{2u}(2\gamma_{p_i}), & H_1 \end{cases} \tag{4.6}$$

where u is the number of samples related with approximation for the decision statistic [14]. We restrict u to be an integer value. χ^2_{2u} denotes a central chi-square distribution with $2u$ degree of freedom and $\chi^2_{2u}(2\gamma_{p_i})$ is a noncentral chi-square distribution with $2u$ degree of freedom and a non-centrality parameter $2\gamma_{p_i}$ [63]. Then, the probabilities of detection and false-alarm in cluster i are formulated as follows.

$$P_{d_i} = Pr[Y_i > \alpha_i | H_1] \tag{4.7}$$

$$P_{f_i} = Pr[Y_i > \alpha_i | H_0] \tag{4.8}$$

where α_i is the decision threshold in cluster i. The exact closed form expressions for (4.7) and (4.8) under a Rayleigh fading channel are given by [14].

$$P_{d_i} = e^{\frac{-\alpha_i}{2}} \sum_{k=0}^{u-2} \frac{1}{k!} \left(\frac{\alpha_i}{2}\right)^k + \left(1 + \lambda_{p_i} r_i\right)^{u-1} \times \left(e^{\frac{-\alpha_i \lambda_{p_i} r_i}{2(1+\lambda_{p_i} r_i)}} - e^{\frac{-\alpha_i}{2}} \sum_{k=0}^{u-2} \frac{1}{k!} \left(\frac{\alpha_i}{2(1+\lambda_{p_i} r_i)}\right)^k \right) \tag{4.9}$$

$$P_{f_i} = \frac{\Gamma(u, \alpha_i/2)}{\Gamma(u)} \tag{4.10}$$

where $\Gamma(.)$ and $\Gamma(.,.)$ are the complete and incomplete gamma functions, respectively [72]. We note that the probability of acquiring spectrum hole successfully in each cluster corresponds to $1 - P_{f_i}$.

4.3 Outage Probability Analysis

In this section, we investigate the performance of the cognitive wireless relay network in terms of the outage probability and diversity order. For a slow fading channel, an appropriate metric is the outage capacity: one can talk about a tradeoff between the outage probability and the supportable rate [48]. The outage occurs when the mutual information (I) falls below a certain transmission rate (R). The outage probability is defined as [48]

$$P_{out} = Pr[I < R] \tag{4.11}$$

The high SNR analysis of the outage probability of a relay network was developed in [29,30]. In the sequel, we focus on this limiting analysis of the outage probability for our system model. We consider three relay transmission schemes at the potential relay nodes and provide high SNR approximation of outage probabilities of each scheme depending on the capability of spectrum acquisition and the statistical existence of spectrum holes. The mutual information expressions for three relay transmission schemes are given as:

- Regenerative Decode-and-Forward (RDF) [29]:

$$I_{RDF} = \frac{1}{M+1}\log\left(1 + \gamma|h_{sd}|^2 + \gamma \sum_{r_i \in R(s)} |h_{r_i d}|^2\right) \tag{4.12}$$

- Nonregenerative Decode-and-Forward (NDF) [29]:

$$I_{NDF} = \frac{1}{M+1}\log\left(1+\gamma|h_{sd}|^2\right) + \frac{1}{M+1}\sum_{r_i \in R(s)} \log\left(1+\gamma|h_{r_i d}|^2\right) \tag{4.13}$$

- Amplify-and-Forward (AF) [30]:

$$I_{AF} = \frac{1}{M+1}\log\left(1+\gamma|h_{sd}|^2 + \sum_{r_i \in R(s)} f\left(\gamma|h_{sr_i}|^2, \gamma|h_{r_i d}|^2\right)\right) \tag{4.14}$$

where all logarithms are base 2, and M is the total number of clusters. We note that $|h_{sd}|^2$, $|h_{sr_i}|^2$, and $|h_{r_i d}|^2$ are exponentially distributed with parameter λ_{sd}, λ_{sr_i}, and $\lambda_{r_i d}$, respectively. $f(x,y) = xy/(x+y+1)$. In our setting, for RDF and NDF, $R(s)$ is the set of the potential relays that successfully acquire spectrum holes and decode the source message correctly. We note that for AF case, $R(s)$ is simply the set of the potential relays that successfully acquire spectrum holes.

For RDF, the source and each relay use the same codeword that is generated independently and identically distributed (i.i.d.) circularly symmetric complex Gaussian and the destination performs maximum-ratio combining (MRC) resulting log-sum mutual information. For NDF, the source and each relay use independently generated code word and the mutual information leads to sum of logarithms. AF nodes simply amplify their received signal with respect to power constraints, and send.

We define K as the number of potential relay nodes that acquire spectrum holes successfully. Then, the outage probability is given as

$$P_{out} = \sum_{k=0}^{M} \sum_{R(s)} Pr[I_{RDF} < R | R(s), K=k] Pr[R(s)|K=k] Pr[K=k] \tag{4.15}$$

where $Pr[K=k]$ is given as

$$Pr[K=k] = \sum_{j=1}^{\binom{M}{k}} \prod_{i \in S_j^k} P_{S_i}\left(1-P_{f_i}\right) \prod_{i \notin S_j^k} \left(1-P_{S_i}\left(1-P_{f_i}\right)\right) \tag{4.16}$$

where P_{S_i} is the probability that a spectrum exists in ith cluster. We assume that the existence of a spectrum hole in each cluster is independent event. S_j^k represents a jth set of k potential relay nodes which successfully acquire spectrum holes. $Pr[R(s)|K=k]$ is the probability of a set of relays that successfully decode the source message, given $K=k$ successfully acquired spectrum holes.

For RDF and NDF relay transmission schemes, the probability of ith potential relay node decodes the source message successfully is given by

$$Pr[I_{sr_i} > R] = exp\left(-\lambda_{sr_i}\frac{2^{(M+1)R}-1}{\gamma}\right) \tag{4.17}$$

where I_{sr_i} is the mutual information between the source and ith relay. Using the approximation technique developed in [29] and since outage occurs independently between relay nodes, we have

$$\begin{aligned} Pr[R(s)|K=k] = & \prod_{r_i \in R(s)} exp\left(-\lambda_{sr_i}\frac{2^{(M+1)R}-1}{\gamma}\right) \times \\ & \prod_{r_i \notin R(s)} \left(1-exp\left(-\lambda_{sr_i}\frac{2^{(M+1)R}-1}{\gamma}\right)\right) \\ \underset{\gamma \to \infty}{\sim} & \left(\frac{2^{(M+1)R}-1}{\gamma}\right)^{k-|R(s)|} \prod_{r_i \notin R(s)} \lambda_{sr_i} \end{aligned} \tag{4.18}$$

where $|R(s)| \in [0,k]$ is the cardinality of the set, $R(s)$. Conditioned on $R(s)$ and K and using the approximation technique developed in [29], the outage probability for RDF is given by

$$Pr[I_{RDF} < R|R(s), K=k] \underset{\gamma\to\infty}{\sim} \left[\frac{2^{(M+1)R}-1}{\gamma}\right]^{|R(s)|+1} \times \lambda_{sd} \prod_{r_i \in R(s)} \lambda_{r_i d} \frac{1}{(|R(s)|+1)!} \tag{4.19}$$

Proof. See Appendix 4.7.1. □

Substituting (4.16), (4.18), and (4.19) into (4.15), we obtain the outage probability for RDF as follows.

$$P_{out} \underset{\gamma\to\infty}{\sim} \sum_{k=0}^{M} \left[\frac{2^{(M+1)R}-1}{\gamma}\right]^{k+1} \sum_{j=1}^{\binom{M}{k}} \prod_{i \in S_j^k} P_{S_i}\left(1-P_{f_i}\right) \prod_{i \notin S_j^k} \left(1-P_{S_i}\left(1-P_{f_i}\right)\right) \Gamma_{RDF_k} \tag{4.20}$$

where Γ_{RDF_k} is given by

$$\Gamma_{RDF_k} = \lambda_{sd} \sum_{R(s)} \prod_{r_i \in R(s)} \lambda_{r_i d} \prod_{r_i \notin R(s)} \lambda_{s r_i} \frac{1}{(|R(s)|+1)!} \tag{4.21}$$

with $|R(s)| \in [0,k]$. Given k, Γ_{RDF_k} is found by the following recursive formula:

$$\Gamma_{RDF_k} = \Gamma_{RDF_{k-1}} + \frac{\lambda_{sd}}{(k+1)!} \sum_{j=1}^{\binom{M}{k}} \left(\prod_{i \in R_j^k} \lambda_{r_i d} \prod_{i \notin R_j^k} \lambda_{s r_i} \right), \quad k \geq 1 \tag{4.22}$$

where $\Gamma_{RDF_0} = \lambda_{sd} \sum_{i=1}^{M} \lambda_{s r_i}$.

Proof. See Appendix 4.7.2. □

R_j^k represents a jth set of k successful potential relay nodes that both successfully decode source message and successfully acquire spectrum holes.

If the spectrum hole always exists in each cluster and the probability of spectrum acquisition is always correct, i.e., $P_{S_i} = 1$, $P_{f_i} = 0$, $\forall i$, the outage probability for RDF can be simplified as [29]:

$$P_{out} \underset{\gamma \to \infty}{\sim} \left[\frac{2^{(M+1)R} - 1}{\gamma} \right]^{M+1} \Gamma_{RDF_M} \tag{4.23}$$

We note that Γ_{RDF_M} has the same expression as (4.21), but $|R(s)| \in [0, M]$. Similarly, given M, Γ_{RDF_M} is obtained by the recursive formula:

$$\Gamma_{RDF_M}(r) = \lambda_{sr_M} \Gamma_{RDF_{M-1}}(r) + \lambda_{r_M d} \Gamma_{RDF_{M-1}}(r+1), \quad M \geq 2 \tag{4.24}$$

where $\Gamma_{RDF_0}(r) = \lambda_{sd}$ and $\Gamma_{RDF_1}(r) = \lambda_{sd}\lambda_{sr_1}/(r)! + \lambda_{sd}\lambda_{r_1 d}/(r+1)!$. That is, the recursion starts with $r = 1$ and the formula is repeated until given M is reached [28]. We note that this system with $P_{S_i} = 1$, $P_{f_i} = 0$, $\forall i$ is equivalent to a "regular" cooperative diversity scenario [28–30] where relays have dedicated resources. Its performance is considered for the purpose of obtaining a benchmark, i.e., an upper bound on the performance of a cognitive wireless relay network.

Similarly, conditioned on $R(s)$ and K, the outage probability for NDF is given by

$$Pr[I_{NDF} < R|R(s), K = k] \underset{\gamma\to\infty}{\sim} \left[\frac{1}{\gamma}\right]^{|R(s)|+1} \times \lambda_{sd} \prod_{r_i \in R(s)} \lambda_{r_i d} G_{|R(s)|+1}((M+1)R) \tag{4.25}$$

where $G_k(t)$ is defined as

$$G_k(t) = \int_0^t G_{k-1}(t-x)2^x ln2 \; dx, \quad k = 2, 3, ... \tag{4.26}$$

where $G_1(t) = 2^t - 1$.

Proof. See Appendix 4.7.1. □

Substituting (4.16), (4.18), and (4.25) into (4.15), we obtain the outage probability for NDF as follows.

$$P_{out} \underset{\gamma\to\infty}{\sim} \sum_{k=0}^{M} \left[\frac{2^{(M+1)R} - 1}{\gamma}\right]^{k+1} \sum_{j=1}^{\binom{M}{k}} \prod_{i \in S_j^k} P_{S_i} \left(1 - P_{f_i}\right) \prod_{i \notin S_j^k} \left(1 - P_{S_i}\left(1 - P_{f_i}\right)\right) \Gamma_{NDF_k} \tag{4.27}$$

where Γ_{NDF_k} is given by

$$\Gamma_{NDF_k} = \lambda_{sd} \sum_{R(s)} \left(2^{(M+1)R} - 1\right)^{-|R(s)|} \prod_{r_i \in R(s)} \lambda_{r_i d} \prod_{r_i \notin R(s)} \lambda_{sr_i} G_{|R(s)|+1}((M+1)R) \tag{4.28}$$

with $|R(s)| \in [0, k]$. Given k, Γ_{NDF_k} is found by the following recursive formula:

$$\Gamma_{NDF_k} = \Gamma_{NDF_{k-1}} + \frac{\lambda_{sd} G_{k+1}((M+1)R)}{\left(2^{(M+1)R} - 1\right)^k} \sum_{j=1}^{\binom{M}{k}} \left(\prod_{i \in R_j^k} \lambda_{r_i d} \prod_{i \notin R_j^k} \lambda_{s r_i} \right), \quad k \geq 1 \tag{4.29}$$

where $\Gamma_{NDF_0} = \lambda_{sd} G_1((M+1)R) \sum_{i=1}^{M} \lambda_{s r_i}$.

Proof. See Appendix 4.7.2. □

If the spectrum hole always exists in each cluster and the probability of spectrum acquisition is always correct, i.e., $P_{S_i} = 1$, $P_{f_i} = 0$, $\forall i$, the outage probability for NDF can be simplified as [27]:

$$P_{out} \underset{\gamma \to \infty}{\sim} \left[\frac{1}{\gamma}\right]^{M+1} \left(2^{(M+1)R} - 1\right)^M \Gamma_{NDF_M} \tag{4.30}$$

We note that Γ_{NDF_M} has the same expression as (4.28), but $|R(s)| \in [0, M]$. In this case, given M, Γ_{NDF_M} is found by a tree-based algorithm depicted in Figure 4.2. We define $T(M, r)$ as follows.

$$\begin{aligned} T(M, r) = \lambda_{sd} \lambda_{s r_1} \left(2^{(M+1)R} - 1\right)^{-(r-1)} G_r((M+1)R) + \\ \lambda_{sd} \lambda_{r_1 d} \left(2^{(M+1)R} - 1\right)^{-r} G_{r+1}((M+1)R) \end{aligned} \tag{4.31}$$

We construct the tree diagram by starting with $T(1, 1)$, creating a left branch by increasing M by one and a right branch by increasing M and r by one, respectively. Each branch is multiplied by a weight L_i and R_i, $i \geq 2$. Then Γ_{NDF_M} for certain M is given

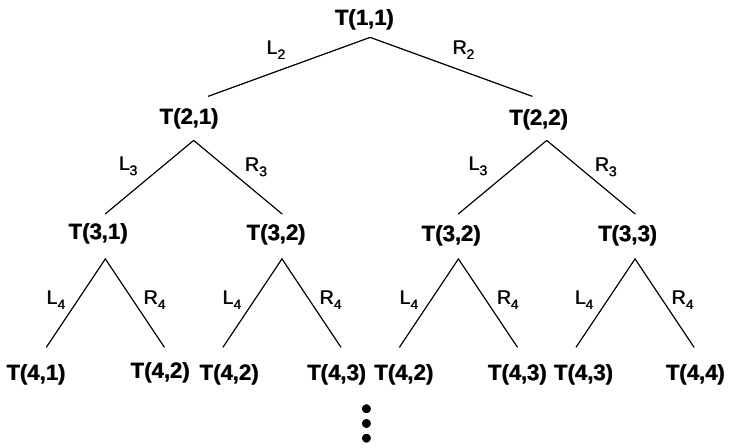

Fig. 4.2. Tree diagram.

by weighted sum of all nodes in the same level of the tree. L_i and R_i are given by λ_{sr_i} and λ_{r_id}, respectively. That is, Γ_{NDF_M} for $M = 1$ is $T(1,1)$. Γ_{NDF_M} for $M = 2$ is $\lambda_{sr_2}T(2,1) + \lambda_{r_2d}T(2,2)$. Γ_{NDF_M} for $M = 3$ is $\lambda_{sr_3}\lambda_{sr_2}T(3,1) + \lambda_{sr_2}\lambda_{r_3d}T(3,2) + \lambda_{sr_3}\lambda_{r_2d}T(3,2) + \lambda_{r_3d}\lambda_{r_2d}T(3,3)$.

Since for AF scheme, there is no decodability constraint, $R(s)$ is simply equal to the set of potential relay nodes that acquire spectrum holes successfully. Thus, the outage probability for AF is given by

$$P_{out,AF} = \sum_{R(s)} Pr[I_{AF} < R|R(s)]Pr[R(s)] \tag{4.32}$$

where $Pr[R(s)]$ is given by

$$Pr[R(s)] = \prod_{r_i \in R(s)} P_{S_i}\left(1 - P_{f_i}\right) \prod_{r_i \notin R(s)} \left(1 - P_{S_i}\left(1 - P_{f_i}\right)\right) \tag{4.33}$$

with $|R(s)| \in [0, M]$. Given $R(s)$, the outage probability for AF is given by

$$Pr[I_{AF} < R|R(s)] \underset{\gamma\to\infty}{\sim} \left[\frac{2^{(M+1)R}-1}{\gamma}\right]^{|R(s)|+1} \times \lambda_{sd} \prod_{r_i \in R(s)} \left(\lambda_{sr_i} + \lambda_{r_i d}\right) \frac{1}{(|R(s)|+1)!} \tag{4.34}$$

Proof. See Appendix 4.7.1. □

Substituting (4.34) and (4.33) into (4.32), we obtain the outage probability for AF as follows.

$$P_{out} \underset{\gamma\to\infty}{\sim} \sum_{R(s)} \left[\frac{2^{(M+1)R}-1}{\gamma}\right]^{|R(s)|+1} \lambda_{sd} \prod_{r_i \in R(s)} \left(\lambda_{sr_i} + \lambda_{r_i d}\right) \prod_{r_i \in R(s)} P_{S_i} \left(1 - P_{f_i}\right) \times \prod_{r_i \notin R(s)} \left(1 - P_{S_i}\left(1 - P_{f_i}\right)\right) \frac{1}{(|R(s)|+1)!} \tag{4.35}$$

Given M, P_{out} for AF is found by the tree diagram shown in Figure 4.2. We define $T(M, r)$ as follows.

$$T(M,r) = \left[\frac{2^{(M+1)R}-1}{\gamma_s}\right]^{r} \lambda_{sd}(1 - P_{S_1}\left(1 - P_{f_1}\right))/(r)! + \left[\frac{2^{(M+1)R}-1}{\gamma_s}\right]^{r+1} \lambda_{sd}\left(\lambda_{sr_1} + \lambda_{r_1 d}\right) P_{S_1}\left(1 - P_{f_1}\right)/(r+1)! \tag{4.36}$$

We construct the tree diagram by starting with $T(1, 1)$, creating a left branch by increasing M by one and a right branch by increasing M and r by one, respectively. Each branch

is multiplied by a weight $L_i = \left(1 - P_{S_i}\left(1 - P_{f_i}\right)\right)$ and $R_i = \left(\lambda_{sr_i} + \lambda_{r_i d}\right) P_{S_i}\left(1 - P_{f_i}\right)$, $\forall i \geq 2$, respectively. Then, P_{out} for certain M is given by weighted sum of all nodes in the same level of the tree.

If the spectrum hole always exists in each cluster and the probability of spectrum acquisition is always correct, i.e., $P_{S_i} = 1$, $P_{f_i} = 0$, $\forall i$, the outage probability for AF can be simplified as [29]:

$$P_{out} \underset{\gamma \to \infty}{\sim} \left[\frac{2^{(M+1)R} - 1}{\gamma}\right]^{M+1} \Gamma_{AF_M} \tag{4.37}$$

where Γ_{AF_M} is given by

$$\Gamma_{AF_M} = \lambda_{sd} \prod_{i=1}^{M} \left(\lambda_{sr_i} + \lambda_{r_i d}\right) \frac{1}{(M+1)!} \tag{4.38}$$

From (4.20), (4.27), and (4.35), we note that full-diversity is not achieved for any relaying scheme whether spectrum exists or not in each cluster.

4.3.1 Intra-Cluster Cooperation

We have observed that even for $P_{S_i} = 1$, $\forall i$, i.e., the spectrum always exists in each cluster, full diversity is not achieved due to the less than perfect spectrum acquisition performance. The natural question to ask then is whether we can improve the outage performance by having neighboring nodes cooperate with the potential cognitive node by sharing spectrum sensing information. This is termed *intra-cluster cooperation*. We assume that all cooperating nodes employ the same energy detector and the same decision

thresholds. For $N \geq 1$ cooperating nodes, the potential relay node decides in favor of the presence of a spectrum hole if at least one of the cooperating nodes detects it. In order words, the potential relay node acts like a fusion center and receives the individual decision from each cooperating relay node. By performing OR logical operation on the received decisions, the potential relay node makes the decision. This decision strategy is a simple fusion rule and shown to perform quite well [17]. The new probabilities of detection and false-alarm for the intra-cluster cooperation at cluster l are given by

$$C_{d_l} = \sum_{k=1}^{N} \sum_{j=1}^{\binom{N}{k}} \prod_{i \in D_j^k} P_{d_i} \prod_{i \notin D_j^k} \left(1 - P_{d_i}\right) \tag{4.39}$$

$$C_{f_l} = \sum_{k=1}^{N} \sum_{j=1}^{\binom{N}{k}} \prod_{i \in F_j^k} P_{f_i} \prod_{i \notin F_j^k} \left(1 - P_{f_i}\right) \tag{4.40}$$

where D_j^k is a jth set of k number of neighboring nodes, which decide H_1 given hypothesis H_1, and F_j^k is a jth set of k number of neighboring nodes, which decide H_1 given hypothesis H_0.

If $P_{d_i} = P_d$ and $P_{f_i} = P_f$, $\forall i$, (4.39) and (4.40) are simplified as [66]

$$C_d = 1 - (1 - P_d)^{N+1} \tag{4.41}$$

$$C_f = 1 - (1 - P_f)^{N+1} \tag{4.42}$$

The outage probabilities for each scheme with intra-cluster cooperation are obtained by (4.20), (4.27), and (4.35), respectively with the new probabilities of detection and false-alarm. We note that $N = 0$ corresponds to the case where intra-cluster cooperation is not used. With the intra-cluster cooperation, as more nodes cooperate, the outage performance improves and the system gets close to obtaining full-diversity.

It can be shown that given M and C_{f_i}, full-diversity can be achieved if there are N cooperating nodes, in each cluster satisfying the following:

$$\Omega(M, \gamma, C_{f_i}, N) \approx 1 \tag{4.43}$$

where $\Omega(M, \gamma, C_{f_i}, N)$ for RDF and NDF is given by

$$\frac{1}{\Gamma_M} \sum_{k=0}^{M} \left[\frac{2^{(M+1)R} - 1}{\gamma} \right]^{k-M} \sum_{j=1}^{\binom{M}{k}} \prod_{i \in S_j^k} (1 - C_{f_i}) \prod_{i \notin S_j^k} C_{f_i} \Gamma_k \tag{4.44}$$

where Γ_k and Γ_M represent Γ_{RDF_k}(or Γ_{NDF_k}) and Γ_{RDF_M}(or Γ_{NDF_M}), respectively. For AF scheme, $\Omega(M, \gamma, C_{f_i}, N)$ is given by

$$\frac{1}{\Gamma_{AF_M}} \left[\frac{2^{(M+1)R} - 1}{\gamma} \right]^{-(M+1)} \Gamma_{I_{AF_M}} \tag{4.45}$$

Equation (4.43) serves as a design rule: we can numerically determine the number of cooperating nodes necessary for each scheme to have (4.44) and (4.45) sufficiently close

to 1 and conclude that having at least that many cooperating nodes will achieve full-diversity. It can easily be seen that when C_{f_i} becomes close to zero, (4.43) is satisfied and we can find the corresponding necessary number of cooperating nodes numerically.

4.4 Overlay Cognitive Wireless Relay Networks

In this section, we consider an overlay cognitive wireless relay network where a source node belonging to the primary network wishes to communicate to its destination via relaying its information using the primary nodes in each cluster. Thus, the source node belonging to the primary network communicates with its destination via primary nodes that have dedicated resources. The source node belonging to the secondary network communicates with its destination via potential cognitive relay nodes that opportunistically acquire spectrum holes. In this setup, if the primary network uses DF (RDF or NDF), the primary relay node relays only when the primary relay node decodes its source message successfully. If the primary network uses AF scheme, the primary relay node in each cluster relays the received signal to the destination of the primary network without the decoding constraint. The system model is depicted in Figure 4.3. It shows the various scenarios that can occur in the overlay cognitive wireless relay networks. For example, for cluster M, the primary relay node using either DF or AF forwards the information of the source node (S_p) and the nearby potential cognitive relay node identifies the transmission successfully, which leads to the successful transmission from the primary relay node to the desired destination node (D_p). For cluster 2, it depicts the scenario when the primary relay node does not decode the source (S_p) message successfully and the resulting spectrum hole is identified by the potential

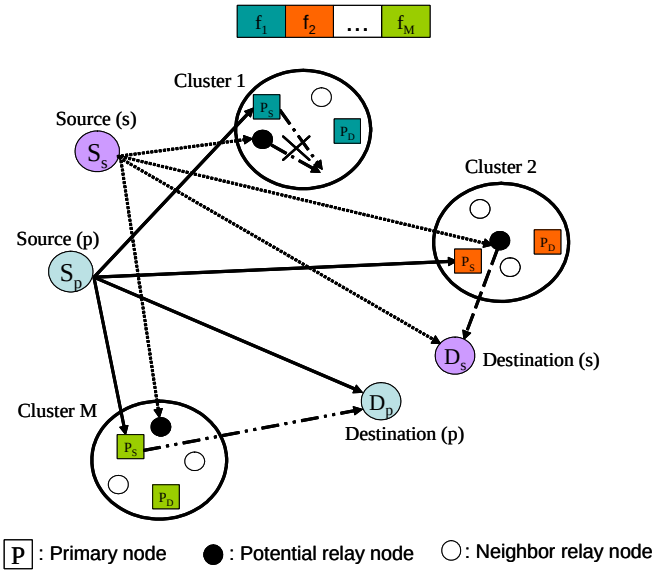

Fig. 4.3. Overlay cognitive wireless relay networks: (s) and (p) stand for the secondary and the primary network, respectively.

cognitive relay node which relays the information of the desired source node (S_s) to the destination node (D_s). If the cognitive relay node identifies the "busy" channel as "idle" and tries to communicate over the channel, collision occurs between these two networks and none of transmissions are successful as illustrated in cluster 1.

For the secondary network, the potential cognitive relay nodes relay to the destination node over the acquired spectrum. The received signals at each relay and the destination for the secondary network are given in (4.1) and (4.2), respectively.

For the primary network, the received signals at each primary relay node and the destination, respectively are given by

$$Y_{r_{p_i}} = h_{s_p r_{p_i}} X_{s_p} + N_{s_p r_{p_i}}, \quad Y_{d_p} = h_{s_p d_p} X_{s_p} + N_{s_p d_p} \tag{4.46}$$

where X_{s_p} is the transmitted signal from the source node of the primary network. The received signal at the destination from the primary relay node, over channel i, is given by

$$Y_{d_{p_i}} = h_{r_{p_i}d_p} X_{r_{p_i}} + N_{r_{p_i}d_p} \tag{4.47}$$

where $X_{r_{p_i}}$ is the transmitted signal from the primary relay node i. $N_{s_p r_{p_i}}$, $N_{s_p d_p}$, and $N_{r_{p_i}d_p}$ are zero-mean, independent, circularly symmetric, complex Gaussian random variables with variance N_0. $h_{s_p r_{p_i}}$, $h_{s_p d_p}$, and $h_{r_{p_i}d_p}$ are the fading coefficients and modeled as zero-mean, independent, circularly symmetric complex Gaussian random variables with variances $1/\lambda_{s_p r_{p_i}}$, $1/\lambda_{s_p d_p}$, and $1/\lambda_{r_{p_i}d_p}$, respectively. The source and primary relays of the primary network all transmit with power P. We define the received SNR at the relay and the destination of the primary network as:

$$\chi_{p_i} = \gamma |h_{s_p r_{p_i}}|^2, \quad \eta_{p_i} = \gamma |h_{s_p d_p}|^2, \quad \rho_{p_i} = \gamma |h_{r_{p_i}d_p}|^2 \tag{4.48}$$

where the transmit SNR is given by $\gamma = P/N_0 W$. We assume that the transmit SNRs of the primary and secondary network are same.

We focus on the case where the spectrum hole is available, i.e., the probability of spectrum existence, $P_{S_i} = 1$, $\forall i$. This implies that in each cluster there is no communication between the primary nodes and one primary node can act as a relay node for the primary source. That is to say, the primary network has dedicated resources to assist the primary source-to-destination communication, while the secondary network does not have dedicated resources and have to sense and acquire the spectrum holes to be able to assist the secondary source.

If the primary relay node in each cluster applies AF, it is easy to note that the secondary network can not be assisted by its cognitive relay nodes because the spectrum is always occupied. Also, if the primary relay node in each cluster applies either RDF or NDF, even though the secondary network can see the spectrum opportunity when the primary relay node fails to decode its source message, at high value of γ, this event does not occur and outage probability for the secondary network becomes one. Thus, for the secondary network, only meaningful outage event is when the source node of the primary network becomes idle. Thus, the outage probability for the secondary network for three relay transmission schemes are identical to those in obtained in section 4.3. For simplicity, we consider $P_{f_i} = P_f$, $\forall i$. Then, the outage probability for the secondary network using RDF can be obtained from (4.20) as follows.

$$P_{out} \underset{\gamma\to\infty}{\sim} \sum_{k=0}^{M} \left[\frac{2^{(M+1)R}-1}{\gamma}\right]^{k+1} \begin{pmatrix} M \\ k \end{pmatrix} \left(1-P_f\right)^k P_f^{M-k} \Gamma_{RDF_k} \tag{4.49}$$

Similarly, the outage probability for the secondary network using NDF can be obtained from (4.27) as follows.

$$P_{out} \underset{\gamma\to\infty}{\sim} \sum_{k=0}^{M} \left[\frac{1}{\gamma}\right]^{k+1} \left(2^{(M+1)R}-1\right)^k \begin{pmatrix} M \\ k \end{pmatrix} \left(1-P_f\right)^k P_f^{M-k} \Gamma_{NDF_k} \tag{4.50}$$

The outage probability for the secondary network using AF can be obtained from (4.35) as follows.

$$P_{out} \underset{\gamma\to\infty}{\sim} \sum_{|R(s)|=0}^{M} \left[\frac{2^{(M+1)R}-1}{\gamma}\right]^{|R(s)|+1} \lambda_{sd} \prod_{r_i\in R(s)} \left(\lambda_{sr_i}+\lambda_{r_id}\right) \times (1-P_f)^{|R(s)|} P_f^{M-|R(s)|} \frac{1}{(|R(s)|+1)!} \tag{4.51}$$

The outage probability for the primary network is defined as:

$$P_{out} = \sum_{R(s)} Pr[I < R|R(s)]Pr[R(s)] \tag{4.52}$$

where for decode-and-forward scheme, $R(s)$ is the set of clusters in which the primary relay node decodes its source message successfully and its transmission is successfully detected by the potential cognitive relay node. Thus, $Pr[R(s)]$ is given by

$$Pr[R(s)] = \prod_{r_i\in R(s)} P_{d_i} P\left[I_{s_p r_{p_i}} > R\right] \prod_{r_i\notin R(s)} \left(1 - P_{d_i} P\left[I_{s_p r_{p_i}} > R\right]\right) \tag{4.53}$$

where $I_{s_p r_{p_i}}$ is the mutual information between the source node of the primary network and ith primary relay node. $P\left[I_{s_p r_{p_i}} > R\right]$ is given by

$$P\left[I_{s_p r_{p_i}} > R\right] = exp\left(-\lambda_{s_p r_{p_i}} \frac{2^{(M+1)R}-1}{\gamma}\right) \underset{\gamma\to\infty}{\sim} 1 \tag{4.54}$$

We note that P_{d_i} corresponds to the probability that the potential cognitive relay node detects the transmitted signal from the primary relay node in ith cluster to its desired

destination. Thus, P_{d_i} is equivalent to (4.9) by replacing $\lambda_{p_i r_i}$ with $\lambda_{r_{p_i} d_p}$. We further assume that $P_{d_i} = P_d$, $\forall i$ (i.e., $\alpha_i = \alpha$ and $\lambda_{r_{p_i} d_p} = \lambda_{r_p d_p}$, $\forall i$). Then, we readily find the outage probability for RDF of the primary network as follows.

$$P_{out} \underset{\gamma \to \infty}{\sim} \sum_{|R(s)|=0}^{M} \left[\frac{2^{(M+1)R} - 1}{\gamma} \right]^{|R(s)|+1} P_d^{|R(s)|} (1 - P_d)^{M-|R(s)|} \Gamma_{RDF_{|R(s)|}} \tag{4.55}$$

where $\Gamma_{RDF_{|R(s)|}} = \frac{\lambda_{s_p d_p} (\lambda_{r_p d_p})^{|R(s)|}}{(|R(s)|+1)}$. Similarly, we find the outage probability for NDF of the primary network as follows.

$$P_{out} \underset{\gamma \to \infty}{\sim} \sum_{|R(s)|=0}^{M} \left[\frac{1}{\gamma} \right]^{|R(s)|+1} P_d^{|R(s)|} (1 - P_d)^{M-|R(s)|} \Gamma_{NDF_{|R(s)|}} \tag{4.56}$$

where $\Gamma_{NDF_{|R(s)|}} = \frac{\lambda_{s_p d_p} (\lambda_{r_p d_p})^{|R(s)|}}{(|R(s)|+1)} G_{|R(s)|+1}((M+1)R)$. $G_k(t)$ is defined as follows.

$$G_k(t) = \int_0^t G_{k-1}(t-x) 2^x ln2 \; dx, \quad k = 2, 3, ... \tag{4.57}$$

where $G_1(t) = 2^t - 1$.

For AF, $R(s)$ is the set of clusters in which the potential cognitive relay node successfully detects the transmission from the primary relay node. Thus, $Pr[R(s)]$ for AF is given by

$$Pr[R(s)] = P_d^{|R(s)|} (1 - P_d)^{M-|R(s)|} \tag{4.58}$$

The outage probability for AF of the primary network is given as

$$P_{out} \underset{\gamma\to\infty}{\sim} \sum_{|R(s)|=0}^{M} \left[\frac{2^{(M+1)R}-1}{\gamma}\right]^{|R(s)|+1} P_d^{|R(s)|} (1-P_d)^{M-|R(s)|} \Gamma_{AF_{|R(s)|}} \tag{4.59}$$

where $\Gamma_{AF_{|R(s)|}} = \frac{\lambda_{s_p d_p} \prod_{r_{p_i}\in R(s)} \left(\lambda_{s_p r_{p_i}} + \lambda_{r_p d_p}\right)}{(|R(s)|+1)}$.

4.5 Numerical Results

In this section, we present numerical results to support our analysis. Specifically, we consider a cognitive wireless relay network consisting of a source and a destination $300m$ (meter) apart, and $M = 4$ clusters that are distributed in a $300 \times 300m^2$ square area, as shown in Figure 4.4. The radius of each cluster is $40m$. Each cluster consists of a primary source node placed in the center, a primary destination node, and group of cognitive relay nodes. Relay nodes that are closest to each primary source node are chosen as potential relay nodes. We assume the path-loss model [54] on fading channels. Thus, we have $1/\lambda_{sd} = C/d_{sd}^{\alpha}$, $1/\lambda_{sr_i} = C/d_{sr_i}^{\alpha}$, $1/\lambda_{r_i d} = C/d_{r_i d}^{\alpha}$, and $1/\lambda_{p_i r_i} = C/d_{p_i r_i}^{\alpha}$ where d_{AB} is the distance between node A and B. α is the path-loss exponent. $C = G_t G_r \lambda_w^2/(4\pi)^2 L$, where G_t is the transmitter antenna gain, G_r is the receiver antenna gain, λ_w is the wavelength, and L is the system loss factor not related to propagation ($L \geq 1$). Throughout the numerical results, the values $\alpha = 3, G_t = G_r = 1, \lambda_w = 1/3m$ (carrier frequency $f = 900MHz$), $L = 1$, are used. The AWGN variances on all communication links are assumed to be 10^{-10}. We assume that $R = 1$, $u = 5$.

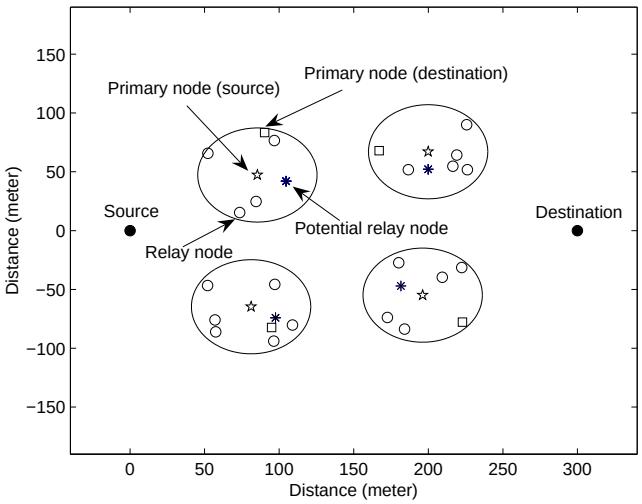

Fig. 4.4. Model of cognitive wireless relay network.

Figure 4.5 illustrates the simulated outage probabilities and the corresponding high SNR approximated outage probabilities of RDF for all possible cases. All simulated outage probabilities are obtained by Monte Carlo simulation of (4.12) over 60000 iterations. Given a randomly generated network topology, each channel gain, i.e., $|h_{sd}|^2$, $|h_{sr_i}|^2$, and $|h_{r_id}|^2$, is generated as independent exponential random variable and the outage occurs if the given rate R is larger than (4.12). We observe that the numerical outage probabilities of RDF are well matched with the simulated outage probabilities, especially at high SNR regime. We note that the same observation can be made for NDF and AF.

Figure 4.6 shows the outage probabilities of three relay transmission schemes for $P_{S_i} = 1$, $\forall i$, i.e., the spectrum hole always exists in each cluster. We observe that all three relay transmission schemes for $P_{f_i} \neq 0$, $\forall i$ do not achieve full-diversity. We observe

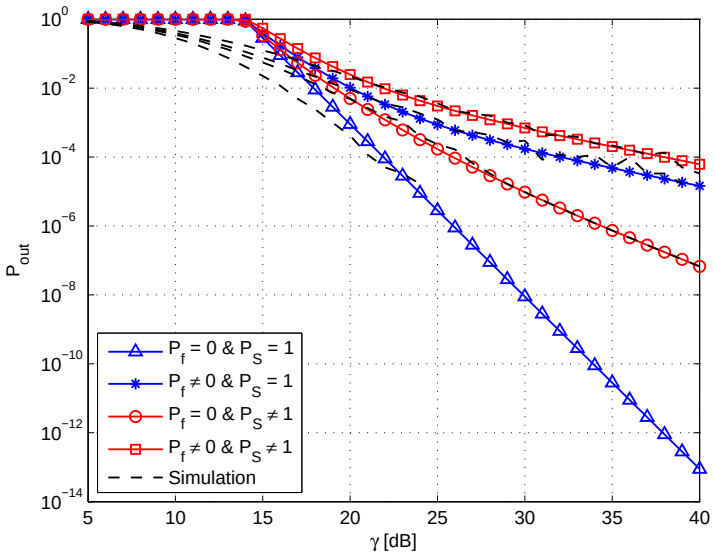

Fig. 4.5. Outage probabilities of RDF.

that AF performs best. This result is expected because both NDF and RDF require the decode constraints at the relay node which constrain the performance of the networks. We observe that NDF performs better than RDF as expected.

Figure 4.7 shows outage probabilities of RDF for different number of cooperating node (N) in each cluster. For simplicity, we assume that $P_{d_i} = P_d$ and $P_{f_i} = P_f$, $\forall i$. Thus, the probability of detection and false-alarm for intra-cluster cooperation is given by (4.41) and (4.42), respectively. We observe that $N = 5$ is required for achieving full-diversity. This is also shown in Figure 4.8 showing $\Omega(M, \gamma, C_{f_i}, N)$ for three relay transmission schemes to find the required number of cooperating node in each cluster for achieving full-diversity. We observe that $N = 5$ is necessary to achieve full-diversity for NDF and RDF. $N = 6$ is the required number of cooperating nodes to achieve full-diversity for AF. We also observe that increasing N beyond these required number does

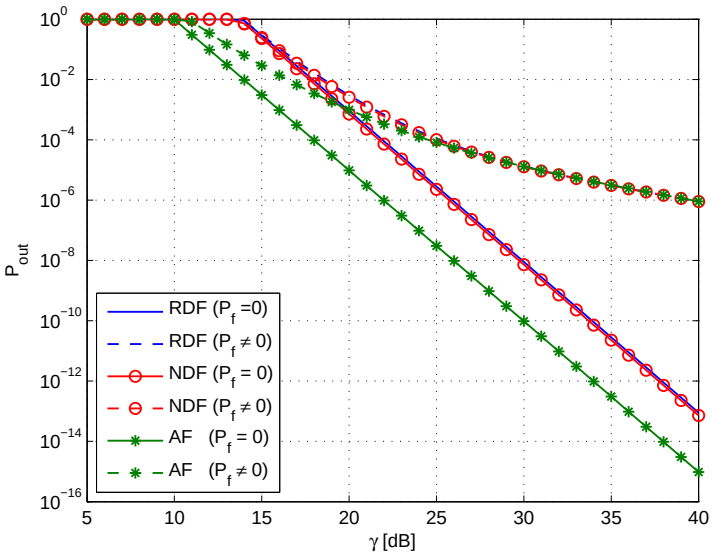

Fig. 4.6. Outage probabilities: $P_{S_i} = 1$, $\forall i$.

not help. Thus, for achieving full-diversity, we do not need more than these required number of cooperating nodes in each cluster.

4.6 Chapter Summary

In this chapter, we have investigated the outage performance of cognitive wireless relay networks where a single pair of source and destination nodes is assisted by a number of cognitive relay nodes that are grouped in clusters, based on their geographical proximity. Specifically, we have analyzed the high SNR approximation of the outage probabilities of three relay transmission schemes (RDF, NDF, and AF) for the general channel conditions. We have found that full-diversity is achieved only if the spectrum hole always exists and the cognitive relay nodes acquire spectrum hole successfully in each cluster. Further, we have investigated intra-cluster cooperation, which allows the

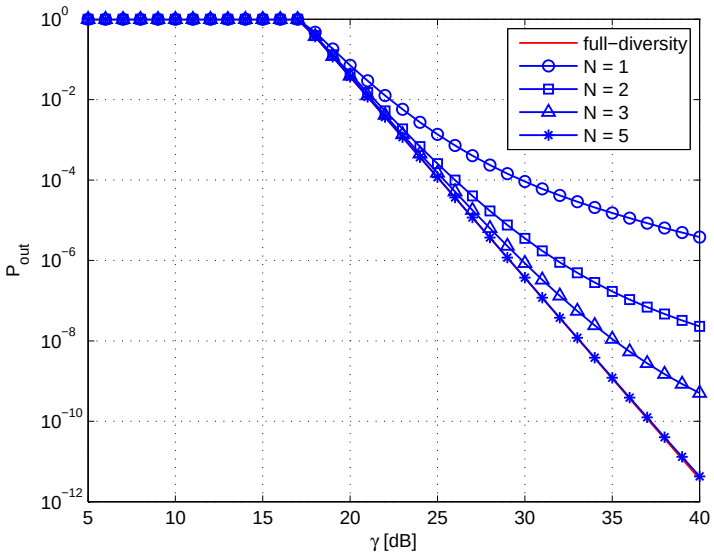

Fig. 4.7. Outage probabilities of RDF for different N.

neighboring relay nodes in a cluster to collaborate with a potential relay node in acquiring the spectrum hole. The intra-cluster cooperation is shown to improve the outage performance. Specifically, we observe that full-diversity is achieved if the proper number of neighboring relay nodes in each cluster participate in intra-cluster cooperation. Finally, we have investigated the outage probability of an overlay cognitive wireless relay networks.

4.7 Appendices

4.7.1 Proof of the conditional outage probability

We provide the proof of the outage probability conditioned $R(s)$ and $K = k$. We rely on the following theorem which is restated as follows.

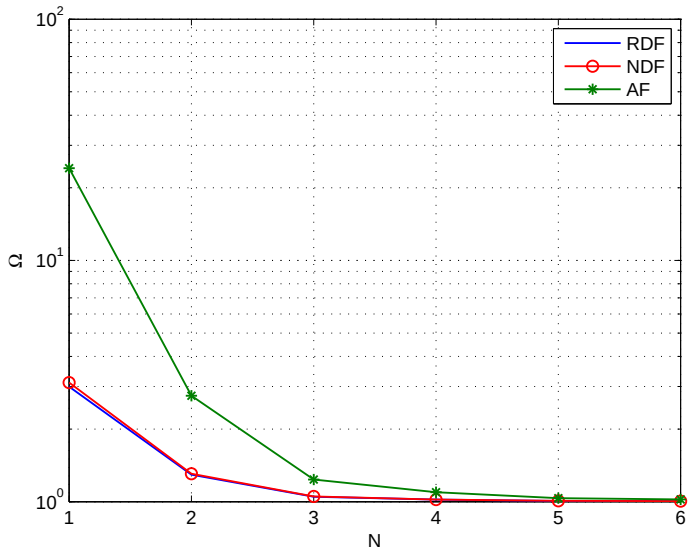

Fig. 4.8. The number of required cooperating nodes for achieving full-diversity.

Theorem 4.1 ([27], Theorem 1)**.** *If $U(s)$ and $V(s)$ are two independent random variables satisfying the following property:*

$$\lim_{s\to\infty} sPr\left[U(s) < t\right] = f(t), \quad \lim_{s\to\infty} s^d Pr[V(s) < t] = g(t) \tag{4.60}$$

where $f(t)$ and $g(t)$ are monotone increasing and integrable, and the first-order derivative of $f(t)$, $f'(t)$ is integrable. Then, the following is true:

$$\lim_{s\to\infty} s^{d+1} Pr[U(s) + V(s) < t] = \int_0^t g(t-x)f'(x)dx \tag{4.61}$$

First, we provide the proof for (4.19). For independent exponential random variables, $|h_{sd}|^2$ and $|h_{r_id}|^2$, we have the following [30]:

$$\lim_{s\to\infty} sPr\left[s|h_{sd}|^2 < t\right] = \lambda_{sd}t \tag{4.62}$$

$$\lim_{s\to\infty} sPr\left[s|h_{r_id}|^2 < t\right] = \lambda_{r_id}t \tag{4.63}$$

Applying Theorem 4.1 with (4.62) and (4.63) with $i = 1$, we obtain the following.

$$\lim_{s\to\infty} s^2Pr\left[s|h_{sd}|^2 + s|h_{r_1d}|^2 < t\right] = \frac{\lambda_{sd}\lambda_{r_1d}}{2}t^2 \tag{4.64}$$

Similarly, applying Theorem 4.1 with (4.64) and (4.63) with $i = 2$, the following is readily obtained.

$$\lim_{s\to\infty} s^3Pr\left[s|h_{sd}|^2 + s|h_{r_1d}|^2 + s|h_{r_2d}|^2 < t\right] = \frac{\lambda_{sd}\lambda_{r_1d}\lambda_{r_2d}}{3!}t^3 \tag{4.65}$$

Repeating this procedure $|R(s)| - 2$ times and using $s = \gamma$ and $t = 2^{(M+1)R} - 1$, we get (4.19).

For the proof of (4.34), since the mutual information of AF is log-sum as RDF case, the proof follows the foregoing step. Instead of using (4.63) at each step, the following is used [30].

$$\lim_{s\to\infty} sPr\left[f(s|h_{sr_i}|^2, s|h_{r_id}|^2) < t\right] = \left(\lambda_{sr_i} + \lambda_{r_id}\right)t \tag{4.66}$$

where $t = 2^{(M+1)R} - 1$.

Since the mutual information of NDF is sum of log, the following is used instead of (4.62) and (4.63).

$$\lim_{s\to\infty} sPr\left[U_j < t\right] = \lambda_j\left(2^t - 1\right) \tag{4.67}$$

where $U_j = \log\left(1 + s|h_j|^2\right)$ and $t = (M+1)R$. Applying Theorem 4.1 with (4.67) for U_{sd} and U_{r_1d}, we obtain the following.

$$\lim_{s\to\infty} s^2 Pr\left[U_{sd} + U_{r_1d} < t\right] = \lambda_{sd}\lambda_{r_1d}G_2(t) \tag{4.68}$$

Similarly, applying Theorem 4.1 with (4.68) and (4.67) with U_{r_2d}, the following is readily obtained.

$$\lim_{s\to\infty} s^3 Pr\left[U_{sd} + U_{r_1d} + U_{r_2d} < t\right] = \lambda_{sd}\lambda_{r_1d}\lambda_{r_2d}G_3(t) \tag{4.69}$$

Repeating this procedure $|R(s)| - 2$ times and using $s = \gamma$, we get (4.25).

4.7.2 Proof of (4.22) and (4.29)

Proof. We provide the proof of the recursive formula (4.22) and (4.29) for Γ_{RDF_k} and Γ_{NDF_k}, respectively. For given $M \geq k$, Γ_{RDF_0} for $k = 0$ is obtained from (4.21) as follow.

$$\Gamma_{RDF_0} = \lambda_{sd}\sum_{i=1}^{M}\lambda_{sr_i} \tag{4.70}$$

For $k = 1$, i.e., $R(s) \in [0, 1]$, Γ_{RDF_1} is readily found from (4.21) as:

$$\Gamma_{RDF_1} = \Gamma_{RDF_0} + \frac{\lambda_{sd}}{2!} \left\{ \lambda_{r_1 d} \prod_{i=1, i\neq 1}^{M} \lambda_{sr_i} + \lambda_{r_2 d} \prod_{i=1, i\neq 2}^{M} \lambda_{sr_i} + , ..., + \lambda_{r_M d} \prod_{i=1, i\neq M}^{M} \lambda_{sr_i} \right\} \tag{4.71}$$

(4.71) can be simplified as follows.

$$\Gamma_{RDF_1} = \Gamma_{RDF_0} + \frac{\lambda_{sd}}{2!} \sum_{j=1}^{\binom{M}{1}} \left(\prod_{i \in R_j^1} \lambda_{r_i d} \prod_{i \notin R_j^1} \lambda_{sr_i} \right) \tag{4.72}$$

Similarly, for $k = 2$, i.e., $R(s) \in [0, 2]$, Γ_{RDF_2} is readily found as:

$$\Gamma_{RDF_2} = \Gamma_{RDF_1} + \frac{\lambda_{sd}}{3!} \sum_{j=1}^{\binom{M}{2}} \left(\prod_{i \in R_j^2} \lambda_{r_i d} \prod_{i \notin R_j^2} \lambda_{sr_i} \right) \tag{4.73}$$

By applying the same procedure, for general k, we obtain (4.22).

Similarly, for given $M \geq k$, Γ_{NDF_0} for $k = 0$ is obtained from (4.28) as follow.

$$\Gamma_{NDF_0} = \lambda_{sd} G_1((M + 1)R) \sum_{i=1}^{M} \lambda_{sr_i} \tag{4.74}$$

For $k = 1$, i.e., $R(s) \in [0, 1]$, Γ_{NDF_1} is readily found from (4.28) as:

$$\Gamma_{NDF_1} = \Gamma_{NDF_0} + \frac{\lambda_{sd} G_2((M+1)R)}{(2^{(M+1)R} - 1)} \left\{ \lambda_{r_1 d} \prod_{i=1, i\neq 1}^{M} \lambda_{sr_i} + \lambda_{r_2 d} \prod_{i=1, i\neq 2}^{M} \lambda_{sr_i} +, ..., + \lambda_{r_M d} \prod_{i=1, i\neq M}^{M} \lambda_{sr_i} \right\} \tag{4.75}$$

(4.75) can be simplified as follows.

$$\Gamma_{NDF_1} = \Gamma_{NDF_0} + \frac{\lambda_{sd} G_2((M+1)R)}{(2^{(M+1)R} - 1)} \sum_{j=1}^{\binom{M}{1}} \left(\prod_{i \in R_j^1} \lambda_{r_i d} \prod_{i \notin R_j^1} \lambda_{sr_i} \right) \tag{4.76}$$

Similarly, For $k = 2$, i.e., $R(s) \in [0, 2]$, Γ_{NDF_2} is readily found as:

$$\Gamma_{NDF_2} = \Gamma_{NDF_1} + \frac{\lambda_{sd} G_3((M+1)R)}{(2^{(M+1)R} - 1)^2} \sum_{j=1}^{\binom{M}{2}} \left(\prod_{i \in R_j^2} \lambda_{r_i d} \prod_{i \notin R_j^2} \lambda_{sr_i} \right) \tag{4.77}$$

By applying the same procedure, for general k, we obtain (4.29). □

Chapter 5

Throughput Enhancing Cooperative Spectrum Sensing Strategies for Cognitive Radios

5.1 Introduction

Cognitive radio allows a secondary (cognitive) user to access a spectrum hole unoccupied by a primary (licensed) user and improves the spectrum utilization while reducing the white spaces in the spectrum [19]. Recent research effort investigates the scenario where a group of neighboring nodes cooperate with a desired cognitive user to improve the spectrum sensing performance of the desired user. It has been shown that such cooperative spectrum sensing provides reliable and fast detection of the presence of primary users [16, 17, 44, 49, 61]. While these cooperative schemes provide the reliable spectrum sensing performance of a desired cognitive user especially when deep fade, these schemes might not be scalable for the more general scenario where multiple cognitive users co-exist and contend over a limited number of frequency channels unused by the primary users.

In this chapter, we consider the general cognitive network where a number of cognitive users seek to access the unused frequency channels licensed to the primary users. One example of this general cognitive network is shown in Figure 5.1. There are a number of primary nodes (P) that communicate with their own destination, either directly or assisted by relay transmission. A number of cognitive nodes (S) communicate with their

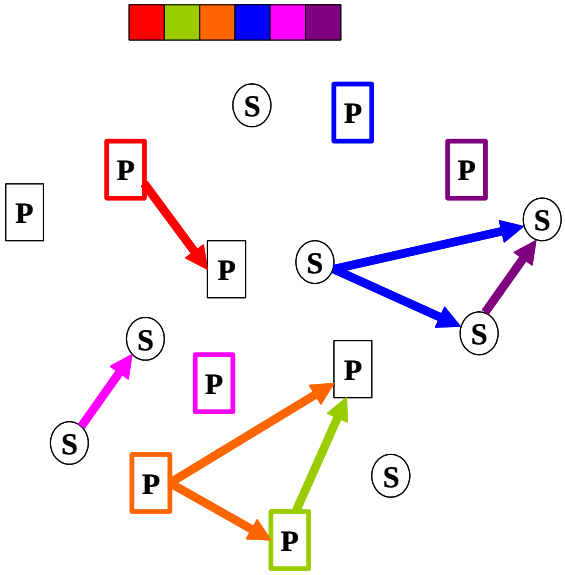

Fig. 5.1. A general cognitive network setup.

desired destination opportunistically by acquiring the spectrum unused by the primary nodes. In this setup, a main challenge is to design a spectrum sensing strategy which enhances the throughput of the cognitive users while the interference to the primary user transmissions is kept to a minimum. Towards addressing this challenge, we propose a *cooperative spectrum sensing strategy* in which cognitive users collaborate by sharing their decisions regarding spectrum occupancy of primary users. To do so, we propose that each cognitive user maintains the list of "busy" channels that it identifies and cognitive users share this information. By exchanging the indices of the busy frequency channels, each cognitive user can obtain more complete occupancy information about the overall occupancy status of the channels, which reduce the possibility to choose a channel in use by a primary user and increase the possibility to choose an idle channel. The proposed

scheme is designed to work in a distributed fashion and only requires one common time-slotted control channel in which each cognitive user broadcasts the frequency channels that it marked as busy.

The simulation results show that as compared with the non-cooperative case, this simple cooperative sensing strategy improves the probability of successful transmission of the cognitive users, leading to improve the throughput of the cognitive users while limiting the interference to the primary users.

5.2 System Model

We consider a cognitive network consisting of M primary users and K cognitive users which transmit their information by opportunistically acquiring spectrum holes unused by the primary users. We assume that one licensed frequency channel is allocated to each primary user. Thus, there are M orthogonal frequency channels and cross channel interference is negligible. Thus, the interference to the primary users by a cognitive user occurs only when the cognitive user transmits over a channel that is being used by a primary user. We assume that the state of being busy or idle for each frequency channel remains unchanged for T time slots. After T, the state of each frequency channel changes independently. Each cognitive user contends over the available frequency channels out of M frequency channels. Each cognitive user knows the total number of frequency channels in the network and has a frequency table in which the user maintains the occupancy information of the frequency channels.

Cognitive users communicate according to the slot structure shown in Figure 5.2. In a slot, each cognitive user randomly picks a frequency channel, senses it using the

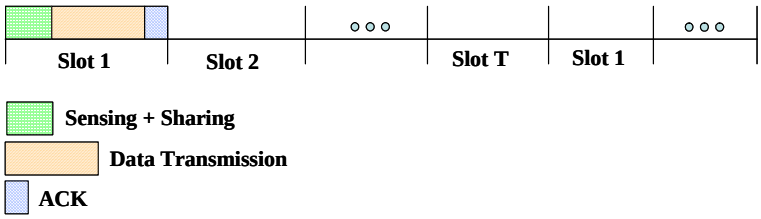

Fig. 5.2. Time-slotted Structure.

energy detector described in chapter 4, and makes a decision regarding the occupancy of the channel, i.e., busy or idle. If the channel sensed is deemed busy, the cognitive user marks the frequency channel in its frequency table and does not pick this channel in the remainder of T-slot frame until the frequency table is refreshed. If the decision is idle, the cognitive user transmits its data over this frequency channel and the transmission is successful if the same channel is not used by other cognitive users, i.e., we consider a collision limited system.

5.3 Cooperative Spectrum Sensing Strategy

In the scenario where multiple cognitive users seek to access unused frequency channels licensed to the primary users, a main challenge is to design the spectrum sensing strategy which will enhance the performance, e.g. throughput of the cognitive users, and limit the interference to the primary users. To address this challenge, we propose a cooperative spectrum sensing strategy in which cognitive users collaborate to share their decisions regarding spectrum occupancy of the primary users.

The idea is that each cognitive user cooperates by reporting the binary index of the frequency channel which is marked as “busy” in its frequency table. The reporting

is done via a common time-slotted control channel with C slots. Each cognitive user broadcasts its report over a slot chosen randomly. The reporting is successful if the same slot is not used by other cognitive users. We assume that the control channel is error-free.

The proposed cooperative spectrum sensing works as follows: If there are more than two frequency channels identified as "busy" in the frequency table, the cognitive user performs a binary XOR (exclusive OR) operation of the binary index numbers of the two of the randomly chosen channels in its frequency table. For example, if the total number of frequency channels is 16 and the current frequency table indicates that channel number 5, 9, and 12 are busy, one possible report is $f_5 \oplus f_{12} = 0110 \oplus 1100 = 1010$. By receiving the XOR-ed information, the remaining cognitive users can improve their frequency table information by decoding the received XOR-ed information, which is possible if the frequency channel f_5 or f_{12} is marked in their frequency tables. If there is only one frequency channel identified as "busy", the user reports the channel without the XOR operation. With the proposed cooperative spectrum sensing, we expect that each user obtains a complete occupancy information of the overall set of frequency channels. Thus, the cognitive users are less likely to choose busy channels for data transmission, leading to limit the collisions with the primary users as well as more likely to choose idle channels for data transmission.

In practice, each user might identify an idle channel as busy due to the non-zero false-alarm probability (P_f) of the energy detector. In this case, reporting the XOR-ed information might lead to missed opportunities for access. For lack of a better term, we will call these "false reports". Hence a false report corresponds to the case where the

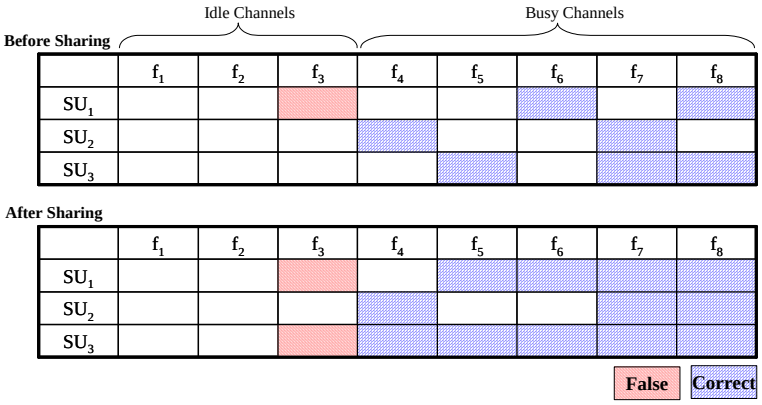

Fig. 5.3. Frequency channel table before and after cooperative spectrum sharing: SU_i, ith cognitive user.

report results in marking an idle channel as busy channel in a frequency table. Similarly, a "correct report" is when the report results in the identification of a new correctly-identified busy frequency channel. Figure 5.3 shows a snapshot of frequency table of a cognitive user before and after a round of the proposed cooperative spectrum sharing strategy.

Next, we study how often the false report and correct reports may occur. We consider a simple network where two cognitive users and M primary users exist and we find the probabilities of correct report (P_{CR}) and false report (P_{FR}) of the first cognitive user. To do so, we define w_1 to be the set of frequency channels of the first cognitive user that are incorrectly identified as busy when the channel is idle. We define c_1 to be the set of frequency channels of the first cognitive user that are identified correctly as busy when the channel is busy. Similarly, w_2 and c_2 are the corresponding sets for the second cognitive user, respectively. The cardinalities of w_i and c_i are W_i and C_i, for $i = 1, 2$. Let $f = f_k \oplus f_l$ be the binary XOR-ed data to be reported from the first cognitive user

after performing binary XOR operation on the frequency channels k and l. Then, P_{FR} and P_{CR} of the first cognitive user are defined as follows:

$$\begin{aligned} P_{FR} = P[f_k, f_l \in w_1]\,(1 - P[f_k, f_l \notin w_2 | f_k, f_l \in w_1] - P[f_k, f_l \in w_2 | f_k, f_l \in w_1]) \\ +2P[f_k \in w_1, f_l \in c_1](1 - P[f_l \notin c_2 | f_k \in w_1, f_l \in c_1] - \\ P[f_k \in w_2, f_l \in c_2 | f_k \in w_1, f_l \in c_1]) \end{aligned} \tag{5.1}$$

$$\begin{aligned} P_{CR} = P[f_k, f_l \in c_1]\,(1 - P[f_k, f_l \notin c_2 | f_k, f_l \in c_1] - P[f_k, f_l \in c_2 | f_k, f_l \in c_1]) \\ +2P[f_k \in w_1, f_l \in c_1](1 - P[f_l \notin w_2 | f_k \in w_1, f_l \in c_1] - \\ P[f_k \in w_2, f_l \in c_2 | f_k \in w_1, f_l \in c_1]) \end{aligned} \tag{5.2}$$

Out of M frequency channels, B frequency channels are busy and I frequency channels are idle. Thus, $M = B + I$. With the probabilities of detection (P_{d_i}) and false-alarm (P_{f_i}), we let $W_i = IP_{f_i}$ and $C_i = BP_{d_i}$. After substituting the corresponding probability expressions for each term in (5.1) and (5.2), we obtain P_{FR} and P_{CR} as follows,

Table 5.1. Performance of P_{CR} and P_{FR}: $B = 8$, $P_f = (0.01, 0.05, 0.1, 0.15)$, and $P_d = (0.8, 0.85, 0.9, 0.95)$.

P_f	0.01	0.05	0.1	0.15
P_{CR}	0.7192	0.7231	0.7165	0.7205
P_{FR}	0.0156	0.0178	0.080	0.0185

respectively.

$$P_{FR} = \frac{\binom{W_1}{2}}{\binom{C_1+W_1}{2}} \left(1 - \frac{\binom{I-2}{W_2}}{\binom{I}{W_2}} - \frac{\binom{I-2}{W_2-2}}{\binom{I}{W_2}} \right) + 2\frac{\binom{C_1}{1}\binom{W_1}{1}}{\binom{C_1+W_1}{2}} \left(1 - \frac{\binom{B-1}{C_2}}{\binom{B}{C_2}} - \frac{\binom{I-1}{W_2-1}\binom{B-1}{C_2-1}}{\binom{I}{W_2}\binom{B}{C_2}} \right) \tag{5.3}$$

$$P_{CR} = \frac{\binom{C_1}{2}}{\binom{C_1+W_1}{2}} \left(1 - \frac{\binom{B-2}{C_2}}{\binom{B}{C_2}} - \frac{\binom{B-2}{C_2-2}}{\binom{B}{C_2}} \right) + 2\frac{\binom{C_1}{1}\binom{W_1}{1}}{\binom{C_1+W_1}{2}} \left(1 - \frac{\binom{I-1}{W_2}}{\binom{I}{W_2}} - \frac{\binom{I-1}{W_2-1}\binom{B-1}{C_2-1}}{\binom{I}{W_2}\binom{B}{C_2}} \right) \tag{5.4}$$

Table 5.1 shows P_{CR} and P_{FR} for $B = 8$ and $M = 16$. This simulation consists of an experiment run 2000 times by changing W_i and C_i based on the random experiment of IP_{f_i} and BP_{d_i}, respectively. Similarly, Table 5.2 shows P_{CR} and P_{FR} for varying B.

Table 5.2. Performance of P_{CR} and P_{FR}: $B = 4, 8, 12$, $P_f = 0.05$, and $P_d = 0.85$.

B	4	8	12
P_{CR}	0.8564	0.7183	0.5598
P_{FR}	0.0436	0.0177	0.0061

We observe that a correct report transpires a lot more frequently than a false report. This encouraging result provides motivation for employing the proposed cooperative spectrum sensing. We note that $P_{CR} + P_{FR}$ is not necessarily equal to one because there might be cases when neither correct report nor false report occurs. That is, the XOR-ed information of the first cognitive user may not be decoded at the second cognitive user.

5.4 Simulation Results

In this section, we present simulation results to support our proposed cooperative spectrum sensing strategy. The total number of potential primary users (M), i.e., the frequency channels is 16. The number of the cognitive users is 5. We assume that the state of the frequency channels remains unchanged during T time slots and changes independently afterwards. Also, we assume that the cognitive users refresh their frequency table every T time slots. Any cognitive user causing interference to the primary users receives a penalty which bans its transmission for $P = 6$ time slots. We assume that $P_{d_i} = P_d$ and $P_{f_i} = P_f$, $i = 1, 2, ..., 5$. We consider three cases of the probability of detection and the probability of false-alarm. i.e., that $(P_d, P_f) = \{(0.8, 0.01), (0.85, 0.05), (0.9, 0.1)\}$. We assume that data rate of the cognitive users is $1Mbps$ and each data packet consists

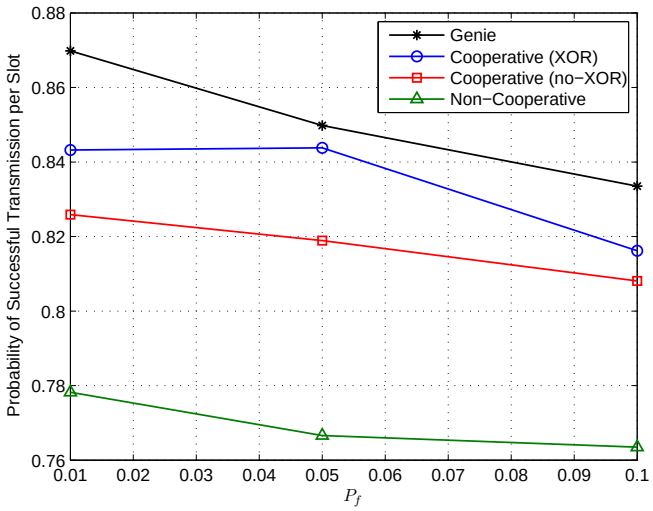

Fig. 5.4. Probability of successful transmission per slot: $T = 14$, $B = 10$, $C = 10$.

of 1000bits. The number of packets transmitted per slot over a frequency is 20. Thus, the duration for data transmission in each slot is $20ms$. The control channel transmission rate is $0.25Mbps$ and the total number of slots for the control channel is C. Thus, the overhead for each slot for the cooperative spectrum sharing is $16 * C\mu s$.[1] The ACK duration is 2 μs. Thus, the slot duration for the cooperative sensing strategy is 20,002 μs + $16 * C\mu s$. The corresponding slot duration for the non-cooperative strategy is 20,002 μs. We ignore the time spent in spectrum sensing as well as guard intervals since they are identical for the non-cooperative and the cooperative scheme. We also consider a simple cooperative scheme in which each cognitive user does not use the XOR operation, but simply forwards one frequency channel marked busy. We run 2000 iterations and

[1] Given $M = 16$, 4 bits are needed to identify each frequency channel. If $C = 10$, the overhead time is $4 * 10 * 4\mu s = 160\mu s$.

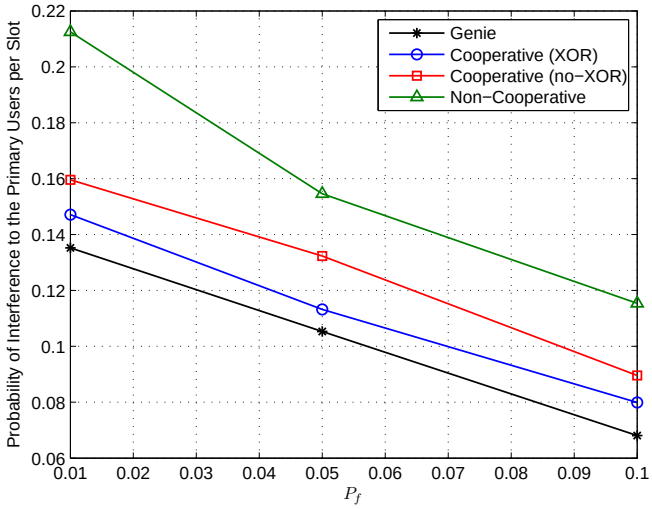

Fig. 5.5. Probability of interference to the primary users per slot: $T = 14$, $B = 10$, $C = 10$.

each iteration terminates when the cognitive users transmit all 200 the packets they have to transmit.

As a bench mark for performance, we also simulate a genie-aided scheme in which each cognitive user instantly knows the sensing decision of all other users related with a "busy channel". Also, an incorrect sensing decision, the event of identifying "idle" channel as "busy", is not shared. Though not practical, this genie-aided scheme clearly provides an upper bound for the performance of any cooperative sensing scheme.

Figure 5.4 clearly indicates that the cooperative spectrum sharing schemes increase successful transmissions by the cognitive users, and the cooperative scheme is close in performance to the genie-aided upper bound. This increase in successful transmissions leads to improved throughput for the cognitive users.

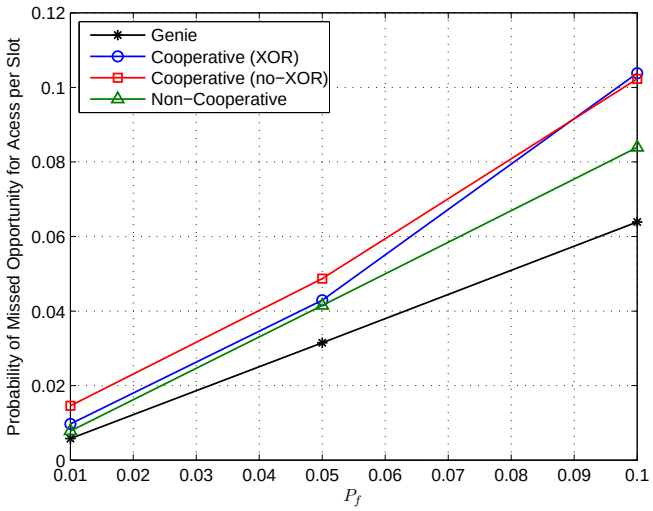

Fig. 5.6. Probability of missed opportunity for access: $T = 14$, $B = 10$, $C = 10$.

Figure 5.5 and 5.6 show the probability of interference to the primary users per slot and the probability of missed opportunity for access, respectively. As we expect, by sharing the channel occupancy information, interference to the primary users is reduced as shown in Figure 5.5. As discussed in section 5.3, sharing the channel occupancy information might result in the propagation of incorrect information leading to an increase in missed opportunities for access to idle frequency channels. We note that this increase is relatively small making the probability of missed opportunity for access comparable to the non-cooperative scheme.

Figure 5.7 shows the performance of the cooperative and the non-cooperative scheme in terms of throughput per user as T varies. We observe that the cooperative

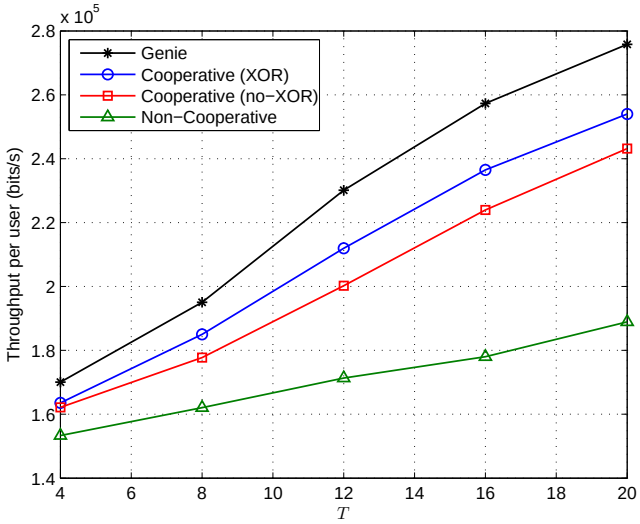

Fig. 5.7. Throughput per cognitive user: $B = 10$, $C = 4$, $P_f = 0.05$, and $P_d = 0.85$.

schemes are always better than the non-cooperative scheme. The throughput gap between the cooperative and the non-cooperative scheme becomes wider when the state of the frequency channels changes less frequently.

Figure 5.8 shows the performance of the cooperative and non-cooperative scheme in terms of throughput per user as B varies. We define R as the ratio of the number of busy channels to the number of total channels, i.e., $R = B/M$. We observe that the cooperative schemes are always better than the non-cooperative scheme. The throughput gap between the cooperative and the non-cooperative scheme becomes smaller when R is either small or large. For small R, most of the cognitive users are more likely to choose idle channels to sense. On the other hand, for large R, most of the cognitive users are likely to choose the busy channels to sense.

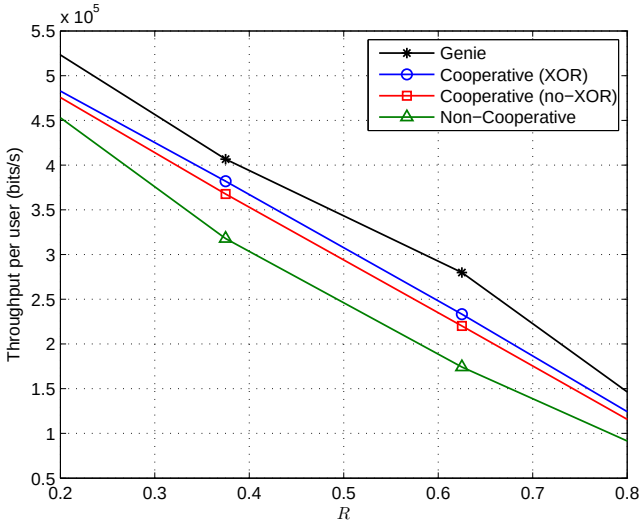

Fig. 5.8. Throughput per cognitive user: $T = 14$, $C = 10$, $P_f = 0.05$, and $P_d = 0.85$.

Figure 5.9 shows the impact of the knowledge of T on the throughput of the cognitive users. When the system state changes every $T = 14$ slots, we observe that the largest throughput gain between the cooperative schemes and the non-cooperative scheme is obtained when the cognitive users know the value of T and refresh their frequency table accordingly.

So far, the performance results were obtained based on the same P_d for all cognitive users. In a more general case, given a P_f, P_d might be different depending on the channel conditions between the cognitive users and the primary users. P_d is affected by $1/\lambda$, the variance of the fading channel, which is modeled as a zero-mean, independent, circularly symmetric complex Gaussian random variable. We assume that $1/\lambda_{AB} = 1/d_{AB}^{\alpha}$, where d_{AB} is the distance between the cognitive user A and the primary user B. α is the path-loss exponent. We let D_{max} as the maximum distance

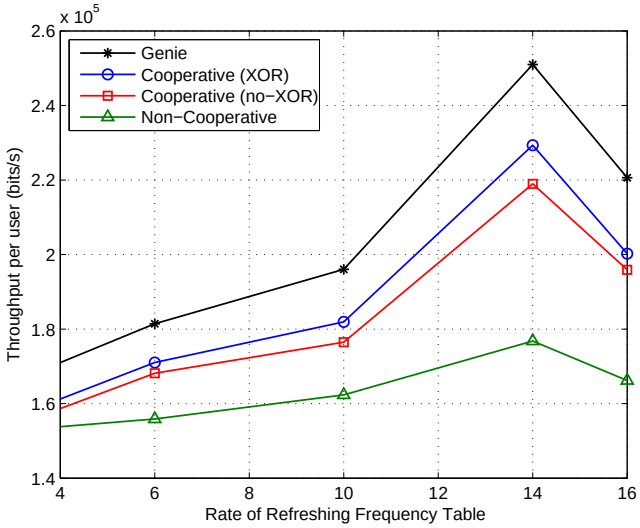

Fig. 5.9. Throughput per cognitive user: $T = 14$, $B = 10$, $C = 10$, $P_f = 0.05$, $P_d = 0.85$.

between any primary user and any cognitive user. The distance between the cognitive users and the primary users are randomly chosen within D_{max}. As shown in Figure 5.10, we observe that the cooperative schemes are always better than the non-cooperative scheme. Also, as D_{max} increases, we observe that the performance degrades because P_{d_i} becomes smaller.

5.5 Chapter Summary

In this chapter, we have considered a wireless communication scenario where multiple unlicensed cognitive users seek to access unused frequency channels licensed to the primary users. We have proposed a simple cooperative spectrum sharing strategy in which cognitive users collaborate by sharing their channel occupancy information. We

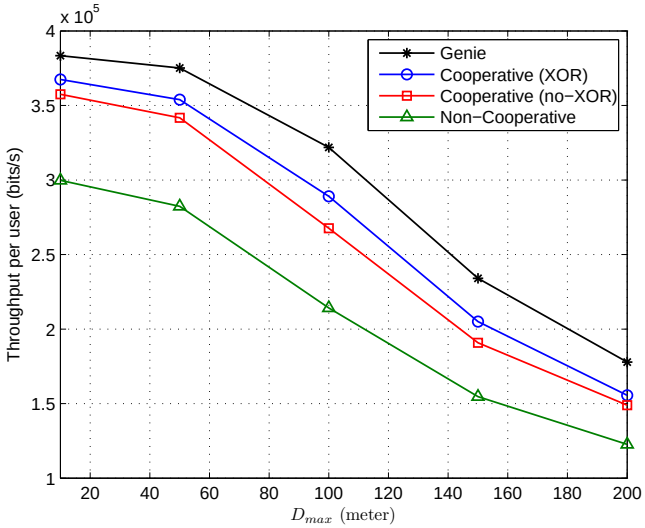

Fig. 5.10. Throughput per cognitive user: $T = 14$, $B = 10$, $C = 10$, $P_f = 0.01$, $\alpha = 3$.

have observed that the throughput of the cognitive users is enhanced and the interference to the primary user is reduced as a result of the cooperative sensing strategy. Surprisingly, these performance benefits require only small price to pay in the form of a slight increase on the probability of missed opportunity for access and a mild overhead brought by a common control channel used for sharing spectrum information.

Chapter 6

Conclusion

6.1 Thesis Summary

In this thesis, we have investigated the performance of cognitive hybrid wireless relay networks from various application aspects of these networks. First, we have investigated the information-theoretic performance of a simple hybrid wireless relay network, termed the Multi-Band Relay Channel (MBRC), where multiple frequency bands available from the source and the relay are mutually orthogonal. Specifically, we have studied the capacity bounds of MBRC where the relay node uses decode-and-forward (DF) scheme, and solved for the joint bandwidth and power allocation that maximize the bounds on the capacity. We have further provided sufficient conditions for when the solution technique can be applied. It is worth emphasizing that the sufficient conditions are general enough so that utility functions other than Shannon capacity can be considered. For a representative example, we have provided the joint power and bandwidth allocation for the case where two orthogonal channels are available from the source node and one orthogonal channel is available from the relay node. We have shown that joint power and bandwidth optimization always yields better performance than power optimization only.

Next, we have investigated the joint optimum source and relay power allocation problem for the MBRC where the relay performs amplify-and-forward (AF) or compress-and-forward (CF). We have found the joint source and relay power allocation strategies that maximize the mutual information for each relay transmission scheme. Given the channel conditions, we have investigated the corresponding power allocation strategies for each scheme. It is shown that CF is always better than AF. We have observed that CF and AF may lead to different power allocation strategies.

Throughout our analysis in chapters 2 and 3, we have assumed that the relay node has dedicated resource to assist its source node transmission. As means of utilizing the radio spectrum more efficiently, the future wireless communication systems, including relay-assisted networks, are likely to have cognitive radios which have to sense and acquire spectrum resources to be able to participate in the network. To understand the impact of employing cognitive radios on the performance of wireless networks, we have investigated *cognitive wireless relay networks* which are defined by source nodes, destination nodes, and a group of network clusters each consisting of a number of secondary (cognitive) relay nodes and pair of primary (licensed) source and destination nodes. Specifically, we have analyzed the high SNR approximation of the outage probabilities of three relay transmission schemes, namely regenerative decode-and-forward, nonregenerative decode-and-forward, and amplify-and-forward in order to examine diversity order of these networks and investigated the impact of spectrum acquisition capability on the diversity order.

We have found that full-diversity is not achieved by any of the relaying schemes even for the case where the spectrum hole exists in each cluster. Hence, to improve

the diversity performance, we have investigated intra-cluster cooperation, which allows the neighboring relay nodes in a cluster to collaborate with a potential relay node in acquiring the spectrum hole. The intra-cluster cooperation is shown to improve the outage performance. Specifically, we observe that full-diversity can be achieved if the proper number of neighboring relay nodes in each cluster participate in intra-cluster cooperation.

Lastly, we have considered the general cognitive wireless networks where a number of cognitive users seek to access unused frequency channels licensed to the primary users. We have investigated cooperative spectrum sensing strategies in which cognitive users collaborate by sharing their decisions regarding spectrum occupancy of primary users. We have shown that the cooperative spectrum sensing strategies enhance the throughput of the cognitive users while reducing the interference to the primary users.

Most of the results presented in this thesis have been presented in various conferences, see [33–38].

6.2 Future Research

Throughout the thesis, we have investigated the performance of two-hop cognitive hybrid wireless relay networks. It will be interesting work to extend this two-hop setting to the multi-hop scenario. In chapter 2 and 3, we have investigated the optimum resource allocation maximizing the capacity bounds for the multi-band relay channel (MBRC). The proposed resource allocation scheme requires each node to know the received SNRs of the whole network. This global information might not be available in practice. Thus, resource allocation scheme based on local information remains to be investigated. In

chapter 4, We have assumed that each relay node uses the energy detector for the spectrum sensing. Investigating the impact of different spectrum sensing schemes on the diversity performance would be interesting.

References

[1] N. Ahmed, M. A. Khojastepour, and B. Aazhang. Outage minimization and optimal power control for the fading relay channel,. In *IEEE Information Theory Workshop, ITW' 04*, pages 458 – 462, October 2004.

[2] S. M. Alamouti. A simple transmit diversity technique for wireless communications. *IEEE Journal on Selected Areas in Communications*, 16(8):1451 – 1458, October 1998.

[3] M. S. Bazaraa, H. D. Sherali, and C. M. Shetty. *Nonlinear Programming: Theory and Algorithms*. Wiley-Interscience, 2006.

[4] D. P. Bertsekas and J. N. Tsitsiklis. *Parallel and Distributed Computation: Numerical Methods*. Athena Scientific, 1997.

[5] H. Bölcskei, R.U. Nabar, O. Oyman, and A.J. Paulraj. Capacity scaling laws in MIMO relay networks. *IEEE Transactions on Wireless Communications*, 5(6):1433 – 1444, June 2006.

[6] J. Boyer, D. D. Falconer, and H. Yanikomeroglu. Multihop diversity in wireless relaying channels. *IEEE Transactions on Communications*, 52(10):1820 – 1830, October 2004.

[7] R. W. Broderson, A. Wolisz, D. Cabric, S. M. Mishra, and D. Willkomm. CORVUS : A cognitive radio approach for usage of virtual unlicensed spectrum. http://bwrc.eecs.berkeley.edu/Research/MCMA/CRWhitepaperfinal1.pdf.

[8] M. Chen, S. Serbetli, and A. Yener. Distributed power allocation for parallel relay networks. *IEEE Transactions on Wireless Communications, submitted December 2005, revised February 2007.*

[9] M. Chen, S. Serbetli, and A. Yener. Distributed power allocation for parallel relay networks. In *IEEE Global Telecommunications Conference, GLOBECOM' 05*, pages 1177 – 1181, 28 Nov.-2 Dec 2005.

[10] T. M. Cover and A. A. El Gamal. Capacity theorems for the relay channel. *IEEE Transactions on Information Theory*, 25(5):572 – 584, September 1979.

[11] T. M. Cover and J. A. Thomas. *Elements of Information Theory.* Wiley Interscience, 2006.

[12] A. del Coso, S. Savazzi, U. Spagnolini, and C. Ibars. Virtual MIMO channels in cooperative multi-hop wireless sensor networks. In *Conference on Information Sciences and Systems, CISS' 06*, pages 75 – 80, March 2006.

[13] N. Devroye, P. Mitran, and V. Tarokh. Achievable rates in cognitive radio channels. *IEEE Transactions on Information Theory*, 52(5):1813 – 1827, May 2006.

[14] F. F. Digham, M. S. Alouini, and M. K. Simon. On the energy detection of unknown signals over fading channels. *IEEE Transactions on Communications*, 55(1):21 – 24, January 2007.

[15] A. A. El Gamal and S. Zahedi. Capacity of a class of relay channels with orthogonal components. *IEEE Transactions on Information Theory*, 51(5):1815 – 1817, May 2005.

[16] G. Ganesan and Y. Li. Cooperative spectrum sensing in cognitive radio, Part I: Two user networks and Part II: multiuser networks. *IEEE Transactions on Wireless Communications*, 6(6):2204 – 2222, June 2007.

[17] A. Ghasemi and E. S. Sousa. Collaborative spectrum sensing for opportunistic access in fading environments. In *First IEEE International Symposium on New Frontiers in Dynamic Spectrum Access Networks, DySPAN'05*, pages 131 – 136, November 2005.

[18] A. Ghasemi and E. S. Sousa. Fundamental limits of spectrum-sharing in fading environments. *IEEE Transactions on Wireless Communications*, 6(2):649 –658, February 2007.

[19] S. Haykin. Cognitive radio: Brain-empowered wireless communications. *IEEE Journal on Selected Areas in Communications*, 23(2):201 – 220, February 2005.

[20] A. Høst-Madsen and J. Zhang. Capacity bounds and power allocation in wireless relay channel. *IEEE Transactions on Information Theory*, 51(6):2020 – 2040, June 2005.

[21] T. Hunter and A. Nosratinia. Coded cooperation under slow fading, fast fading, and power control. In *Thirty-Sixth Asilomar Conference on Signals, Systems and Computers,*, pages 118–122, November 2002.

[22] Intel. http://www.intel.com/pressroom/archive/releases/20040908techb.htm. Intel News Release: First Multi-Band OFDM-Based UWB Technology Interoperability Over Wireless USB Demonstrated.

[23] Y. Jing and B. Hassibi. Cooperative diversity in wireless relay networks with multiple-antenna nodes. In *IEEE International Symposium on Information Theory, ISIT 05'*, pages 815 – 819, September 2005.

[24] M. A. Khojastepour, A. Sabharwal, and B. Aazhang. On the capacity of cheap relay networks,. In *Conference on Information Sciences and Systems, CISS' 03*, March 2003.

[25] V. I. Kostylev. Energy detection of a signal with random amplitude. In *IEEE International Conference on Communications, ICC'03*, pages 1606 – 1610, May 2002.

[26] G. Kramer, M. Gastpar, and P. Gupta. Cooperative strategies and capacity theorems for relay networks. *IEEE Transactions on Information Theory*, 51(9):3037 – 3063, September 2005.

[27] J. N. Laneman. Limiting analysis of outage probabilities for diversity schemes in fading channels. In *IEEE Global Telecommunications Conference, GLOBECOM'03*, pages 1242 – 1246, December 2003.

[28] J. N. Laneman. Network coding gain of cooperative diversity. In *IEEE Military Communications Conference, MILCOM'04*, pages 106 – 112, November 2004.

[29] J. N. Laneman, D. N. C. Tse, and G. W. Wornell. Distributed space-time-coded protocols for exploiting cooperative diversity in wireless networks. *IEEE Transactions on Information Theory*, 49(10):2415 – 2425, October 2003.

[30] J. N. Laneman, D. N. C. Tse, and G. W. Wornell. Cooperative diversity in wireless networks: Efficient protocols and outage behavior. *IEEE Transactions on Information Theory*, 50(12):3062 – 3080, December 2004.

[31] J. N. Laneman and G. W. Wornell. Energy-efficient antenna sharing and relaying for wireless networks. In *IEEE Wireless Communication and Networking Conference, WCNC 00'*, September 2000.

[32] E. Larsson and Y. Cao. Collaborative transmit diversity with adaptive radio resource and power allocation. *IEEE Communications Letters*, 9(6):511–513, June 2005.

[33] K. Lee and A. Yener. On resource allocation for multi-band relay channel. In *Conference on Information Sciences and Systems, CISS' 05*, March 2005.

[34] K. Lee and A. Yener. On the achievable rate of three-node cognitive hybrid wireless networks. In *International Conference on Wireless Networks, Communications and Mobile Computing, WirelessCom' 05*, pages 1313 – 1318, June 2005.

[35] K. Lee and A. Yener. Iterative power allocation algorithms for amplify/estimate/compress-and-forward multi-band relay channels. In *Conference on Information Sciences and Systems, CISS' 06*, March 2006.

[36] K. Lee and A. Yener. Outage performance of cognitive wireless relay networks. In *IEEE Global Telecommunications Conference, GLOBECOM'06*, November 2006.

[37] K. Lee and A. Yener. Spectrum-sensing opportunistic wireless relay networks: Outage and diversity performance. In *40th Annual Asilomar Conference on Signals, Systems, and Computers, Asilomar'06*, October 2006.

[38] K. Lee and A. Yener. Throughput enhancing cooperative spectrum sensing strategies for cognitive radios. In *41th Annual Asilomar Conference on Signals, Systems, and Computers, Asilomar'07*, November 2007.

[39] Y. Liang, V. Veeravalli, and V. Poor. Resource allocation for wireless fading relay channels: Max-min solution. *To appear in the IEEE Transactions on Information Theory - Special Issue on Models, Theory and Codes for Relaying and Cooperation in Communication Networks*, 53(10), October 2007.

[40] Y. Liang and V. V. Veeravalli. Gaussian orthogonal relay channel: optimal resource allocation and capacity. *IEEE Transactions on Information Theory, 2005*, 51(9):3284 – 3289, September 2005.

[41] H. Luo, R. Ramjee, P. Sinha, L. Li, and S. Lu. UCAN : A unified cellular and ad-hoc network architecture. In *ACM MOBICOM'03*, pages 353 – 367, September 2003.

[42] J. Luo, R. S. Blum, L. j. Greenstein L. J. Cimini, and A. M. Haimovich. Decode-and-forward cooperative diversity with power allocation in wireless networks. *IEEE Transactions on Wireless Communications*, 6(3):793 – 799, March 2007.

[43] I. Maric and R. D. Yates. Forwarding strategies for Gaussian parallel-relay networks. In *Conference on Information Sciences and Systems, CISS' 04*, pages 591 – 596, March 2004.

[44] S. M. Mishra, A. Sahai, and R. W. Brodersen. Cooperative sensing among cognitive radios. In *IEEE International Conference on Communications, ICC'06*, June 2006.

[45] J. Mitola and G. Q. Maguire Jr. Cognitive radio: making software radios more personal. *IEEE Personal Communications*, 6(4):13 – 18, August 1999.

[46] R. U. Nabar, H. Bölcskei, and F. W. Kneubühler. Fading relay channels: performance limits and space-time signal design. *IEEE Journal on Selected Areas in Communications*, 22(6):1099 – 1109, August 2004.

[47] A. Narula, M.D. Trott, and G. W. Wornell. Performance limits of coded diversity methods for transmitter antenna arrays. *IEEE Transactions on Information Theory*, 45(7):2418 – 2433, November 1999.

[48] L. H. Ozarow, S. Shamai, and A. D. Wyner. Information theoretic considerations for cellular mobile radio. *IEEE Transactions on Vehicular Technology*, 33(2):359 – 378, May 1994.

[49] E. Peh and Y.C. Liang. Optimization for cooperative sensing in cognitive radio networks. In *Conference on Wireless Communications and Networking Conference, WCNC'07*, March 2007.

[50] J. G. Proakis. *Digital Communications*. New York: McGraw-Hill, Inc., Fourth ed., 2001.

[51] C. Qiao, H. Wu, and O. Tonguz. Load balancing via relay in next-generation wireless systems. In *2000 First Annual Workshop on Mobile and Ad Hoc Networking and Computing, MobiHOC'00*, pages 149 – 150, August 2000.

[52] Qualcomm. http://www.qualcomm.com/press/releases/2002/press1110.html.

[53] IEEE 802.22 Wirelesss RAN. Functional requirements for the 802.22 WRAN standard, IEEE 802.22 - 05/0007r46, October, 2005.

[54] T. S. Rappaport. *Wireless communications: Principles and Practice.* Prentice-Hall, 1996.

[55] A. K. Sadek, Z. Han, and K. J. R. Liu. Multi-node cooperative resource allocation to improve coverage area in wireless networks. In *IEEE Global Telecommunications Conference, GLOBECOM' 05*, pages 3058 – 3062, 28 November - 2 December 2005.

[56] A. Sahai, N. Hoven, and R. Tandra. Some fundamental limits on cognitive radio. In *Allerton conference on Communications, Control, and Computing*, 2004.

[57] B. Schein and R. G. Gallager. The Gaussian parallel relay network. In *IEEE International Symposium on Information Theory, ISIT 00'*, page 22, 2000.

[58] A. Sendonaris, E. Erkip, and B. Aazhang. User cooperation diversity part I: System description; part II: Implementation, aspects and performance analysis. *IEEE Transactions on Communications*, 51(11):1927 – 1948, November 2003.

[59] S. Serbetli and A. Yener. Relay assisted F/TDMA ad hoc networks: Node classification, power allocation and relaying strategies. *IEEE Transactions on Wireless Communications, accepted for publication, November 2006.*

[60] S. N. Shankar, C. Chou, K. Challapali, and S. Mangold. Spectrum agile radio: Capacity and QoS implication of dynamic spectrum assignment. In *IEEE Global Telecommunications Conference, GLOBECOM' 05*, pages 2510 – 2516, 28 November - 2 December 2005.

[61] C. Sun, W. Zhang, and K. B. Letaief. Cooperative spectrum sensing for cognitive radios under bandwidth constraints. In *Conference on Wireless Communications and Networking Conference, WCNC'07*, March 2007.

[62] I. E. Telatar. Capacity of multi-antenna Gaussian channels. *European Transactions on Telecommunications*, 10(6):585 – 595, November/December 1999.

[63] H. Urkowitz. Energy detection of unknown deterministic signals. *Proceedings of the IEEE*, 55(4):523 – 531, April 1967.

[64] E. van der Meulen. Three terminal communications channels. *Advanced Applied Probability*, 3(5):120 – 154, September 1971.

[65] A. Vardy. *Codes, Curves, and Signals: Common Threads in Communications*, pages 173 – 191. Kluwer Academic Publishers, 1998.

[66] P. K. Varshney. *Distributed Detection and Data Fusion*. Springer, 1997.

[67] B. Wang, J. Zhang, and A. Høst-Madsen. On the capacity of MIMO relay channels. *IEEE Transactions on Information Theory*, 51(1):29 – 43, January 2005.

[68] H. Wu, C. Qiao, S. De, and O. K. Tonguz. Integrated cellular and ad-hoc relay systems: iCAR. *IEEE Journal on Selected Areas in Communications*, 19(10):2105 – 2115, October 2001.

[69] A. D. Wyner and J. Ziv. The rate-distortion function for source coding with side information at the decoder. *IEEE Transactions on Information Theory*, 22(1):1 – 10, January 1976.

[70] Q. Zhao, L. Tong, A. Swami, and Y. Chen. Decentralized cognitive MAC for opportunistic spectrum access in ad hoc networks: A POMDP framework. In *IEEE Journal on Selected Areas in Communications (JSAC): Special Issue on Adaptive, Spectrum Agile and Cognitive Wireless Networks*, volume 25, pages 589 – 600, April 2007.

[71] H. Zheng and C. Peng. Collaboration and fairness in opportunistic spectrum access. In *IEEE International Conference on Communications, ICC'05*, pages 3132 – 3136, May 2005.

[72] D. Zwillinger. *Standard Mathematical Tables and Formulae*. CRC Press, 1996.

Vita

Kyounghwan Lee

- 2000 B.S. in Electrical Engineering, University of Seoul, Seoul, Korea
- 2002 M.S. in Information and Communication Engineering, Gwangju Institute of Science and Technology, Gwangju, Korea
- 2007 Ph.D. in Electrical Engineering, The Pennsylvania State University, University Park